INTERNATIONAL ATOMIC ENERGY AGENCY
UNITED NATIONS EDUCATIONAL, SCIENTIFIC AND CULTURAL ORGANIZATION

INTERNATIONAL CENTRE FOR THEORETICAL PHYSICS
34100 TRIESTE (ITALY) - P.O.B. 586 - MIRAMARE - STRADA COSTIERA 11 - TELEPHONE: 2240-1
CABLE: CENTRATOM - TELEX 460392-1

SMR/220-25

COLLEGE ON SOIL PHYSICS
2 - 20 November 1987

"Quantification of Soil Moisture Through Passive Microwave Remote Sensing Techniques"

Dr. K.S. RAO
Centre of Studies in Resources Engineering
Indian Institute of Technology
Bombay, India

Quantification of Soil Moisture Through Passive Microwave Remote Sensing Techniques

K. S. Rao, Y. Subrahmanyeswara Rao, Girish Chandra, Suresh Raju and P. V. Narasimha Rao

Center of Studies in Resources Engineering
Indian Institute of Technology, Powai, Bombay - 400 076, India.

Abstract: To study the quantification of soil moisture through microwave remote sensing techniques, a test site has been selected in Pune College Agricultural Farm Land, Pune, India. The representative soil moisture and temperature vertical profiles are derived by analysing the field data. A study has been made on dielectric and brightness temperature models with a view to select the appropriate one. Newton's equivalent soil moisture (EQSM) has been modified by incorporating soil moisture slope parameter to improve its accuracy. The soil textural dependence of Microwave emission and penetration depths of Microwaves into moist soil medium has been studied. Finally a methodology has been developed for the selection of multifrequencies to extract soil moisture and temperature vertical profile parameters. Computer software package has been developed to implement the above models. Thus this paper presents a consolidated work on modelling aspects of Passive Microwave Remote Sensing.

1.0 INTRODUCTION

Microwave Remote Sensing of soil moisture is becoming one of the major activities of research in view of its wider applications (Rao et al. 1986a). During the last one decade, considerable effort is made to draw general conclusions for the

quantification of soil moisture based on laboratory and field experiments. Extension of the applicability of these conclusions for the analysis of Airborne/satellite data is being realised. Simultaneously, efforts are being made to develop theoretical models to derive the conclusions drawn on the basis of experimental data analysis. The recent research trend is to develop multifrequency models and to optimize system parameters to maximize the efficiency of data analysis and interpretation.

Through this paper, an attempt is made to review the present state of development of passive microwave remote sensing of soil moisture and develop models relevent to a particular test site. For this purpose, a test site in Agrimet Observatory, located in agricultural college farm land, Pune, India, is selected.

As a first step, the soil samples are collected and are analysed in terms of its physical and chemical properties. One year data on soil moisture and physical temperature vertical profiles have been studied with a view to simulate soil moisture and temperature vertical profiles. These profiles and the soil properties are the major inputs for the development of models. These results are presented in section 2.

Subsequently, a detailed study has been made on the available models for the estimation of dielectric constant with a view to select the suitable model applicable to the test site. From these studies, it has been found that the semiempirical model developed by Dobson et al. (1985) is more general and

applicable to wider range of soil texture and frequency. The details of these studies are discussed in section 3.

Next aspect needs attention is the estimation of brightness temperature(TB) under varying vertical properties of soil moisture and physical temperature. Basically, there are two categories of models namely coherent (Tsang et al. 1975 and Wilheit 1978) and noncoherent (Burke et al.1979). From a detailed study of these models and comparison with the experimental results, it has been found, in general, that the coherent models are more accurate than noncoherent model. The details of these studies are summarized in section 4.

Under natural conditions, the soil moitsure varies with depth. As microwaves penetrate deep into the soil medium and gives rise to an integrated effect of the soil moisture profile, it is necessary to know the equivalent soil moisture which can be used to replace the varying soil moisture profile. Newton's (1977) equivalent soil moisture (EQSM) is supposed to serve this purpose. A detailed study on the validity of EQSM reveals its limitations and therefore a modified EQSM (MEQSM) has been suggested whose details are given in section 5.

A study has been made to understand the relation between soil moisture and brightness temperature. A comparison is also made with the experimental observations. It has been noticed that the TB is linearly dependent on soil moisture at higher frequencies whereas low (TB) is linearly dependent on soil moisture at lower frequencies. The outcome of this study gave the

means to identify the frequency region suitable for the study of soil moisture. The details of this work is given in section 6.

The penetration depth of microwaves is studied as a function of soil moisture, frequency, soil texture and physical temperature. The calculated penetration depths are, in general, in agreement with the experimental investigations. The penetration depth varies from 0 to 10 cm. The details of this study is presented in section 7.

It has been observed by Schmugge (1980) and Ulaby et al. (1979) that the microwave emission dependence on soil texture can be minimized by expressing soil moisture in terms of percentage of field capacity units. An examination of this aspect has been done in this paper by deriving the statistical relations for water holding capacities of soils and using these relations to express soil moisture in terms of percentage of field capacity. This study, as can be seen from section 8, reveals that the expressing the soil moisture in terms of $(m_v - W_t)$ minimizes the emissivity dependence on soil texture. Here W_t is the transmission moisture as defined by Wang and Schmugge (1980).

Finally a methodology has been developed for the selection of multifrequencies whose combination will give rise to the estimation of soil moisture and temperature profile parameters. It has been observed that the set of four frequencies 1.0, 3.0, 6.0 and 30 GHz coupled with one more measurement at thermal band will lead to the estimation of soil moisture and soil temperature profile parameters. These aspects are explained in section 9.

A software package has been developed around in house 16/32 bit microcomputer to implement all the models described above. The package has been used extensively for the last two years. Thus this paper presents a consolidated work on passive microwave remote sensing of soil moisture.

2.0 REPRESENTATIVE PROFILES OF SOIL MOISTURE AND TEMPERATURE OF BLACK SOILS OF PUNE

2.1 The Test Site

To study the above aspects mentioned in introduction, Pune Agricultural farm land has been chosen as a test site. The soil moisture and temperature data have been collected from the Agrimet Observatory located in the above farm land. Two sets of three soil samples at two different places and at three different depths are analysed in terms of physical and chemical properties. The average of analysed results are given in Table 2.1. According to the analysis, the soil of the test site comes under clay with greyish black colour. The annual rainfall in this area ranges from 700 to 1730 mm. The temperature varies from 6.5° C minimum to 48.9° C maximum. The drainage is slow to medium and internal drainage is poor. The crops grown in this land are pulses, cereals, cotton, sugarcane, paddy, jowar, bajra and vegetables rotationally.

2.2 Data Collection and Selection

The Agrimet Department collects the vertical profiles of soil moisture and physical temperature data regularly. The test site is specially prepared for this purpose. The vertical

profile of soil moisture is collected once in a week (every Thursday before sun rise). The gravimetric technique is used for the determination of soil moisture. The soil samples are taken at surface and at depths of 7.5, 15.0, 22.5, 30.0 and 45.0 cm. The data on temperature are collected three times every day (0730 hrs., 1430 hrs and 1730 hrs) at surface and at depths 5.0, 10.0, 15.0, 20.0 and 30.0 cm using soil thermometers. The data used in this analysis belong to the time period of January-December 1985 and consists of 52 soil moisture profiles and 1100 temperature profiles.

An observation of temperature profiles indicates that the data is consistent. It has also been noticed that the variations in temperature from day to day are not appreciable. Therefore, it was decided to consider only one set of temperature profiles in each month (around the middle of every month has been chosen). Each set of temperature profiles consists of three profiles at 0730 hrs., 1430 hrs. and 1730 hrs., respectively. All soil moisture and temperature profiles considered are given in Rao et al. (1986b).

2.3 Models to represent the soil moisture and temperature profile data

From a careful observation of the soil moisture profiles shown in Fig. 2.1, it is clear that the profiles, in general, follow a multiparameter exponential trend with a finite value at the surface. This can be mathematically represented as follows (Hildebrand, 1956).

$$\rho(z) = \rho_0 + \sum_{i=1}^{n} \Delta\rho_i \exp[\beta_i z] \qquad (2.1)$$

where ρ_0 is the constant soil moisture, $\Delta\rho_i$ is the fractional change in the soil moisture, β_i is the coefficient of variation (similar to infiltration coefficient) and n is the number of exponential terms.

The higher the value of n, the greater the number of exponential terms and so better fitting. However, to evaluate the coefficients of this expression, there should be a large number of remote sensing observations at different frequencies which is difficult to realize. Therefore, the smaller the number of parameters, better the feasibility. Considering two exponential terms only, equation (2.1) can be written as :

$$\rho(z) = \rho_s + \Delta\rho_1(1 - \exp(\beta_1 z)) + \Delta\rho_2(1 - \exp(\beta_2 z)) \qquad (2.2)$$

where ρ_s is surface soil moisture, $\Delta\rho_1$ and $\Delta\rho_2$ are constants indicating the variations in the soil moisture. A few soil moisture profiles follow the trend of the above equation. However, most of the soil moisture profiles (Fig. 2.1) show a regular trend in which case Eq. (2.2) can be further simplified to

$$\rho(z) = \rho_s + \Delta\rho(1 - \exp(\beta z)) \qquad (2.3)$$

In this expression, $\Delta\rho$ has no physical significance except that it represents the total change in the soil moisture at infinite depth. None of the soil moisture profiles can be extended to infinite depth. Therefore, Njoku and Kong (1977) have normalized the expression upto a depth d and it is given as:

$$\rho(z) = \rho_s + \Delta\rho' \frac{(1 - \exp(\beta z))}{(1 - \exp(-\beta d))} \qquad (2.4)$$

where $\Delta\rho$ is the increment of the soil moisture at a depth d below the surface.

From the study of temperature profiles at 0730 hrs., 1430 hrs., and 1730 hrs., it has been observed that temperature profiles data acquired at 0730 hrs. (Fig. 2.2a) and 1430 hrs., can be conveniently fitted to the following expression :

$$T(z) = T_0 + \Delta T \exp(\gamma z) \qquad (2.5)$$

It has been observed from Fig. (2.3) that though there are variations in temperature at surface and subsurface for 0730 hrs., 1430 hrs., and 1730 hrs., all the profiles appear to converge to a constant temperature below 20 cm depth. Therefore, it is convenient to represent T_0 as a constant temperature at deeper depths.

The data acquired at 1730 hrs., can be fitted to the following expression because their trend is increasing and decreasing with depth.

$$T(z) = T_0 + \Delta T_1 \exp(\gamma_1 z) + \Delta T_2 \exp(\gamma_2 z) \qquad (2.6)$$

The terms T_0, ΔT_1, ΔT_2, γ_1 and γ_2 have similar meanings as in Eq. (2.2).

Using least square principle and bisection method, the best parameters of Eqs. (2.4) and (2.5) will be estimated by

fitting the soil moisture and temperature data.

For the calculation of parameters in the two exponential term equations (2.2) and (2.6), Prony's method (Hildebrans 1956) has been used.

2.4 Data analysis, results and discussions

A careful observation of individual soil moisture profiles indicates that the variation of soil moisture with depth does not follow any definite trend. However, an observation of a group of profiles definitely indicates a systematic trend in the soil moisture profile. Based on this concept, soil moisture profiles are grouped and then fitted in a combined way to get a single profile. The fitted profiles with dashed lines are shown in Fig. 2.1 as an example. In few cases, some profiles are fitted individually due to their convenience in fitting to a model.

Unlike the soil moisture profiles each temperature profile shows very clear and systematic trend as shown in Fig. 2.2a. These curves can be conveniently fitted to the one exponential function (Eq. 2.5) and the fitted curves are shown in Fig. 2.2b. Similarly, the temperature profiles at 1430 hrs also fitted to the same equation because their trend follows one exponential function. The temperature profiles at 1730 hrs., however, show increasing and decreasing trends. Therefore, these profiles can be fitted only with a two exponential term function.

2.5 Recommended Soil Moisture and Temperature Profiles

The criteria for selecting representative profiles are that these profiles should represent all possible conditions including extreme conditions of soil moisture and temperature variations. Thus, one profile is chosen corresponding to the lowest soil moisture conditions (June). The second profile is chosen corresponding to the highest soil moisture conditions (August, September). The third and fourth profiles represent the intermediate soil moisture conditions. The fifth soil moisture is selected to account for the abnormal situations. The selected representative moisture profiles are shown in Fig. 2.4 and the parameters corresponding to these profiles are given in Table 2.2(a).

In the case of temperature, two profiles are chosen to indicate the lowest and highest possible temperature profile at 0730 hrs., two profiles are chosen to indicate highest and lowest possible temperature profile at 1430 hrs. and one profile has been chosen to indicate temperature variation at 1730 hrs. All the five representative profiles are shown in Fig. 2.5 and the parameters of these profiles are shown in Table 2.2(b).

These representative profiles are useful for the calculation of TB and thereby the development of multifrequency model.

3.0 DIELECTRIC CONSTANT MODELS AND DIELECTRIC PROFILES

The dielectric constant ( ) is the electrical property of the materials in the microwave region. The dielectric

constant of dry soil is of the order of 3 to 5 in the microwave region, whereas, for water it is around 80. Different percentage combinations of water with soil give rise to a variation from 3 to 20. This range of ϵ variation is responsible for about 100°K change in brightness temperature (TB). In view of this, in this paper, an attempt is made to study and compare the existing models for the computation of ϵ with a view to examine the appropriate model. Subsequently, the frequency and soil texture dependence on ϵ have been investigated using the examined model. Finally, the model has been implemented for calculation of representative dielectric constant profiles of clay soils of Pune agricultural farm land.

3.1 Theoretical models for dielectric constant

Several authors have conducted dielectric constant (ϵ) measurements of soil as a function of soil moisture, texture, bulk density, temperature and frequency and observed that ϵ is dependent on the above parameters (Hallikainen et al. 1985). Their observations also confirmed that the behaviour of ϵ is different for bound water and for free water contents of soil medium. The experimental observations have shown that the dielectric constant of soil-water medium is an integrated effect of the dielectric properties of soil solid, free water, bound water and air constituents in proportion of their volume fractions. In the past few years, several attempts have been made to develop the dielectric constant models of soil-water systems. The majority of these models examined by Wang and Schmugge (1980) are a function

of two constituents such as soil solid and water. These models are inadequate to describe the dielectric constant properties at complete soil moisture, soil texture and frequency range.

Wang and Schmugge (1980) have given an empirical model which accounts for moist soil constituents such as bound water, free water, air and soil solids. Recently, Dobson et al (1985) and Hallikainen et al. (1985) have proposed three dielectric constant models such as empirical, physical and semiempirical. The first one is only applicable to a particular value of frequency. It is nothing but a polynomial fitting of measured dielectric constant data as a function of soil moisture and soil texture. The second one (physical model) requires an effective soil surface area data which is not readily available whereas the third one (semiempirical model) requires a readily available data and accounts for all moist soil constituents.

It can be seen that the empirical model and semiempirical model proposed by Wang and Schmugge(1980) and Dobson et al. respectively are required a readily available data and both of the models account for the experimental observations. Therefore, an attempt is made to compare these two models in this section.

Wang and Schmugge Model : The expressions for the dielectric constant of moist soil are given by :

$$\epsilon_m = W_c \epsilon_x + (P - W_c)\,\epsilon_a + (1 - P)\,\epsilon_r \quad \text{for } W_c \le W_t$$

with $$\epsilon_x = \epsilon_i + (\epsilon_w - \epsilon_i)\,\frac{W_c}{W_t}\,\gamma$$

and $$\epsilon_m = W_t \epsilon_x + (W_c - W_t)\,\epsilon_w + (P - W_c)\,\epsilon_a \quad \text{for } W_c > W_t$$

with $\epsilon_x = \epsilon_i + (\epsilon_w - \epsilon_i)\gamma$

Where W_c is the water content (in volumetric) and P ($= 1 - \rho_b/\rho_s$) where ρ_b, ρ_s are bulk density, specific density of dry soil) is porosity. ϵ_a, ϵ_w, ϵ_r, ϵ_i are the dielectric constants of air, water, associated soil rock, ice respectively. ϵ_x stands for the dielectric constants of initially absorbed water. WP, W_t and γ are the wilting point, transition moisture and free adjustable parameters.

Dobson et al model : The expression for the calculation of dielectric constant is as follows :

$$\epsilon_m^\alpha = 1 + \rho_b/\rho_s\,(\epsilon_s^\alpha - 1) + m_v^\beta\,\epsilon_{fw}^\alpha - m_v$$

where coefficient α ($=0.65$) is the shape factor and β depends on the textural composition of the soil. The β can be computed by :

$$\beta = \left(1 \beta_{\epsilon'}^2 + \beta_{\epsilon''}^2 1\right)^{1/2}$$

$$\beta_{\epsilon'} = (127.48 - 0.519\ (\%\text{sand}) - 0.152\ (\%\text{clay}))/100$$

$$\beta_{\epsilon''} = (1.33797 - 0.603\ (\%\text{sand}) - 0.166\ (\%\text{clay})/100$$

ϵ_s & ϵ_{fw} represent the dielectric constant of dry soil and free water which can be calculated by the following equations.

$$\epsilon_s = (1.01 + 0.44\ \rho_s)^2 - 0.062$$

$$\epsilon_{fw} = \epsilon_{w\infty} + \frac{\epsilon_{w0} - \epsilon_{w\infty}}{1 + j2\pi f \tau_w} - j\,\frac{\sigma_{eff}}{2\pi f \epsilon_0}\,\frac{\rho_s - \rho_b}{\rho_s}$$

where ϵ_0 ($= 8.854 \times 10^{-12}$ F/m) is the permittivity of free space and f is frequency. σ_{eff} (mho/m) is the effective conductivity of

water which is given by:

$$\sigma_{eff} = -1.645 + 1.939\,\rho_b - 0.02013\ (\%\text{sand}) + 0.01594\ (\%\text{clay})$$

τ_w is the relaxation time of water, ϵ_{w0} and $\epsilon_{w\infty}$ ($= 4.9$) are the static ($2\pi f \tau_w \ll 1$) and high frequency ($2\pi f \tau_w \gg 1$) dielectric constants of water respectively. The expressions for the calculation of τ_w and ϵ_{w_c} are given as follows (Stogryn, 1971).

$$\epsilon_{wc} = \epsilon_{w_c}(T,N) = \epsilon_{w_c}(T,0)\ a\ (N)$$

$$\tau_w = \tau_w(T,N) = \tau_w(T,0)\ b\ (N,T)$$

$$N = S[1.707 \times 10^{-2} + 1.205 \times 10^{-5}\ S + 4.058 \times 10^{-9}\ S^2]$$

$$a(N) = 1.000 - 0.2551\ N + 5.151 \times 10^{-2}\ N^2 - 6.899 \times 10^{-3}\ N^3$$

$$b(N,T) = 0.1463 \times 10^{-2}\ NT + 1.000 - 0.04896\ N - 0.02967\ N^2 + 5.644 \times 10^{-3}\ N^3$$

$$\epsilon_w(T,0) = 87.74 - 0.400087\ T + 9.398 \times 10^{-4}\ T^2 + 1.410 \times 10^{-6}\ T^3$$

$$\tau_{w0}(T,0) = (1.1109 \times 10^{-10} - 3.824 \times 10^{-12}\ T + 6.938 \times 10^{-14}\ T^2 - 5.096 \times 10^{-16}\ T^3)/2\pi$$

where T is the water temperature in degree centigrade. N is the normality of the solution and S is the salinity.

3.2 Comparison of Models

To compare the models discussed above, the common ranges of validity has been chosen in terms of frequency as well as soil texture. Thus a detailed comparison is made by calculating the ϵ values at three frequencies 1.4, 4.0 and 18.0 GHz and by choosing three soil types namely, sandy loam, silt loam and clay.

At 1.4 GHz the real part of dielectric constant (ϵ') for silt loam and sandy loam soils match well for both the models whereas, for clay soil there is large difference between two models. Regarding the imaginary part of the dielectric constant(ϵ'') as the clay content increases the difference between the models increases. The trends of the dependence of ϵ on m_v is same for both the models (Figure 3.1a - 3.1c). Similar observations have been observed at 4.0 and 18.0 GHz. At 4.0 GHz, they match reasonably well all through the soil moisture range for silt loam and sandy loam whereas for clay the difference increases as the soil moisture increases. The ϵ'' for all three textures reasonably match for both the models. At 18.0 GHz, there is a fairly good agreement between the two models for sandy loam and silt loam soils whereas for clay soil, the difference in ϵ' of both the models increases as the soil moisture increases. In general Wang and Schmugge model predict lower values compared to that of Dobson et al. model. The frequency dependence of ϵ for both the models at 0.3 m for sandy loam, silt loam and clay loam soils shows that the for Wang &Schmugge and Dobson et al. models predict more or less same results for silt loam and sandy loam soils whereas for clay soil, the difference between the models is considerably high all through the frequency range (Fig. 3.2(a) to 3.2(c))

Thus it can be concluded that both the models predict more or less same values above 3 GHz except for high clay content soils. Below 3.0 GHz the trends of ϵ are in the reverse direction. However, the trends shown by Dobson et al. agrees with experimental data (Hallikainen et al 1985) and also low

frequency model proposed by Wang (1980). Thus Dobson et al model is more general, applicable in wide frequency range, considers large amount of experimental data and has no adjustable free parameters. In view of the above, the Dobson et al. model has been used to generate the representative dielectric profiles of clay soils of Pune through representative profiles of soil moisture and temperature (Fig. 2.4 and 2.5). The dielectric profiles are shown in Fig. 3.3 ~~and 3.4~~.

4.0 COMPARISON OF MODELS FOR BRIGHTNESS TEMPERATURE CALCULATIONS

During the recent years considerable amount of work has been carried out on passive microwave remote sensing of the soil moisture both theoretically and experimentally (theoretical: Tsang 1975, Njoku and Kong 1977, Wilheit 1978, Burke et al. 1979; experimental: Newton 1977, Newton et al. 1982, Wang et al. 1982, Schmugge et al. 1983). Schmugge and Choudhury (1981) made an attempt to compare all the models for the calculation of brightnes temperature (TB). But in their calculation they used only the interpolated dielectric data and dielectric constant dependence on temperature was not considered. In view of this it is felt necessary to make a detailed comparitive study on different TB models by making use of the latest dielectric constant models and also soil moisture & temperature representative profiles of Pune test site (Rao, et. al. 1986b).

4.1 Different TB models and their comparison

It is well known that for a homogeneous media, emissivity can be calculated by using the Fresnel reflection equations

(Jackson 1962). However, in natural conditions the soil moisture and temperature vary with depth and hence dielectric profile also vary. In this case, Radiative transfer models developed by Tsang et al. (1975), Wilheit (1978) and Burke et al. (1979) take into account the varying properties of the soils with depth. These models have been developed based on the stratification of a medium (Fig. 4.1) into number of layers having constant dielectric property for each layer and may vary from one layer to another. The microwave radiation is generated in the soil medium due to its temperature. The amount of energy thus generated at any layer is dependent upon the dielectric property (soil moisture) and temperature. As energy propagates upward through the soil volume from its point of origin, it gets reflected and transmitted at the interface of the layers as a function of the difference in dielectric properties of the layers along the path of propagation. In addition as the energy crosses the air-soil interface, it is further reduced by the effective transmission coefficient of that interface.

There are two approaches (coherent and noncoherent) for the calculation of the microwave emission from inhomogeneous medium. The radiative transfer models developed by Tsang et al. (1975) and Wilheit 1978) are the coherent models. Tsang et al. model is based on the radiative transfer formulation of Stogryn (1970) for thermally and dielectrically nonhomogeneous medium. By following an approach parallel to that of Stogryn but using reciprocal properties of dydic Green's function in the solutions of the boundary value problem, the brightness temperature of a

stratified medium is solved and is given below:

$$T_{B_h}(\theta) = \frac{K}{\cos\theta}\sum_{\ell=1}^{N}\frac{\epsilon_\ell T_\ell}{\epsilon_0}\left[\frac{|A_\ell \exp(-iK_{\ell z}d_\ell)|^2}{2K''_{\ell z}}\left\{1-\exp\left[2K_{\ell z}(d_{\ell-1}-d_\ell)\right]\right\}\right.$$

$$-\frac{|B_\ell \exp(iK_{\ell z}d_\ell)|^2}{2K''_{\ell z}}\left\{1-\exp\left[-2K''_{\ell z}(d_{\ell-1}-d_\ell)\right]\right\}$$

$$-\frac{[A_\ell \exp(-iK_{\ell z}d_\ell)]\,[B_\ell \exp(iK_{\ell z}d_\ell)]^*}{2iK'_{\ell z}}\left\{1-\exp\left[-i2K'_{\ell z}(d_{\ell-1}-d_\ell)\right]\right\}$$

$$\left.+\frac{[A_\ell \exp(-iK_{\ell z}d_\ell)]^*\,[B_\ell \exp(iK_{\ell z}d_\ell)]}{2iK'_{\ell z}}\left\{1-\exp\left[i2K'_{\ell z}(d_{\ell-1}-d_\ell)\right]\right\}\right)$$

$$+\frac{K}{\cos\theta}\frac{\epsilon_L T_L}{\epsilon_0}\frac{|T_h|^2\exp(-2K'_{Lz}d_\ell)}{2K''_{Lz}}$$

The subscript ℓ and h refers to the quantities in the i th layer of the medium and horizontal polarization respectively. d is the depth below the surface of the interface between the ℓ and $\ell+1$ layers. The A_ℓ, B_ℓ, and T_h are wave amplitudes and are related to one another by propagation matrices (Kong 1975). K and $K_{\ell z}$ are wave vectors in the air and th soil layer respectively.

In Wilheit model also soil is treated as layered medium. Solutions of Maxwell's equations and boundary conditions at interfaces are used to calculate the electric field in each layer. These electric field values are used to calculate the energy fluxes and thus obtain fractional absorption (f_i) in each layer. If T_i is the temperature of the i th layer, the layer radiates energy equal to the product of the fractional absorption (f_i) and temperature (T_i). Similarly the radiant energy or TB can be calculated for all layers. The microwave emission model developed by Burke et al. (1979) is based on the

assumption of incoherent radiation. The radiation intensity is calculated from the solution of radiative transfer equation. The radiative tranfer equation for each layer is solved. The tranfer of energy between layers is determined by reflectivity from Fresnel equation. The sum of intensitities from N layers gives the total brimhtness temperature

To study the difference in coherent and noncoherent models in detail, theoretical calculations for TB have been made using the representative soil moisture profiles with a temperature profile (see Fig. 2.4 and 2.5) of black soils of Pune. The calculated TB dependence on frequency for different soil moisture and temperature profile combinations have been shown in Fig. 4.2. There is a good agreement among the models for all conditions. However, at lower frequencies (below 5.0 GHz) coherent and incoherent model predictions are significantly different particularly for soil moisture profiles with high gradient. As far as the simplicity, computation time and coincidence of TB with that of experimental values are concerned, Wilheit model is the best one.

4.3 Comparison with Experimental Results

A comparison has been made between the TB calculated using Wilheit model and the value obtained experimentally by Schmugge et al 1974 at 19.35 GHz (Aircraft Experiment). There is a great difference between theoretical and experimental results. This difference may be attributed to surface roughness, atmospheric conditions and errors in the consideration of the

sampling depth. In addition to this, the comperison has also been made with the experimental results obtained by Newton et al (1977) at 1.4 GHz for nadir look angle. The calculated and experimental normalized TB values with EQSM have been shown in Fig. 4.3. It can be seen from the above figure that normalized TB is higher for the experimental results than that of theoretical predictions which has been attributed to errors in taking sampling depth for the soil moisture estimation. Therefore, there is a need to carry out systematic experiments with proper simultneous ground truth to study the dependence of sampling depth as a function of soil moisture and frequency.

5.0 PARAMETERIZATION OF SOIL MOISTURE

5.1 Need for a parameter to represent soil moisture

In natural situation, the soil moisture is not uniform with depth. In those cases, a problem arises in interpreting soil moisture information with the estimates from microwave data because the microwave energy is coming from soil volume and not from a single layer. Therefore, it is necessary to identify a parameter which will be equivalent to the soil moisture profile. This parameter will serve as a reference soil moisture in interpreting the microwave data.

5.2 Definition of different soil moisture parameters

Several attempts are made to determine such a parameter. They are broadly as follows :

(a) Equivalent skin depth moisture content [Lee, 1974]

In this approach, electromagnetic attenuation profile of the soil is calculated based on the permittivity profile. Then the profile is integrated to determine the skin depth. Finally the equivalent skin depth moisture content is calculated that would produce same skin depth.

(b) Attenuated soil moisture in a skin depth

This parameter is calculated by performing a weighted average of soil moisture upto the skin depth. The weighting function is the attenuation constant of the soil from i th layer to the surface as given below :

$$m_A = \frac{\sum_{i=1}^{N} SM(i) \exp\left(-\sum_{j=1}^{i} \alpha(j)\right)}{\text{Skin depth}} \qquad (5.1)$$

where m_A - attenuated soil moisture in a skin depth

$\alpha(j)$ - attenuated constant at each layer

SM(j) - soil moisture in each layer

(c) Equivalent Soil Moisture (EQSM)

Newton [1977] identified a parameter which is known as equivalent soil moisture (EQSM). This is defined as a weighted integral of the soil moisture times the thermal microwave emission profile. The parameter can be expressed in the following manner :

$$EQSM = \frac{\sum_{i=1}^{N} SM(i)\, TB(i)}{TB\ total} \qquad (5.2)$$

where SM(i) - soil moisture content for the i th layer

TB (i) - brightness contribution from i th layer

TB total - total brightness temperature contributions at the surface

N - number of layers

It may be noted that the approaches (a) and (b) have no direct effect on the soil temperature. Whereas, the emission process is a function of physical temperature of the soil. Therefore, it is appropriate to consider the soil temperature into account while defining the parameter. This has been taken into account in the definition of Newton EQSM.

5.3 Validity of Newton's EQSM

According to the definition of Newton EQSM, it is expected that soil medium should produce the same brightness temperature for all possible distributions of soil moisture in the soil medium provided the EQSM is constant. The EQSM is maintained at a constant value using linear shifting approach (Rao et al, 1987a) for different soil moisture profiles. These profiles are shown in Fig. 5.1.

Frequency dependence of EQSM

Figures 5.2 to 5.5 represent the TB calculation as a function of profile shape parameter (β). The data has been presented for frequencies 1.4, 5.0, 19.35 and 30.0 GHz respectively. It can be seen from the figures 5.2 to 5.5 that

the TB varies with β values. Thus for constant EQSM the relative differences varies from 10^{0}K (at 1.4 GHz and 6.4% soil moisture by weight) to 1^{0}K (at 30.0 GHz and 20% soil moisture. The brightness temperature is also calculated using Fresnel's equation for constant moisture profiles whose value is equivalent to EQSM (using 300^{0} K physical temperature). These values are plotted in the same figures. A difference between TB values calculated using profiles and that of Fresnel equation predictions using EQSM soil moisture is referred as absolute difference. It can be seen from the figures 5.2 to 5.5 that the absolute differences are considerably higher than relative differences. These differences decreases as the frequency increases.

Soil moisture dependence of EQSM

It can be seen from the figures 5.2 to 5.5 that the relative as well as absolute differences decreases as the soil moisture increases. This confirms that estimation of EQSM using Newton's approach is not adequately representing the soil moisture distribution in the soil medium.

Temperature dependence of EQSM

Sample calculations have been performed at 1.4 GHz and at 17.0% soil moisture by weight to study the temperature dependence of EQSM. Two types of temperature profiles are considered namely constant temperature profiles (at 280.0, 300.0, 320.0 and 340^{0} K) and varying profiles applicable to black soils of Pune as discussed in section 2. It has been observed that EQSM is fairly constant showing the least dependence on temperature.

5.7 Modified EQSM

As per the analysis presented above, it is clearly brought out that for constant EQSM the soil medium gives rise to different TB values for different distribution of soil moisture in the soil medium. This proves that EQSM has not taken into account precisely the distribution of soil moisture in the soil medium.

In view of the above discrepancy an attempt is made to modify the EQSM formula by incorporating either the dielectric constant slope with depth or soil moisture slope with depth. The modified EQSM is given as follows :

$$MEQSM = \frac{\sum_{i=1}^{N} SM(i)\ TB_i\ S_i}{\sum_{i=1}^{N} TB_i\ S_i}$$

where S_i is slope of moisture profile or dielectric constant profile.

5.8 Study on the validity of MEQSM

Calculations were made to estimate MEQSM from 1.0 to 30.0 GHz frequency range for all profiles shown in Fig. 5.1. The results are shown in Figs. 5.2 to 5.5 for comparison with EQSM predictions and also with Fresnel equation predictions. It can be seen from Figs. 5.2 to 5.5 that the MEQSM are far superior to those of EQSM. A comparison of TB predicted by coherent model and TB predicted by Fresnel equation using MEQSM indicates that the MEQSM is slightly under estimated leading to an error of 3%

12

at 1.4 GHz and less than 1% at 30.0 GHz. One of the limitations of MEQSM is that the model fails for uniform soil moisture profile because of zero slope. However, this limitation is not a major problem because the MEQSM can be made equal to uniform soil moisture itself.

6.0 BRIGHTNESS TEMPERATURE DEPENDENCE ON SOIL MOISTURE AND FREQUENCY

In view of the advantages/merits of microwave remote sensing for soil moisture, Newton's et al (1980), Wang et al (1982), Wang et al (1983) and Vyas et al (1985) have conducted a series of field experiments to study the relation between soil moisture and TB. From their experimental data analysis, they observed a linear relation between soil moisture ~~soil moisture~~ and TB in the frequency range 1.4 and 19.35 GHz. Schmugge et al. (1974) and Schmugge (1980) analysed the airborne TB data at 1.4, 19.35 and 37.0 GHz. They also observed a linear relation between TB and soil moisture at 1.4 and 19.35 GHz. Analysing the data from the sensors on board skylab, Eagleman and Lin (1976) observed that there is a non-linear relationship at 1.4 GHz. Thus it appears that there is a discrepancy between Eagleman and Lin and other investigators cited above, regarding the relation between brightness temperature and soil moisture.

In view of these differences in opinion, it is felt necessary to resolve the discrepancy observed through experimental data analysis by deriving the relation between TB and soil moisture theoretically using the recently developed model of Dobson et al. (1985) for dielectric constant and Tsang et al. (1975) model for the calculation of TB (Rao et al. 1987).

From the theoretical models of Dobson et al. (1985) and Tsang et al. (1975) it can be seen that there is a need to know the vertical profiles of soil moisture and temperature and other soil properties. For this purpose, the soil moisture and soil temperature profiles given in Fig. 2.4 and 2.5 have been used.

6.1 Relation between TB and soil moisture

Using semiempirical model of Dobson et al. (1985) for the calculation of dielectric constant and Tsang et al. (1975) model for the calculation of brightness temperature, a study has been made on the relation between brightness temperature and EQSM at frequencies ranging from 0.1 to 30.0 GHz. It can be seen from Fig. 6.1 that the relation between TB and EQSM is reasonably linear at higher frequencies (above 20 GHz) and it becomes non-linear as frequency decreases. The linearity observed over 20.0 GHz is in confirmation with those of Schmugge et al. (1974, 1980) and Vyas et al. (1985). However, below 19.0 GHz Newton et al. (1980), Wang et al. (1982), Wang et al. (1983) and Schmugge et al. (1974) have found linear relation whereas Eagleman and Lin (1976) found nonlinearity. Thus the present theoretical results support the predictions of Eagleman and Lin (1976) below 20 GHz. When the same data has been plotted (Fig. 6.2) in semi-logarithmic scale, it is seen that the log (TB) is linearly related to EQSM above 1 GHz. The non-linearity starts appearing below 1.0 GHz. So it is concluded that the log TB is linearly related to soil moisture in the frequency range above 1.0 GHz.

Relation between TB and Frequency

To study the relation between brightness temperature and microwave frequency Fig. 6.3 has been plotted with frequency against TB as a function of ERSM at 2%, 10%, 20% and 30% by weight. The fisure clearly demonstrates that as frequency increases the TB increases.

7.0 PENETRATION DEPTH OF MICROWAVES

One of the greatest advantages of microwave remote sensing is the ability of microwaves to penetrate deep into the soil medium, thereby giving rise to the means for the quantitative estimation of soil moisture. So far, no attempt has been made to study the dependence of microwave penetration into the moist soils and the influence of parameters such as soil moisture, soil texture, soil temperature and microwave frequency on the penetration depth. These type of studies are useful for planning ground truth collection campaigns and also to know upto what depth the ground truth data has to be collected.

As explained earlier, the brightness temperature recorded by radiometers originates from different layers of the soil medium. Using the theoretical models (will be discussed later), calculations are made to find out the cumulative percentage contribution to the total brightness temperature as a function of depth of soil medium. The following observations have been made at 1.4 and 5.0 GHz for clay soils of Pune.

-- This cumulative contribution increases exponentially with depth showing a saturation effect.

-- The rate of increase is a function of soil moisture: higher the soil moisture, higher the rate of increase.

-- The percentage contribution is nonlinearly dependent on frequency and soil moisture.

As the percentage contribution exponentially depends on the depth of soil medium, to distinguish the microwave ability to penetrate into soils of different moisture contents and at different frequencies, it is necessary to define the parameter known as penetration depth by introducing a cutoff value for the percentage contribution.

Thus, the penetration depth is defined as the depth from the soil surface upto which the integrated contribution is (1 - 1/e) times the total contribution. It will turn out to be 63% of the total contribution.

In the following section, a detailed study on the dependence of penetration depth as a function of microwave frequency, soil moisture, temperature and texture have been made.

7.1 Theoretical Models

The percentage contribution (PC) can be defined as follows :

$$PC = \frac{\sum_{(i)}^{N} TB\ (i)}{TB\ total} \times 100$$

where TB(i) is the contribution of brightness temperature of the i th layer of thickness d, TB total is the total brightness temperature and N refers to the total number of layers at which

the integrated percentage contribution to the brightness temperature will be 63% from which Pd can be calculated as

$$Pd = N \times d$$

7.2 Pd dependence on soil moisture and frequency

Using the above model the depth of penetration is calculated in the frequency range 1.0 to 30.0 GHz, soil moisture range 2.0 to 30.0 (by weight percentage), temperature range 280 to 320 K and for soil textures clay, silt loam and sandy loam.

Fig. 7.1 shows the dependence of penetration depth (Pd) on equivalent soil moisture (EQSM) at different frequencies (1.0, 3.5, 5.0, 7.5, 10.0 and 30.0 GHz). The representative soil moisture profiles of clay soils of Pune have been used for the Pd calculations. For convenience of plotting each soil moisture profile is represented by its EQSM as defined earlier. As per the definition of EQSM, any soil moisture profile can be represented by a parameter which will produce same the TB as that of original profile. It can be seen from the above figure that the Pd decreases as the soil moisture increases at all frequencies. Similarly, it can be seen from Fig. 7.2 that the Pd decreases almost exponentially as the frequency increases. The highest Pd is of the order of 5 cm for 1.0 GHz and 2.0 %soil moisture by weight for clay soil.

7.3 Pd dependence on temperature

To study the temperature dependence on TB, a case study has been made for clay soils at soil moisture content of 15% by weight. The calculations have been made as a function of

frequency for uniform temperature profiles at 280, 300 and 320 K. The Fig. 7.3 shows that there is an influence of temperature on Pd. The difference is maximum around 6.0 GHz and decreases on either side. Similar trends have been observed for complete soil moisture range also.

7.4 Pd dependence on soil texture

To study the textural dependence of Pd, in addition to clay soil, the calculations are made for silt loam and sandy loam soils. It has been observed that the Pd dependence on frequency shows similar trends for all soil textures and complete soil moisture range. However, their numerical values are different. To study the Pd dependences on texture with frequency and soil moisture, different textural data have been plotted in Figs. 7.4 and 7.5. It can be seen from Fig. 7.4 that at 15% soil moisture by weight, there is no significent texture dependence above 10.0 GHz. The textural dependence increases at lower frequencies. With regard to the soil moisture, the Pd is different for different textures althrough the soil moisture range. However, the difference decreases as the soil moisture increases.

From the above studies, it has been observed that Pd depends on soil moisture, soil temperature, texture and microwave frequency.

8.0 INFLUENCE OF SOIL TEXTURE ON BRIGHTNESS TEMPERATURE

It is of great concern, in the context of microwave remote sensing of soil moisture, regarding the units in which the soil moisture has to be expressed. This problem arises due to the

different degrees of sensitivity of normalized brightness temperature to different soil textures. Thus the estimation of soil moisture through microwave remote sensing becomes a function of soil texture. Several attempts have already been made to find out the manner in which the soil moisture has to be expressed so that the textural dependence on microwave emission can be minimized.

As early as 1977, Newton has indicated that if the soil moisture is expressed in volumetric units, the textural effects on microwave emission can be minimized as he felt that the dielectric constant is mainly dependent on the number of dipoles of water molecules in the soil medium. Schmugge (1980) concluded that the representation of soil moisture in terms of percentage of field capacity can minimize the textural effect on microwave emission on the basis of analysis of airborne data at 19.35 and 1.4 GHz. The data had been acquired over the test sites covering the complete range of soil textures. Subsequently Ulaby et al (1981) have conducted a series of field experiments to study the feasibility of microwave sensors (active) for the estimation of soil moisture. These experiments were conducted over the sandy loam, clay loam and silty clay at 4.26 GHz and the analysis —— had been carried out expressing soil moisture in terms of gravimetric and volumentric units and normalised field capacity. Finally they could conclude that expressing soil moisture in terms of percentage of FC would eliminate the texture effect on backscattering coefficient but they have suggested that there should be improved models for the estimation of field capacity.

However, Rouse (1983) in his theoretical studies concluded that representation of soil moisture in terms of volumetric units will minimize the textural effects and it further increases the divergence between different textures when it is expressed in percentage of FC.

In view of the different opinions of Rouse (1983) and Schmugge (1980), Dobson et al. (1984) felt the need to reexamine their earlier conclusion (Ulaby et al. 1981) that the soil moisture in percentage of FC is an optimum choice for representation of soil moisture. They have made a theoretical study using the experimental dielectric constant data (Hallikainen et al. 1985) at 1.4 and 5 GHz, considering the complete range of soil texture and the analysis has been carried out expressing soil moisture in gravimetric, volumetric units and percentage of FC. In their analysis they observed that bulk density of soils varies with the soil moisture content. They have finally concluded that expressing soil moisture in terms of volumetric units and percentage of FC will lead to more or less the same results and additional efforts should be devoted to accurate quantification of the true soil bulk density by obtaining bulk density concurrent with the gravimetric moisture determination in field experiments. Pampaloni et al. (1986) have also felt that the problem of eliminating influence of soil texture on microwave emission has to be further investigated.

In view of the above, it is felt necessary to examine the problem in the context of Indian environmental conditions using Indian soil characteristics. To examine the above problem, there

16

is a need to know the water retention characteristics and their dependence on soil physical properties.

8.1 Water retention characteristics of soils

Some studies have already been made (Gupta et al. 1979) Schmugge et al. 1976, 1980) to find out the statistical relations between water retention characteristics of soils (field capacity, wilting point and available water) and physical properties. However, Ulaby et al. (1978,1979) indicated the inadequacy of existing models and pointed out the need for improving the above models. In view of this, an attempt is made to study the water retention characteristics considering the data of Indian soils.

The Benchmark Soils India (1982) gives a consolidated data on soils of India and their physical, chemical and mineralogical properties. The field capacity and wilting point data for 25 soils series (each soil series contain 4 to 6 sample sets of data) have been analysed (Rao et al. 1984) and the following equations are recommended.

FC = 23.6475 - 0.2259 * SAND + 0.1987 * CLAY

with r = 0.9761, σ = 0.0952

FC = 32.1793 - 0.3184 * SAND + 0.4174 * CLAY

with r = 0.9490 and σ = 0.1332

WP = 6.8322 - 0.0636 * SAND + 0.1628 * CLAY

with r = 0.9536 and σ = 0.1555

WP = 8.6871 - 0.0680 * SAND + 0.2570 * CLAY

with r = 0.9246 and σ = 0.1773

where SAND and CLAY stand for percentage contents of sand and clay respectively in the soils. r, σ are correlation coefficient

and coefficient of variation.

8.2 Test site and data collection

In order to carry out the study to eliminate the texture influence on TB, three test sites namely, agriculture farm land with clay soils, Karjat observatory with clay loam soils and at Gotri with sandy clay loam soils have been selected. The first site comes under semi arid zone, second under heavy rainfall with no laterite soils and the third one under subtropical humid climatic zone. The physical and chemical properties of these soils are summerised in Table 8.1.

Using the Hallikainen et al. (1985) polynomial model, the dielectric constant of the soils at various constant soil moisture values have been calculated. Since the Fresnel reflection equations are valid for smooth and constant soil moisture, the emissivity values have been estimated for all three soils at different soil moisture values using the above equations.

8.3 Textural dependence on microwave emissivity

The analysis has been carried out as a function of frequency expressing soil moisture in gravimetric (m_g), volumetric (m_v), percentage field capacity and the volumetric soil moisture reduced by the transition moisture content of soil. The transition moisture (W_t), above which the dielectric constant of any soil begins to show a steep rise has been calculated using the model (Wang and Schmugge 1980)

W_t = 0.49 WP + 0.165

where WP is wilting point, which is estimated from the regression equations given earlier.

Figure 8.1 shows the dependence of emissivity on soil texture, where the soil moisure is in gravimetric units. The above figure clearly shows the influence of soil texture on emissivity at frequencies 1.4 GHz. Similar trends have been observed at 8.0 and 18.0 GHz also. Figure 8.2 represents the dependence of emissivity on soil moisture expressed in percentage of FC. To express soil moisture in percentage of FC, the statistical relations given earlier have been used. From figure 8.2, it is clear that divergence among the curves belonging to different textures increases when soil moisture is expressed in percentage of FC. This is in agreement with the observations of Rouse (1983) and Dobson et al. (1984).

When volumetric soil moisture is drawn against the emissivity values, the textural influence on emissivity is found to be reduced marginally. A careful observation of behaviour of dielectric constant values of soil over complete range of soil moisture shows that below a certain soil moisture content (W_t), the dielectric constant is very low with little variation as soil moisture varies. Whereas above W_t, the dielectric constant of soils rises steeply with increase in soil moisture. The values of W_t is found to be different for different soils, being high for clay soils and low for sand soils (Wang and Schmugge, 1980). This gives a clue to consider that W_t is the parameter which has to be considered for the removal of textural influences on emissivity. Thus, when volumetric soil moisture is reduced by W_t

for each soil texture and drawn against the emissivity values, the textural influence on emissivity is minimized as can be seen from Fig. 8.3. From these theoretical studies, it can be concluded that the soil textural influence on microwave emission can be minimized by expressing soil moisture in terms of ($m_v - W_t$)

9.0 SELECTION OF MULTIFREQUENCIES

During the recent years efforts are being made to extract the soil moisture and temperature profile parameters using multifrequency microwave remote sensing approaches including the data of thermal region. The methodology adopted is the statistical inversion technique. As explained in section two, the vertical profile of soil moisture and temperature can be expressed using exponential functions. The number of parameters to be estimated for each profile is three in number. For efficient extraction of profile parameters, there is a need to select the best suitable microwave frequencies.

9.2 Criteria for the selection of multiple number of frequencies

As stated above, there are 6 parameters to represent soil moisture and temperature profiles(3 for soil moisture and 3 for temperature profile). Therefore, to estimate these 6 parameters it is required to make the measurement of TB at a minimum of 6 frequencies. With the help of thermal remote sensing, the surface soil temperature can be estimated, thus reducing the number of parameters to 5. A study on the possible soil moisture profiles indicates that (particularly under the irrigation conditions) their slope can be considered as constant at least up to the depth of 5 cm. Making use of this property, the number of

18

parameters can be reduced to 4. Therefore, there is a need to have at least 4 measurements of TB at 4 microwave frequencies to estimate these 4 parameters. These four parameters are surface soil moisture, slope of soil moisture profile at the surface, change in physical temperature divided by the surface temperature and temperature profile shape parameter(Njoku and Kong 1977).

Here, the problem of selecting the multifrequencis for the estimation of the above four parameters has been considered in two parts namely, (1) the selection of multifrequency range and (2) the selection of intermediate frequencies.

9.3 Criteria for the selection of multifrequency range

The criteria for the selection of microwave frequency range for the study of soil moisture is as follows:

- As far as possible, it is advantageous to have a linear relation between soil moisture and TB (or a parameter which is a simple function of TB) in the selected range of microwave frequencies. This will facilitate to easy interpolation for extraction of information.
- The second criteria is the saturation limit of TB as a function of frequency.

Selection of lowest frequency limit

Fig. 6.2 shows the Log (TB) as a function of EQSM at different frequencies. Using the least square principle, the curves shown in Fig. 6.2 are fitted to a second degree polynomial as given below:

$$\text{Log}(TB) = a_0 + a_1 SM + a_2 SM \qquad (9.1)$$

It is expected that for the frequencies for which a linear

relationship exists, the constant a_2 will turn out to be very small and therefore the smaller value of a_2 is the indication of linearity of the relation. the computed a_2 values are plotted as a function of frequency as shown in figure 9.1. It can be seen from this figure that a_2 remains more or less constant upto 1 GHz and below 1 GHz, a_2 increases steeply indicating the starting point of nonlinearity. Thus from the first criterian for the selection of frequency range, the lowest frequency for the study of soil moisture is 1.0 GHz.

Selection of higher frequency limit

Figure 6.3 shows the TB as a function of frequency at various EQSM values. It can be seen from the above figure that the TB increases as the frequency increases. However, the rate of increase in TB decreases with frequency indicating a saturation limit. From the study of these curves, although the soil moisture range, it appears that the upper limit of the microwave frequency can be around 30 GHz.

9.4 Criteria for the selection of intermediate multifrequencies

The criterion for the selection of intermediate frequencies can be as follows:

1. The frequencies should be selected in such a way that they should be the optimum frequencies although the soil moisture range and temperature range.
2. These frequencies should give the best estimation of profile parameters.

As can be seen from the earlier discussion, the first and the last frequencies can be 1.0 and 30.0 GHz. The following methodology has been adopted to find out the intermediate

19

frequencies.

- The brightness temperature varies as a function of frequency as can be seen from figure 6.3, for the same soil moisture and physical temperature. This variation in the brightness temperature has been used as a criterian for the selection of intermediate frequencies. That means, the difference in brightness temperature between 1.0 and 30 GHz is equally divided and its corresponding frequencies have been interpolated. Table 9.1 shows the interpolated multifrequencies as a function of soil moisture. It can be seen from the table that the selected frequencies changes with soil moisture. Therefore, this methodology can not be adopted for the selection of frequencies.
- In the second criterian, instead of TB differences, the logarithmic TB between 1.0 and 30.0 GHz differences have been used. That means the logarithmic differences of TB is equally divided and its corresponding frequencies have been interpolated. Table 9.1 shows the intermediate multifrequencies obtained on the basis of this methodology. Even in this case (as can be seen from table 9.1) also, the selected frequencies vary with soil moisture. Therefore, these can not be considered as the optimum frequencies.
- Fig. 7.1 and 7.2 show the dependence of Pd on frequency and soil moisture. In the third approach the penetration depth of microwaves has been used as a criterion for the selection of multifrequencies. That is the difference in the penetration depth between 1.0 GHz and that of 30.0 GHz is divided into equal interval and the corresponding frequencies have been interpolated.

Table 9.1 shows the intermediate multifrequencies as a function of soil moisture based on the this methodology. The results are shown in Fig. 9.1 for pictorial view of the results. It can be seen from Fig. 9.1 that the selected frequencies remains fairly constant although the soil moisture range above 5 % by weight. The average value of these frequencies are 1.0, 3.0, 6.0 and 30.0 GHz. It may be noted that these frequencies are obtained for black soils of Pune test site. The applicability of these frequencies for other soil types is to be investigated.

However, the constancy of these frequencies with temperature has to be examined. Finally, the selected frequencies are to be varified for the optimization in the extraction of the profile parameters.

10.0 Conclusions

This paper presents a consolidated work on the theoretical models for the study of soil moisture through passive microwave remote sensing techniques. These models are aimed at obtaining the multifrequencies that are better suitable for the extraction of soil moisture profiles particularly applicable to black soils of Pune. The further work in this direction needs to be carried out to optimize the multifrequencies to take into account the physical temperature variations and also the effect of surface roughness and vegetation cover. The applicability of these frequencies can be judged on the basis of their efficiency in extracting the profile parameters through inversion technique. This aspect is to be studied.

A soft ware package has been developed around inhouse

20

computer (Orion - 6000 Microcomputer system) facilities to impliment all the models discussed in this paper.

Acknowledgements

The authors are thankful to Prof. R. K. Kutti, Head, CSRE, for providing the necessary facilities to carry out this research work. The authors are also thankful to Department of Science and Technology for sponsoring this project. Useful discussions with Mr. B. K. Mohan and Mrs. (Dr.) P. Venkatachalam are thankfully acknowledged. The assistance extended by Mr. S. Choudhury is also acknowledged.

REFERENCES

Burke, W.J., Schmugge, T., and Paris, J.F. (1979), Comparison of 2.8 and 21 cm microwave radiometer observations over soils with emission model calculations, J.Geophs. Res. 87: 287-294.

Dobson, M.C., and Ulaby, F.T., (1981), Microwave backscattering dependence on surface roughness, Soil Moisture, and soil texture : Part III - Soil tension, IEEE Trans. Geosci. Remote sensing, GE-19: 51-61.

Dobson, M. C., Kouyate, F., and Ulaby, F. T. (1984), A reexamination of soil texture effects on microwave emission and backscattering, IEEE trans. Geosci. Remote Sensing, GE-22: 530-533.

Dobson, M.C., Ulaby, F. T., Hallikainen, M.T., and El-Rayes, M. A. (1985), Microwave dielectric behaviour of wet soil -Part II: dielectric mixing models, IEEE Trans. Geosci. Remote Sensing, GE-23: 35-46.

Eagleman J. R. and Lin W.C. (1976), Remote Sensing of soil moisture by a 21 cm passive radiometer, J. Geophy. Res. 81: 3660-3666. ~~1976~~

Gupta, S.C., and Larson, W.E. (1979), Estimating soil water retention characteristics from particle size distribution, organic matter percent and bulk density, Water Resources Res. 15: 1633-1635.

Hallikainen, M.T., F.T. Ulaby, M.C. Dobson, M.A. El-Rayes and Linkun Wu (1985), Microwave dielectric behaviour of wet soil - Part I : Empirical models and experimental observation, IEEE Trans. Geosci. Remote Sens. GE-23: 25-33.

Hildebrand, F.B. (1956), Introduction to numerical analysis, New York, McGraw Hill, pp 378-382.

Jackson, J.D. (1962), Theory of electromagnetic waves, John Wiley and Sons, New York.

Lee, S.L., (1974), Duel frequency microwave radiometer measurements of soil moisture for bare and vegetated rough surfaces, Technical Report RSC-56, Remote Sensing Centre, Texas A&M University.

Newton, R.W. (1977), Microwave remote sensing and its applications to soil moisture detection, Tech. Rep. RSC-81, Texas A&M Univ., College Station , 56pp and 309pp..

Newton R.W. and Rouse J.W. (1980) Microwave radiometer measurements of soil moisture content, IEEE Trans. Ant. and Propos. AP-28: 680-686.

21

Newton, R.W., Black, R.Q., Makanvand, S., Blanchard, A.J. and Jean, B.R. (1982), Soil moisture information and thermal microwave emission, IEEE Trans. Geosci. Remote Sens. GE-20: 275-281.

Njoku, E.G., and Kong, J.A. (1977), Theory of passive microwave remote sensing of near-surface soil moisture, J.Geophys. Res. 82: 3108-3118.

Pampaloni, P., Paloscia, S., and Chiarantini, L. (1986), Contribution of passive microwave remote sensing in soil moisture and evapotranspiration measurements. Proc.ISLSCP Conf. Rome, Italy, 327pp.

Rao, K.S., Rao, P.V.N., Chandra, G., Rao, Y.S., Mohan, B.K., and Venkatachalam, P. (1986a), Quantitative study of soil moisture through multifrequency - multispectral (regions) remote sensing techniques: An integrated approach, state of the art report, DST project.

Rao, K.S., Rao, Y.S., Chandra, G., Mohan, B.K., and Venkatachalam, P. (1986b), Representative profiles of soil moisture and temperature of black soil in the context of microwave remote sensing, Presented in the seminar of Association of Hydrologists of India.

Rao, K.S., Rao, Y.S., and Raju, C.S. (1987u), Improved model for parameterization of soil moisture in microwave remote sensing, Communicated to Int. J. Remote Sensing.

Rao, K.S., Chandra G., and Raju, C.S. (1987b), A comparative study of different dielectric models - computation of representative dielectric profiles of black soils, Ind. J. of Remote Sens, to be published.

Rao, K.S., Girish Chandra and Narasimha Rao, P.V. (1987c), A study on relation between brightness temperature and soil moisture: Selection of frequency range for microwave remote sensing" to be published in Int.J. of Remote Sensing.

Rao, K.S., Narasimha Rao, P. V., Mohan, B.K., Venkatachalam, P. (1987d), Study on relation between water retention characteristics of soils and their physical parameters, communicated to Int. Journal of Remote Sensing.

Rouse, J.W. (1983), Comments on the effects of texture on microwave emission from soils, IEEE Trans. Geosci. Remote Sensing, GE-21: 508-511.

Schmugge T.J. (1980), Effect of texture on microwave emission from soils", IEEE Trans. Geosci. Remote Sensing, GE-18: 353-361.

Schmugge, T.J. (1983), Remote Sensing of soil moisture with microwave radiometers, Trans. A.S.A.E. 26: 748-753.

Schmugge, T.J., and Choudhury, B.J. (1981), A comparison of radiative transfer models for predicting the microwave emission from soils, Radio Sci. 16: 927-979.

Schmugge, T.J., Wilheit, T., Webster, W., and Gloersen, P. (1976), Remote sensing of soil moisture with microwave radiometers -II, NASA Tech. Note, TND-8321 (NTIS No.N76-32625).

Schmugge T.J., Gloersen P., Wilhit T. and Geiser F. (1974), Remote sensing of soil moisture with microwave radiometers, J. Geophy. Res. 79: 317-323.

Stogryn, A. (1970), The brightness temperature of a vertically structured medium, Radio Sci. 5: 1397-1406.

Stogryn A. (1971), Equation for calculating the dielectric constant of saline water, IEEE Trans. Microwave Theory Tech. MTT-19, 733-736.

Tsang, L., Njoku, E. and Kong, J.A. (1975), Microwave thermal emission from a stratified medium with nonuniform temperature distribution, J. Applied Phy. 46: 5127-5133.

Ulaby, F.T. and Bare, J.E. (1979), Look direction modulation function of radar backscattering coefficient of agricultural fields, Photogravi. Eng. Remote Sens. 45: 1495-1506.

Ulaby, F.T., Baltiwala, P.P., and Dobson, M.C. (1978), Microwave backscatter dependence on surface roughness, soil moisture and soil texture: Part I - Bare soil, IEEE Trans. Geosci. Remote Sens. GE-16, 286-295.

Ulaby, F.T., Bradley, G.A., and Dobson, M.C. (1979), Microwave backscatter dependence on surface roughness, soil moisture and texture: Part II Vegetation - covered soils, IEEE Trans. Geosci. Electron. GE-17: 33-40.

Dobson, M.C., and Ulaby, F.T. (1981), Microwave backscatter dependence on surface roughness, soil moisture and soil texture: Part III - Soil tension, IEEE Trans. on Geosci. Remote Sensing, GE-19: 51-61.

Vyas, A.D., Trivedi A.J., Calla O.P.N., Rana S.S. and Raju, G., Passive microwave remote sensing of soil moisture, Int. J. Remote Sens. 6: 1153-1162.

Wang J.R. (1980), The dielectric properties of soil-water mixtures at microwave frequencies, Radio Sci. 15: 977-985.

Wang J.R. and Schmugge, T.J. (1980), An empirical model for the complex dielectric permittivity of soils as a function of water content, IEEE Trans. Geosci. Remote Sensing, GE-18: 288-293.

Wang, J.R., McMurtrey, J.E., Engman, E.T., Jackson, T.J, Schmugge, T.J., Gould, W.I., Fuchs, J.E., and Glazar, W.S. (1982),

22

Radiometric measurements over bare and vegetated fields at 1.4 GHz and 5 GHz. frequencies. Remote Sensing of Environ. 12: 295-311.

Wang J.R., O'Neil P.E., Jackson T.J. and Engman E.T. (1983), Multifrequency measurements of the effects of soil moisture, soil texture and surface roughness. IEEE Trans. Geosci. Remote sensing. GE-21: 44-50.

Wilheit, T.T. (1978), Radiative transfer in a plane stratified dielectric. IEEE Trans. Geosci. Elect. GE-16: 138-143.

Table 2.3 Physical and chemical properties of the Pune test site.
(a) Physicl properties.

Depth (Cm.)	Sand %	Silt %	Clay %	Moisture holding capacity %	Apparent density (gm/cc)	Pore space %	Volume expansion %
0-5	13.76	30.34	55.90	61.03	1.47	53.36	16.26
5-15	23.96	32.48	43.55	61.27	1.595	55.10	17.06
15-45	17.56	32.69	49.75	63.37	1.325	51.82	19.16

(b) Chemical properties

Depth (Cm.)	Saturation %	pH (Paste)	pH (extract)	ECe (millimhos/Cm.)	<--- meq./litre---> Ca^{++}	Mg^{++}	Na^{+}	HCO_3^{-}	Cl^{-}	SAR	ESP
0-5	66.04	7.70	7.8	0.5	2.16	2.34	1.70	4.84	2.4	1.13	0.2
5-15	60.60	7.75	7.8	0.4	2.18	2.30	1.55	3.20	1.2	1.09	0.2
15-45	60.46	7.8	8.0	0.39	2.17	2.33	1.325	3.2	1.2	1.54	0.2

Table 2.2 Soil Moisture and temperature Parameters Corresponding to Recommended Profiles

(a) Moisture Profile Parameters:

Profile	ρ_s	Δf_1	Δf_2	$\beta(m^{-1})$	$\beta(m^{-1})$	d(m)
1.	2.34	0.34	0.0	2.20	0.0	0.45
2.	32.90	-5.20	0.0	24.70	0.0	0.45
3.	2.24	11.40	0.0	8.10	0.0	0.45
4.	7.80	14.40	0.0	9.00	0.0	0.45
5.	33.20	12.12	5.58	13.4+j16.0	13.4-j16.0	0.45

(b) Recommended temperature profile parameters:

Pro-file	$T_c^\circ C$	$\Delta T_1^\circ C$	$\Delta T_2^\circ C$	$\gamma_1(cm^{-1})$	$\gamma_2(cm^{-1})$
1.	26.20	-17.50	0.00	0.087	0.0
2.	32.20	-8.30	0.00	0.172	0.0
3.	22.80	18.30	0.00	0.121	0.0
4.	33.20	15.49	-7.26	0.102-j0.178	0.102+j0.178
5.	24.80	37.80	0.00	0.081	0.0

Table 8.1 Physical and chemical properties of different test sites.

Test site	Sand %	Silt %	Clay %	Bulk density (gm/cm)	Moisture holding capacity %	ECe (milli mhos/cm)	PH	Organic content %
Pune	18.43	31.84	49.73	1.46	61.25	0.45	7.75	0.75
Karjat	28.8	41.4	29.8	1.15	52.3	0.2	6.8	0.60
Gotri	21.7	20.6	57.7	1.47	50.6	0.14	7.1	--

Table 9.1 Four frequency model for Pune soil moisture profiles

% EQSM (by weight)	Multifrequencies (GHz)											
	TB as a Criteria				Low(TB) as a Criteria				Pd as a Criteria			
	1st	2nd	3rd	4th	1st	2nd	3rd	4th	1st	2nd	3rd	4th
2.0	1.0	1.50	3.75	30.0	1.0	1.25	1.75	30.0	1.0	3.50	8.00	30.0
5.0	1.0	1.75	3.00	30.0	1.0	1.50	2.00	30.0	1.0	3.30	7.75	30.0
10.0	1.0	5.00	16.00	30.0	1.0	2.50	9.00	30.0	1.0	3.25	6.50	30.0
15.0	1.0	15.00	22.50	30.0	1.0	12.50	16.00	30.0	1.0	3.00	5.75	30.0
20.0	1.0	14.00	20.00	30.0	1.0	11.25	15.00	30.0	1.0	2.75	5.25	30.0
25.0	1.0	7.50	13.00	30.0	1.0	3.50	9.00	30.0	1.0	2.50	4.75	30.0
30.0	1.0	7.00	15.00	30.0	1.0	2.50	7.50	30.0	1.0	2.25	4.50	30.0

Caption of Figures:

Figure 2.1 Moisture profiles of August and September

Figure 2.2 Temperature profiles of different dates at 7.30 a.m. (a) Before fitting (b) After fitting

Figure 2.3 Temperature profiles of a day at different times

Figure 2.4 Recommended representative soil moisture profiles

Figure 2.5 Recommended representative temperature profiles

Figure 3.1 Soil moisture dependence of dielectric constant (ε) at 1.4 GHz calculated by semiempirical models for (a) Haldi series (sandy loam) (b) Hathiapathar series (silt loam) (c) Jambha series (clay)

Figure 3.2(a) Frequency dependence of the semiempirical models at moisture content (m_v = 0.3) for Haldi series

Figure 3.2(b) Frequency dependence of the semiempirical models at moisture content (m_v = 0.3) for Hathiapathar series

Figure 3.2(c) Frequency dependence of the semiempirical models at moisture content (m_v = 0.3) for Jambha series

Figure 3.3(c) Representative dielectric constant profiles for black soil of Pune at 3.0 GHz

Figure 4.1 Concept of straification of a soil into layers (Tsang et al. 1975)

Figure 4.2 Frequency dependence of brightness temperature for different soil moisture profiles (SMP) with temperature profile 2 combination

Figure 4.3 Comparison between theoretic1 (Wilheit & Burke) and experimental (Newton 1977) normalized brightness temperature at 1.4 GHz as afunction of EQSM for nadir look angle

Figure 5.1 Simulated soil moisture profiles for constant EQSM (16.4 weight % at 1.4 GHz)

Figure 5.2 Brightness temperature dependence of β for same values of EQSM and MEQSM at 1.4 GHz

Figure 5.3 Brightness temperature dependence of β for same values of EQSM and MEQSM at 5.0 GHz

Figure 5.4 Brightness temperature dependence of β for same values of EQSM and MEQSM at 19.35 GHz

Figure 5.5 Brightness temperature dependence of β for same values of EQSM and MEQSM at 30.0 GHz

Figure 6.1 TB vs EQSM (by weight %) for constant soil moisture profile at different frequencies (T = 300°k)

Figure 6.2 Log(TB) vs EQSM (by weight %) for constant soil moisture profile at different frequencies (T = 300°k)

Figure 6.3 TB vs frequency for constant soil moisture profiles

Figure 7.1 EQSM vs depth of penetration (Pd) for representative profiles of clay soils of Pune at different frequnencies

Figure 7.2 Frequency vs depth of penetration (Pd) for representative profiles of clay soils of Pune at different soil moisture conditions (weight %)

Figure 7.3 Frequency vs depth of penetration (Pd) for different soil physical temperature

Figure 7.4 Frequency vs depth of penetration (Pd) for different soil textures

Figure 7.5 Soil moisture (SM) vs depth of penetration for different soil textures

Figure 8.1 Calculated emissivity at 1.4 GHz and 0° incident angle as a function of gravimetric soil moisture(m_g).

Figure 8.2 Calculated emissivity at 1.4 GHz and 0° incident angle as a function of soil moisture in percentage of field

Figure 8.3 Calculated emissivity at 1.4 GHz and 0° incident angle as a function of volumetric soil moisture(m_v).
Figure 8.4 Calculated emissivity at 1.4 GHz and 0° incident angle as a function of soil moisture in terms of ($m_v - W_t$).

Figure 9.1 a_1 vs frequency for constant soil moisture profile

Figure 9.2 Four frequency models for Pune soil moisture profiles

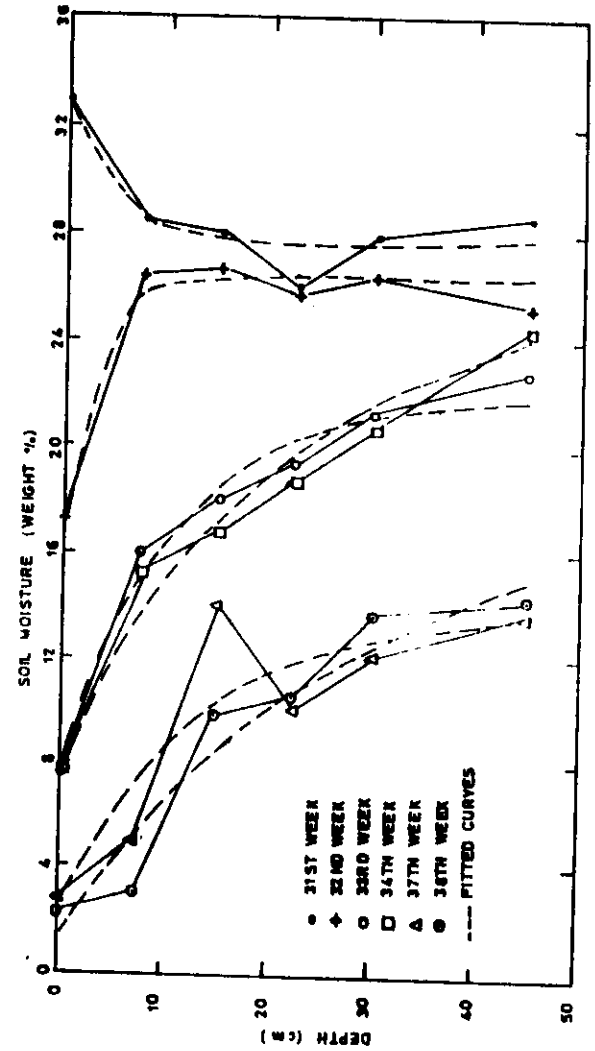

FIG 2·1 Moisture profiles of August and September

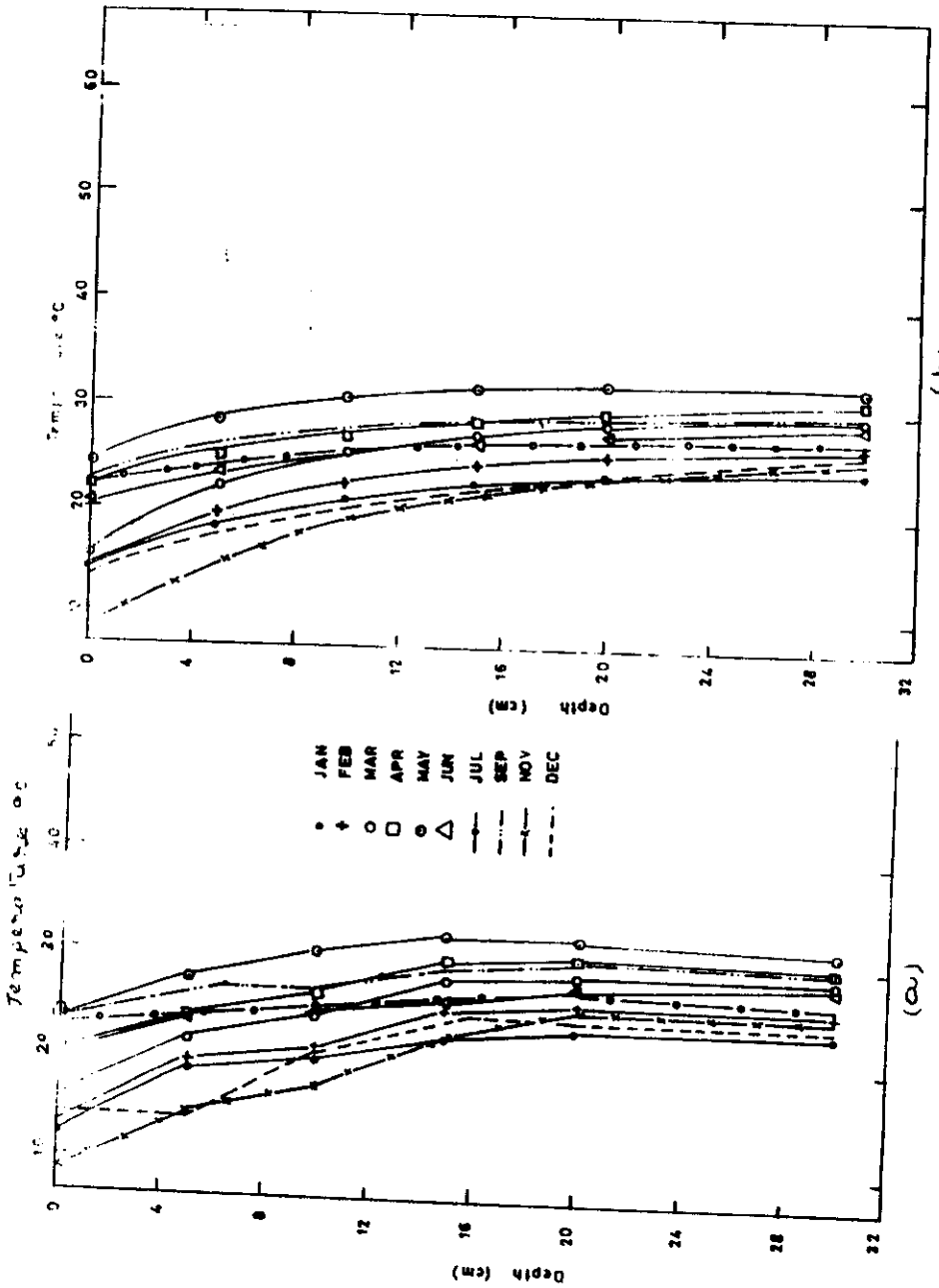

Figure 2.2 Temperature fluctuations of August at different dates at 7.30 a.m.
(a) Before tilling (b) After tilling.

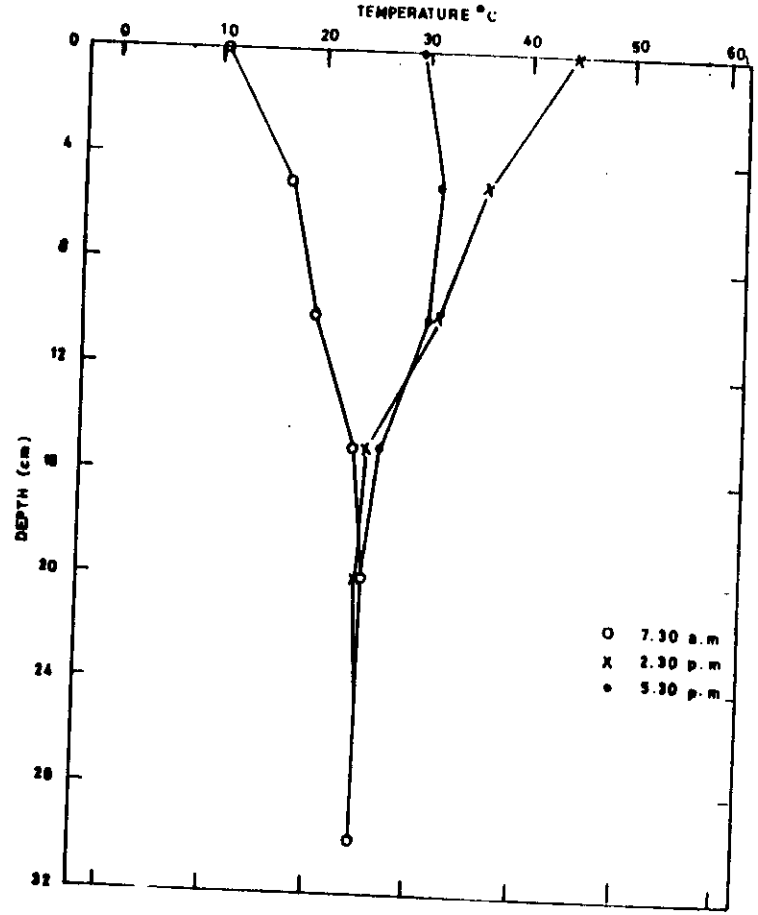

FIG 2.3 Temperature profiles of a day at different times

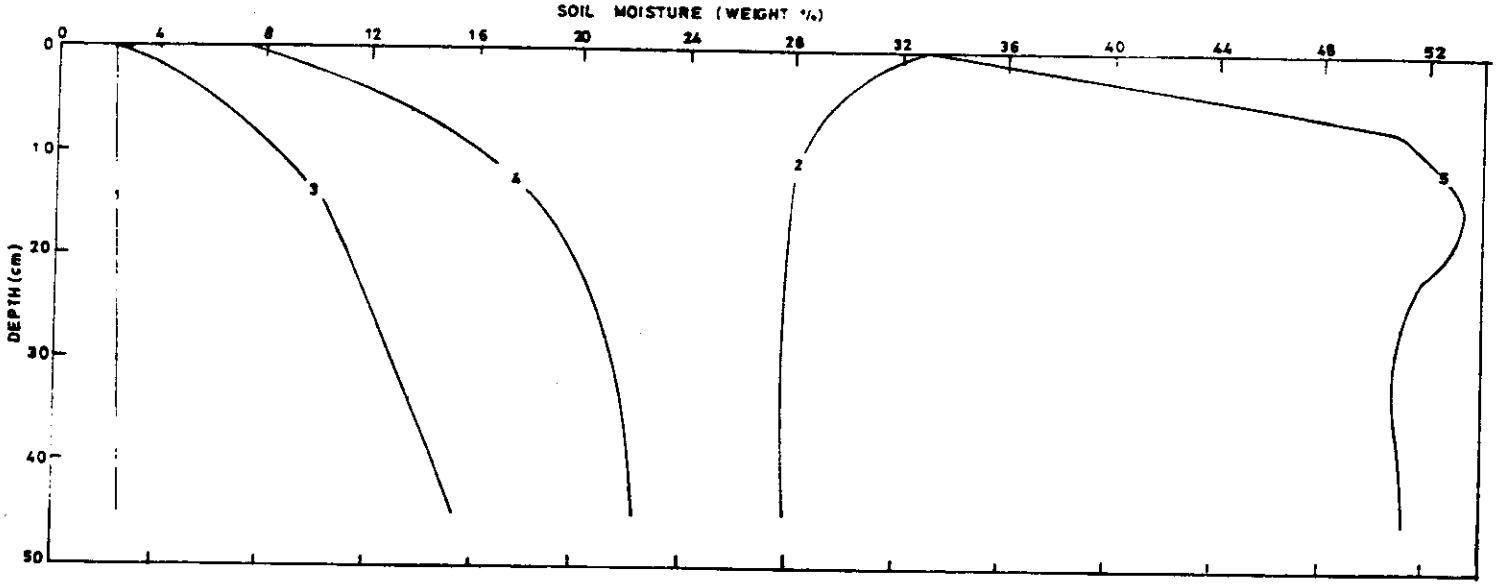

FIG 2.4: Recommended representative soil moisture profiles

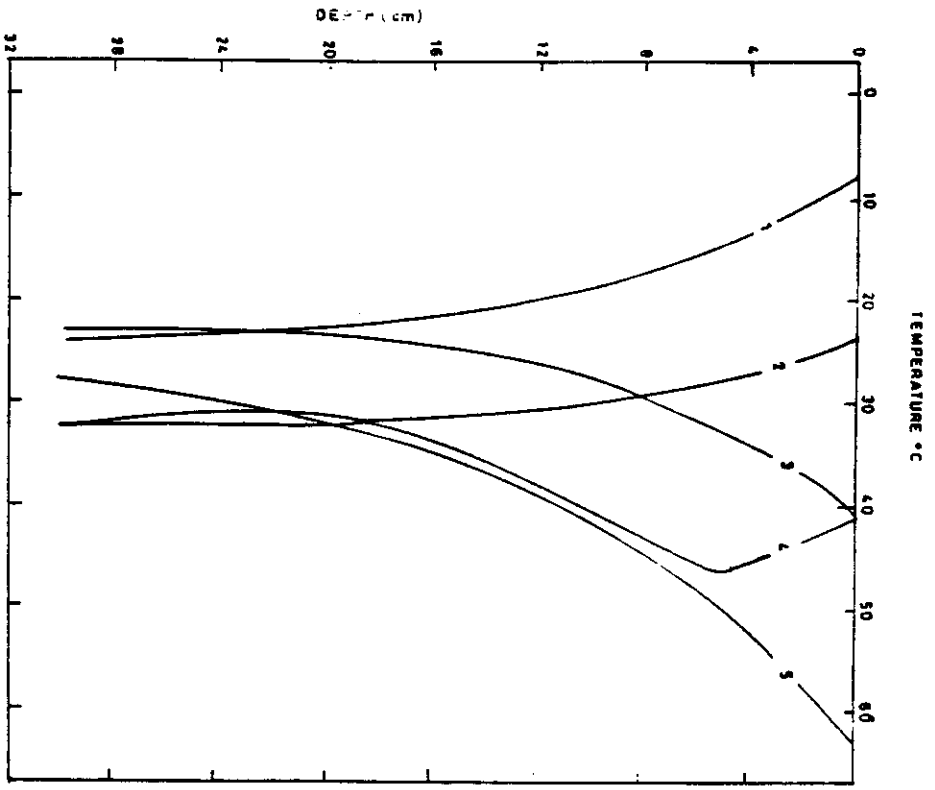

FIG 2.5 Recommended representative temperature profile.

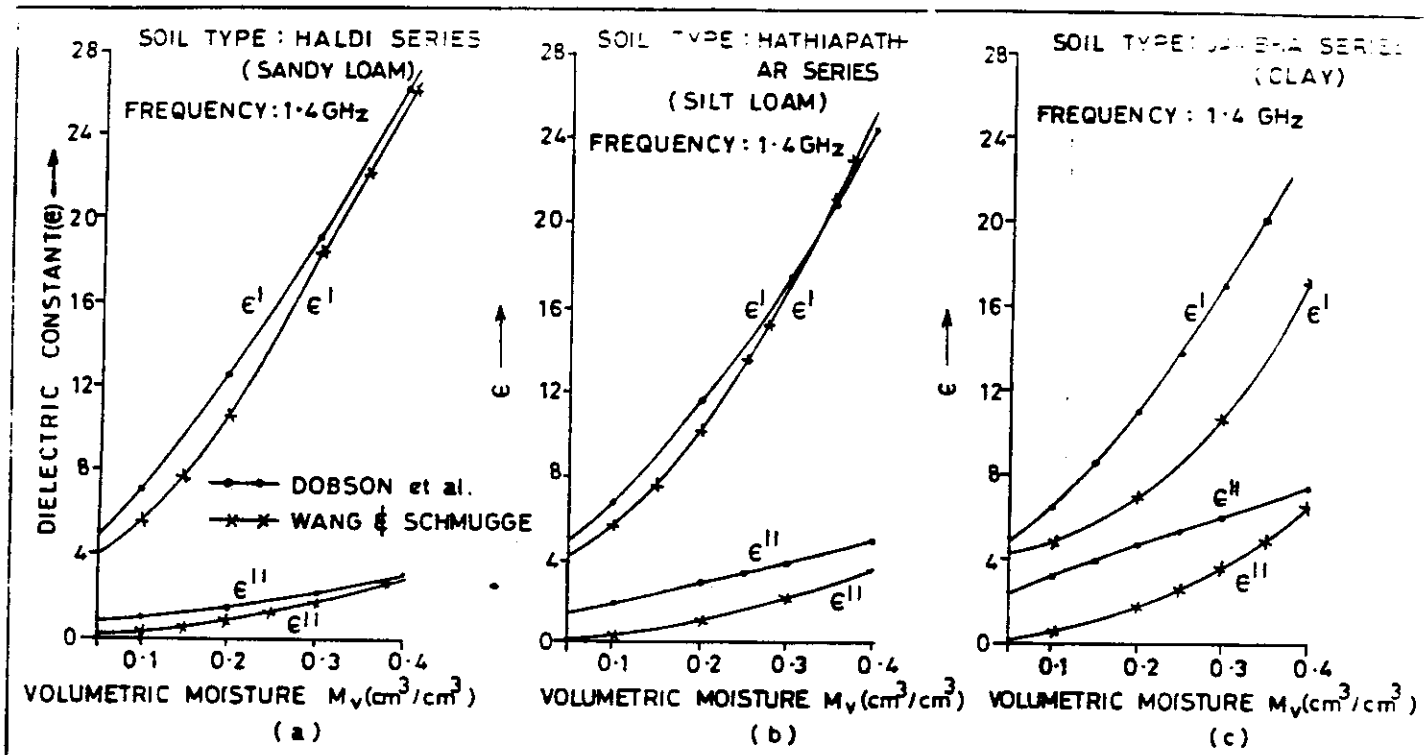

FIG. 3·1 SOIL MOISTURE DEPENDENCE OF DIELECTRIC CONSTANT (ε) AT 1·4 GHz CALCULATED BY SEMIEMPIRICAL MODELS FOR (a) HALDI SERIES (SANDY LOAM) (b) HATHIAPATHAR SERIES (SILT LOAM) (c) JAMBHA SERIES (CLAY)

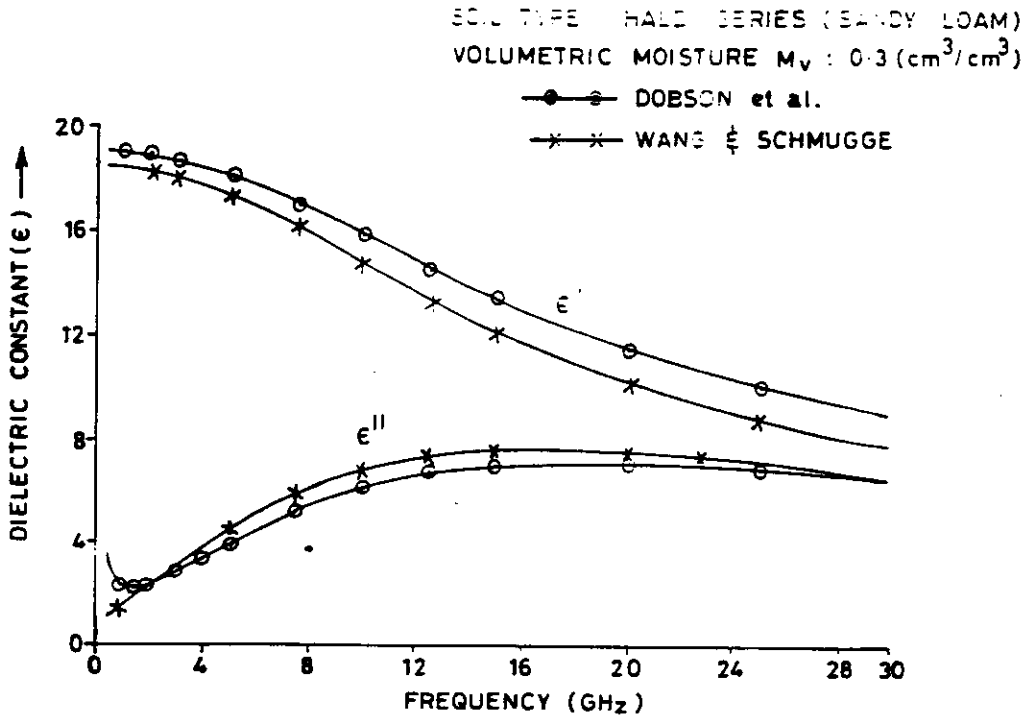

FIG. 3·2(a) FREQUENCY DEPENDENCE OF THE SEMIEMPIRICAL MODELS AT MOISTURE CONTENT (M_v = 0·3) FOR HALDI SERIES

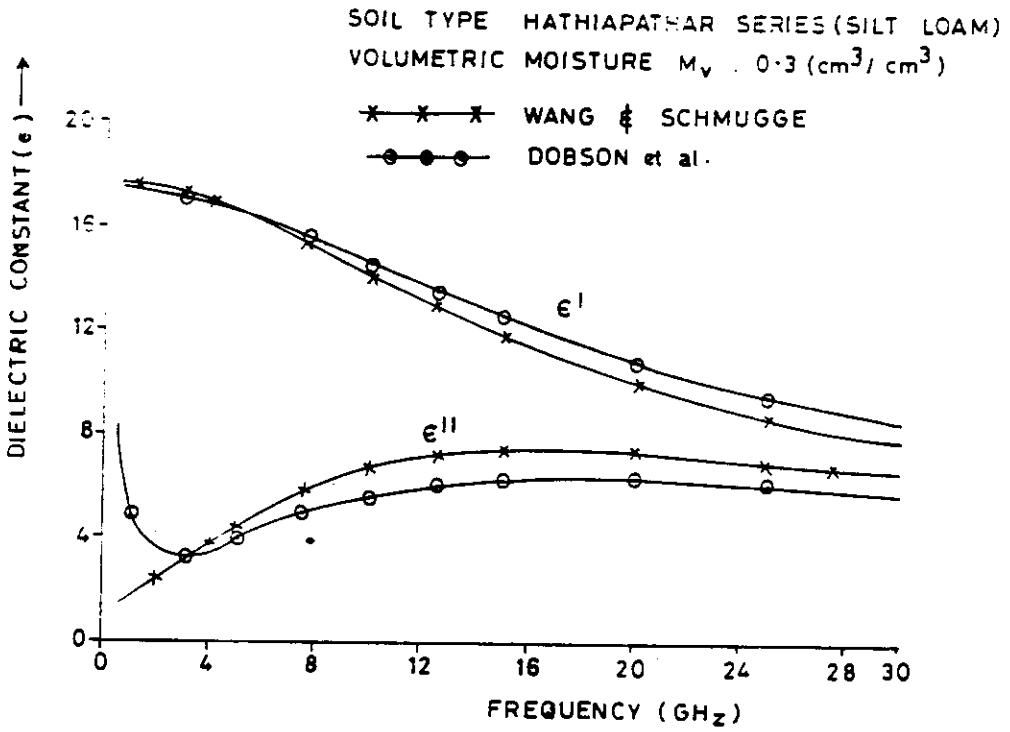

FIG 3·2(b) FREQUENCY DEPENDENCE OF THE SEMIEMPIRICAL MODELS AT MOISTURE CONTENT (M_v = 0·3) FOR HATHIAPATHAR SERIES.

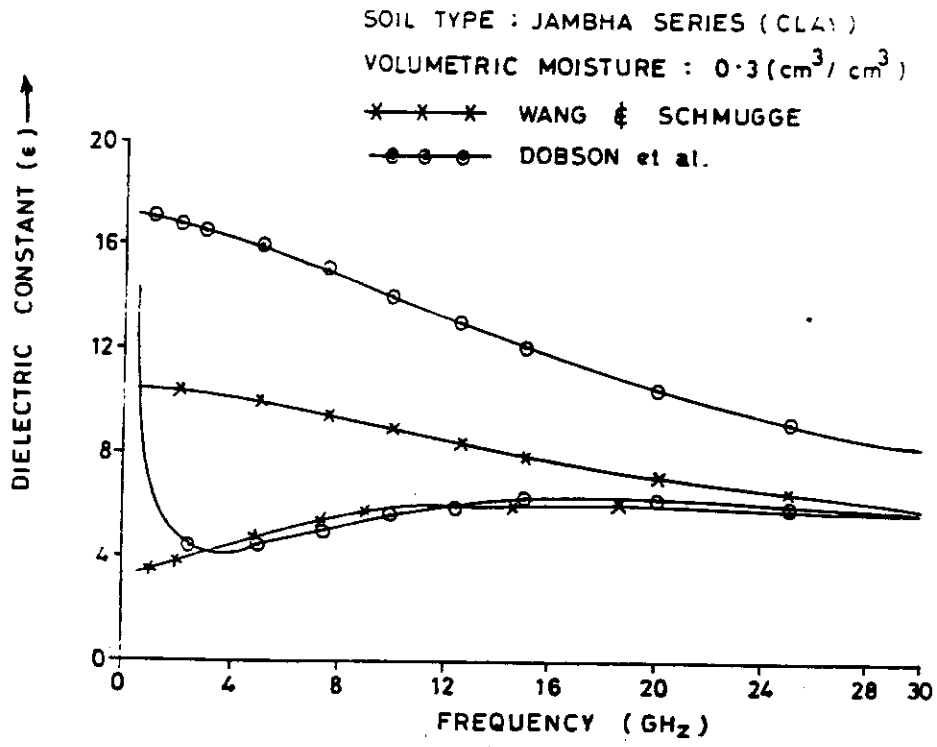

FIG. 3·2(c) FREQUENCY DEPENDENCE OF THE SEMIEMPIRICAL MODELS AT MOISTURE CONTENT (M_v = 0·3) for JAMBHA SERIES.

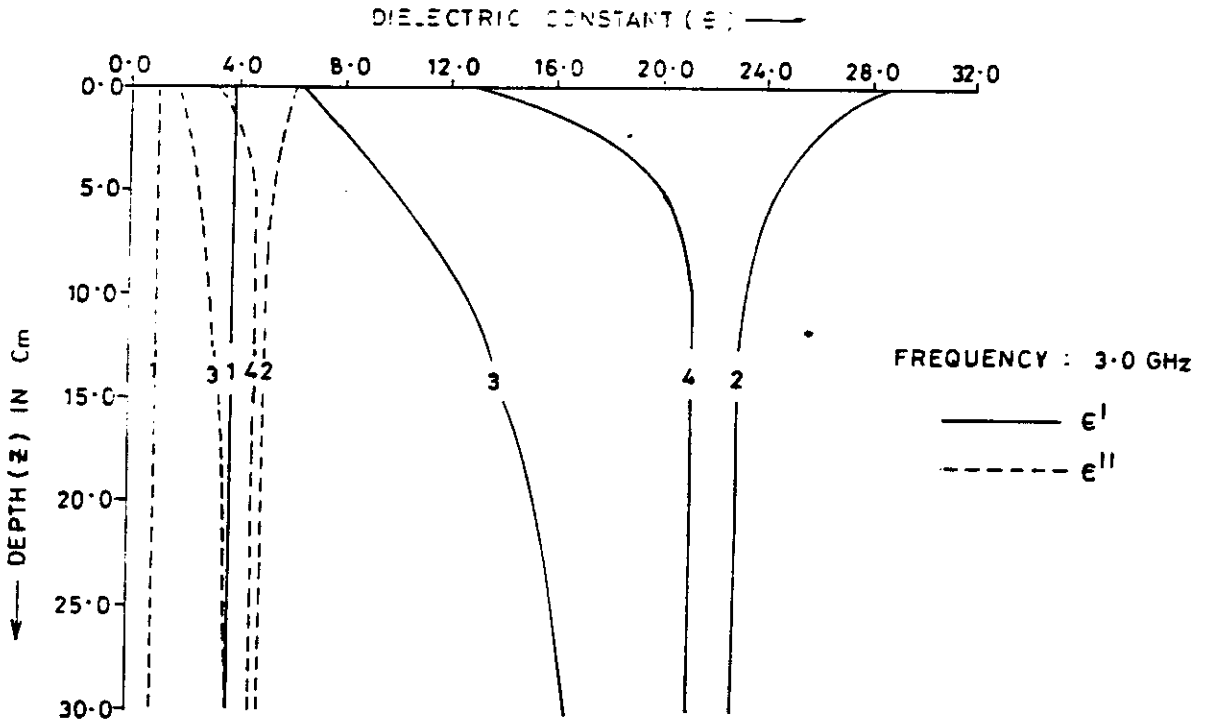

FIG. 3.3 REPRESENTATIVE DIELECTRIC CONSTANT PROFILES FOR BLACK SOIL OF PUNE AT 3·0 GHz

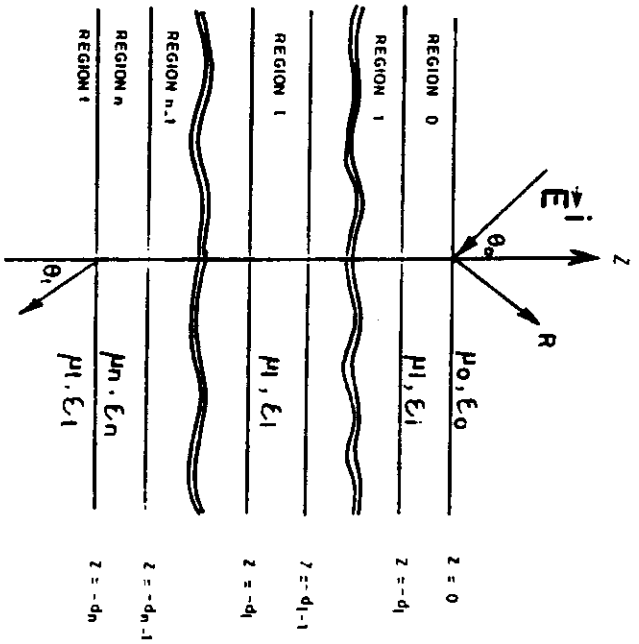

Fig. 4.1 [illegible] et al. 1975).

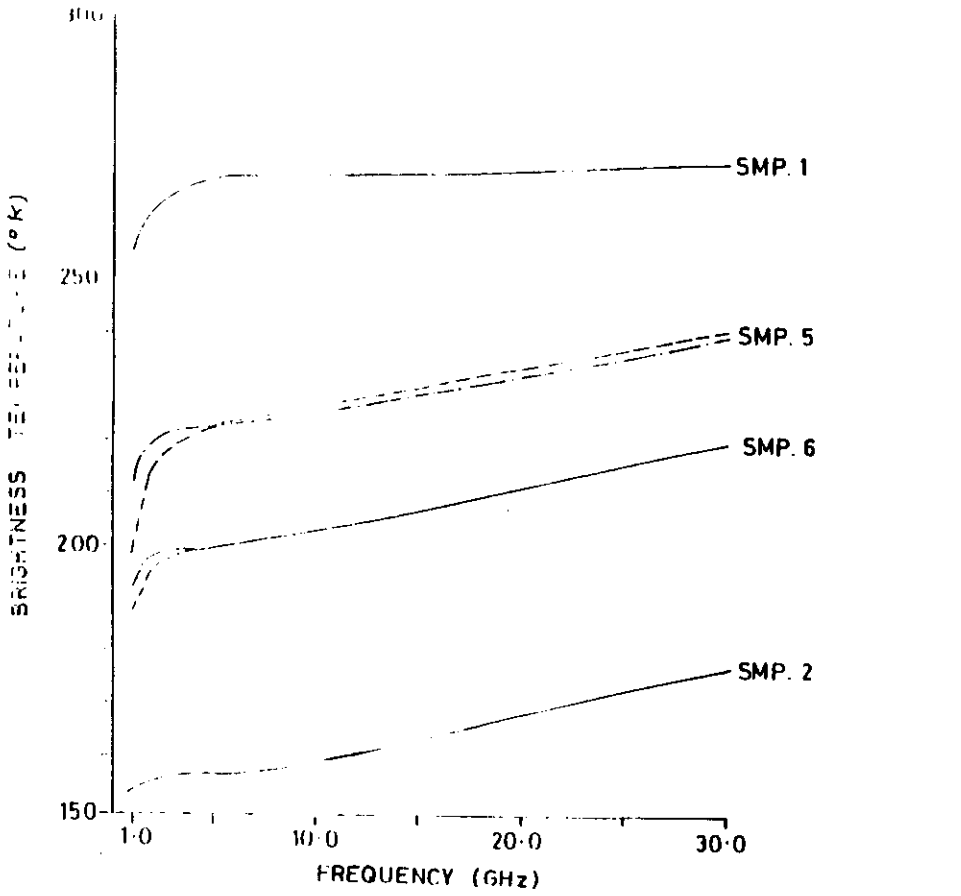

FIGURE 4.2 Frequency dependence of brightness temperature for different soil moisture profile (SMP) with temperature profile combination.

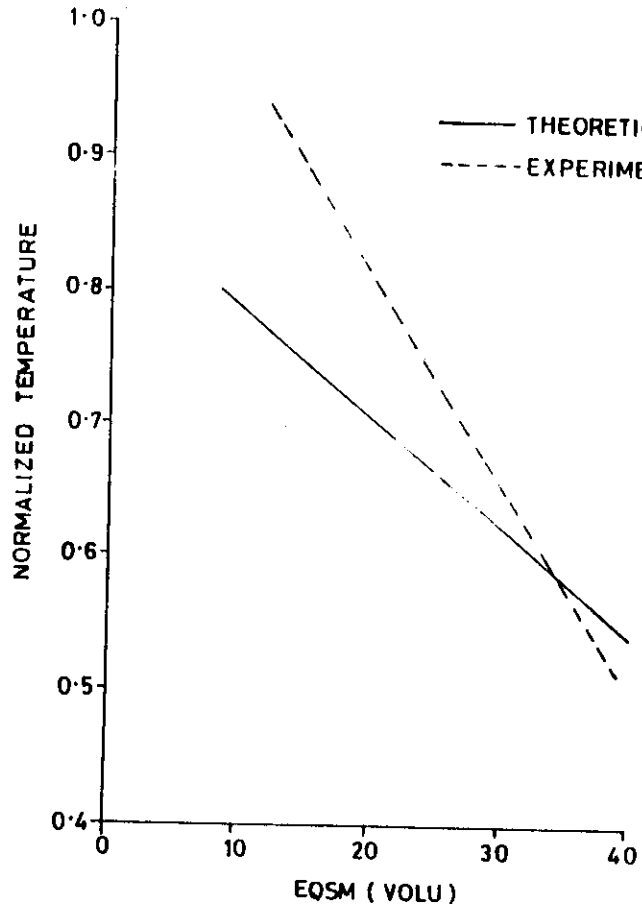

FIGURE 4.3 Comparison between theoretical (Wilheit & Burke) and experimental (Newton 1977) normalized brightness temperature at 1.4 GHz as a function of EQSM for nadir look angle.

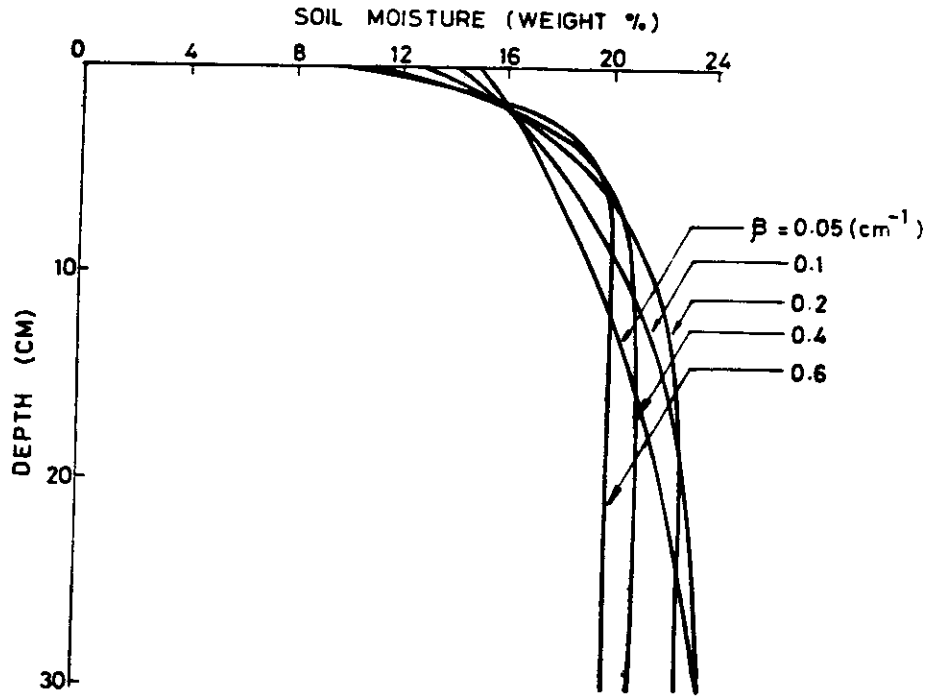

Figure 5.1 Simulated soil moisture profiles for constant EQSM (16.4 weight % at 1.4 GHz)

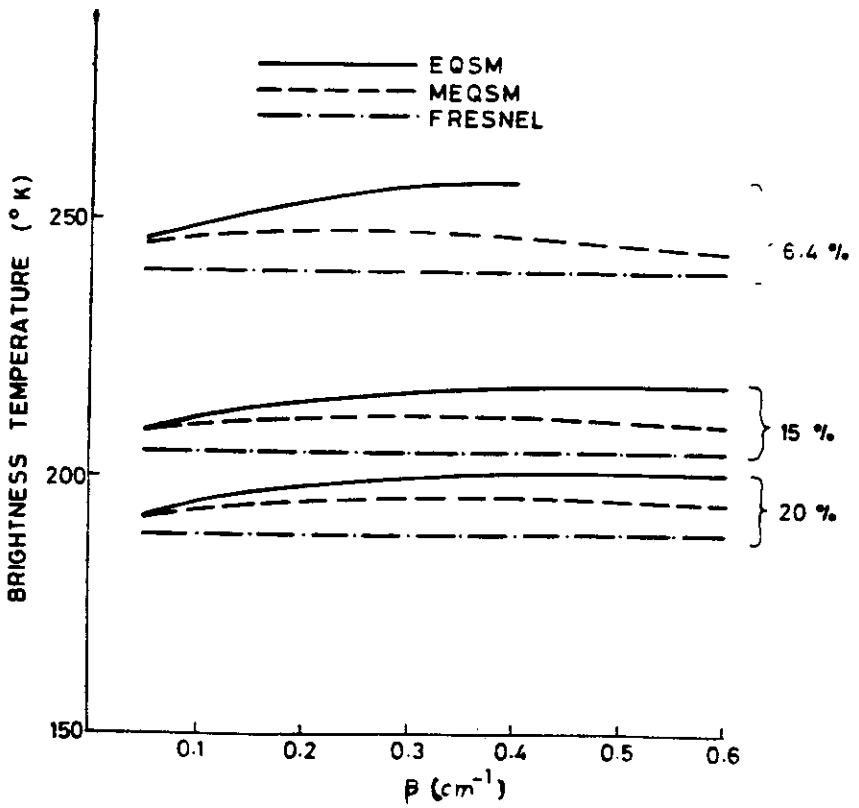

Figure 5.2 Brightness temperature dependence of β for same values of EQSM and MEQSM at 1.4 GHz

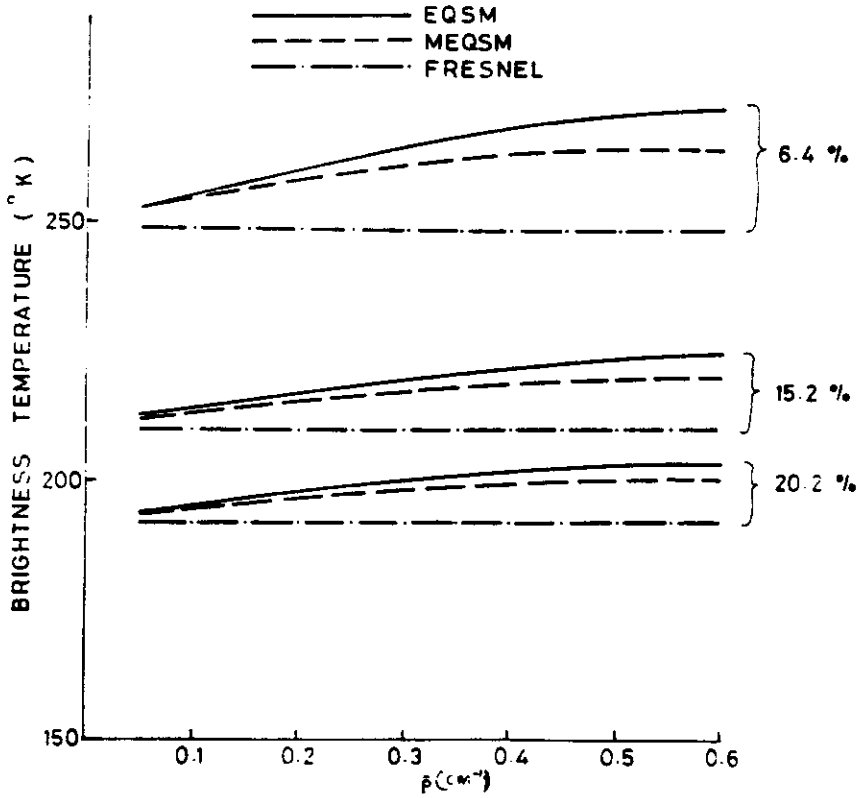

Figure 5.3 Brightness temperature dependence of β for same values of EQSM and MEQSM at 5.0 GHz

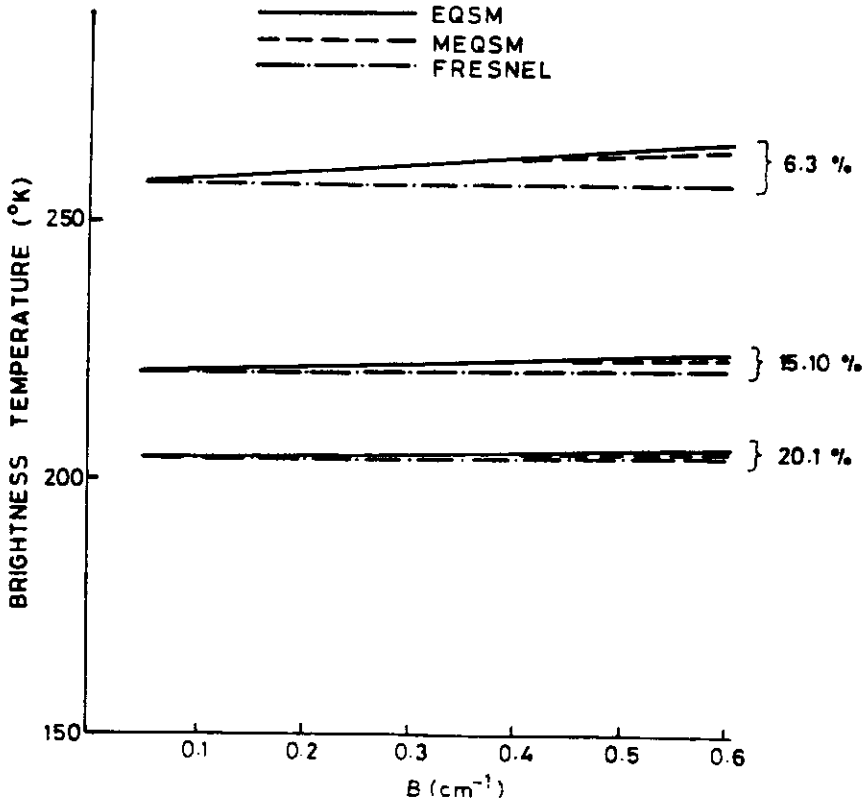

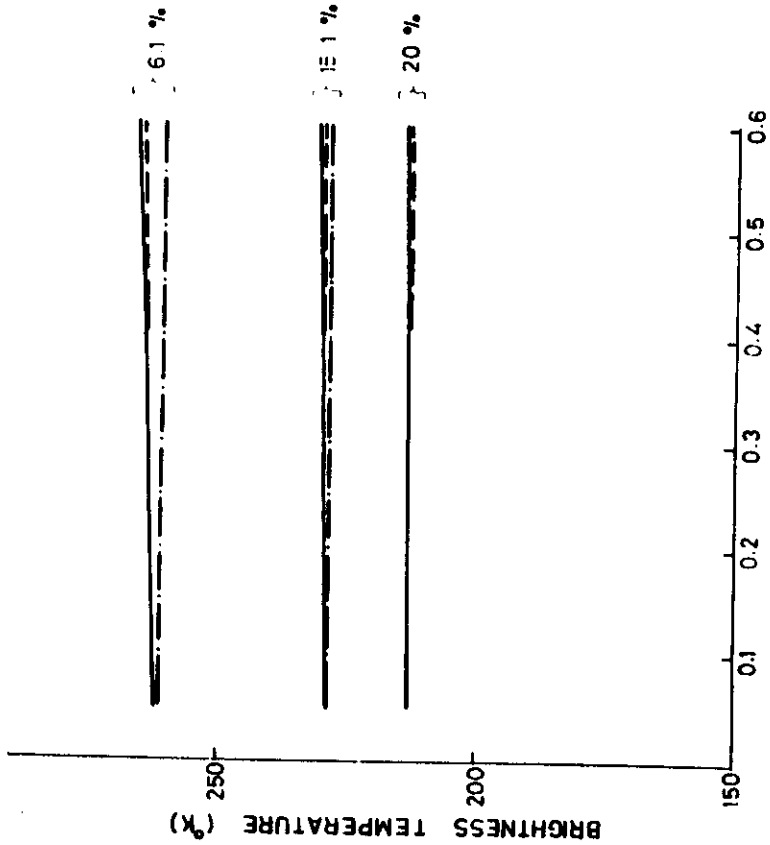

Figure 5.5 Brightness temperature dependence of B for same values of EQSM and MEQSM at 30.0 GHz

-69-

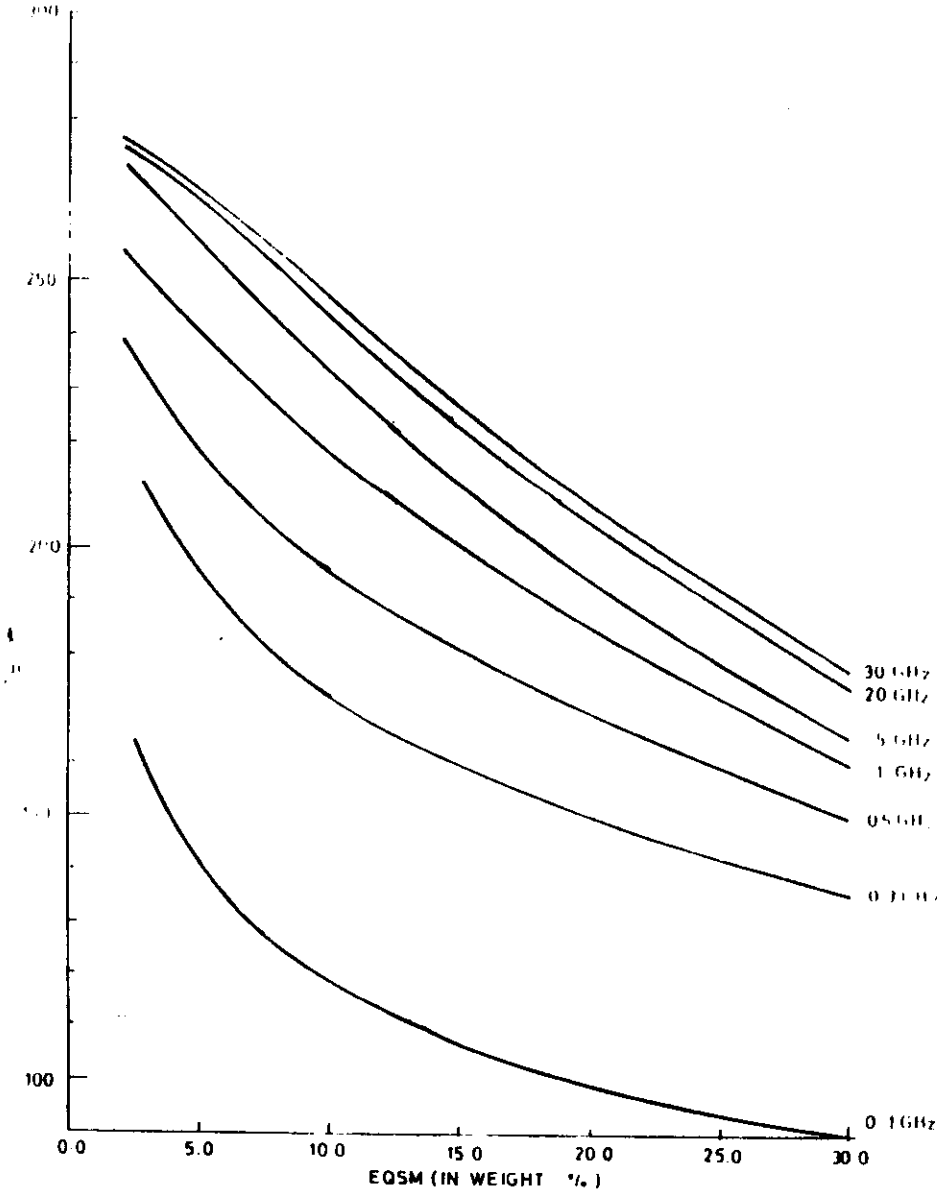

Fig. 6·1 T_B Vs EQSM (in weight %) for constant soil moisture profile at different frequencies (T = 300°k)

35

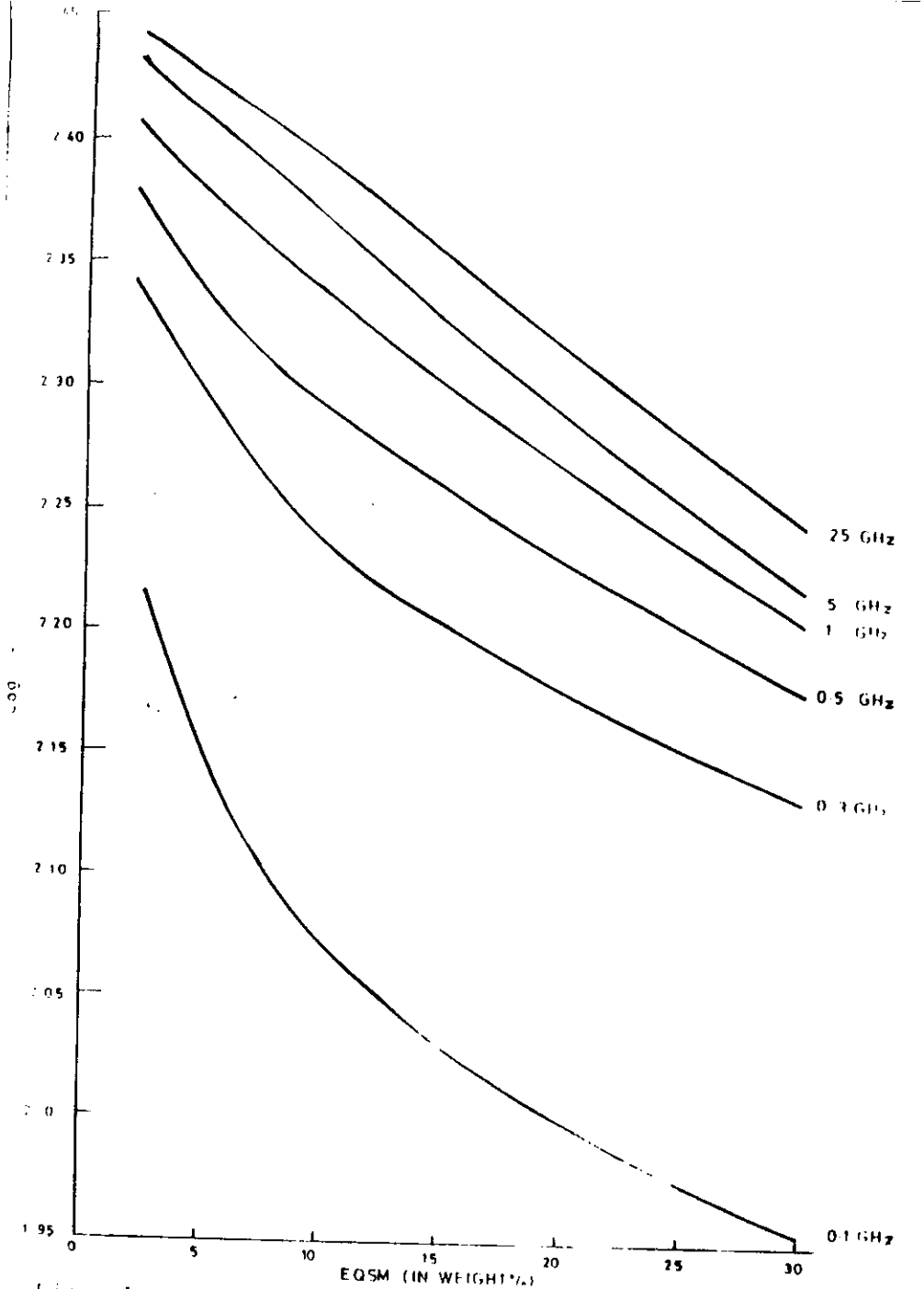

Fig 6.2 Log (T_B) Vs EQSM (in weight %) for constant soil moisture profiles at different frequencies (T=300 °k)

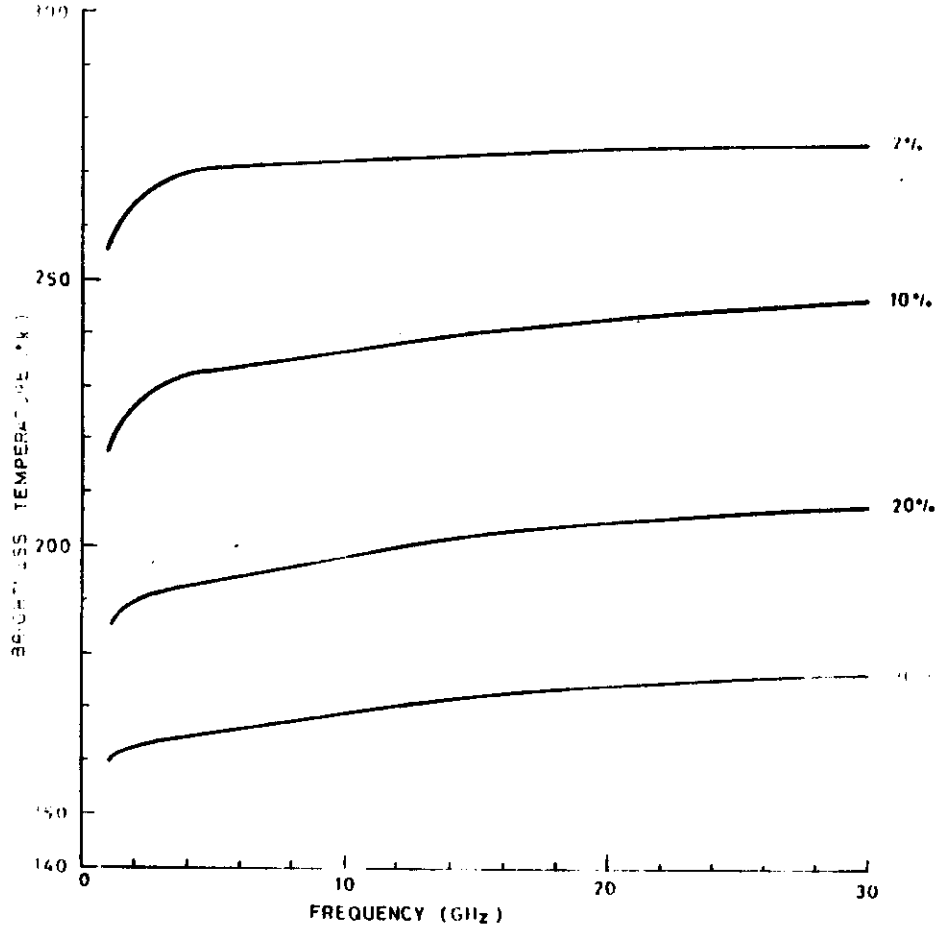

Fig.6.3 T_B Vs Frequency for constant soil moisture profiles

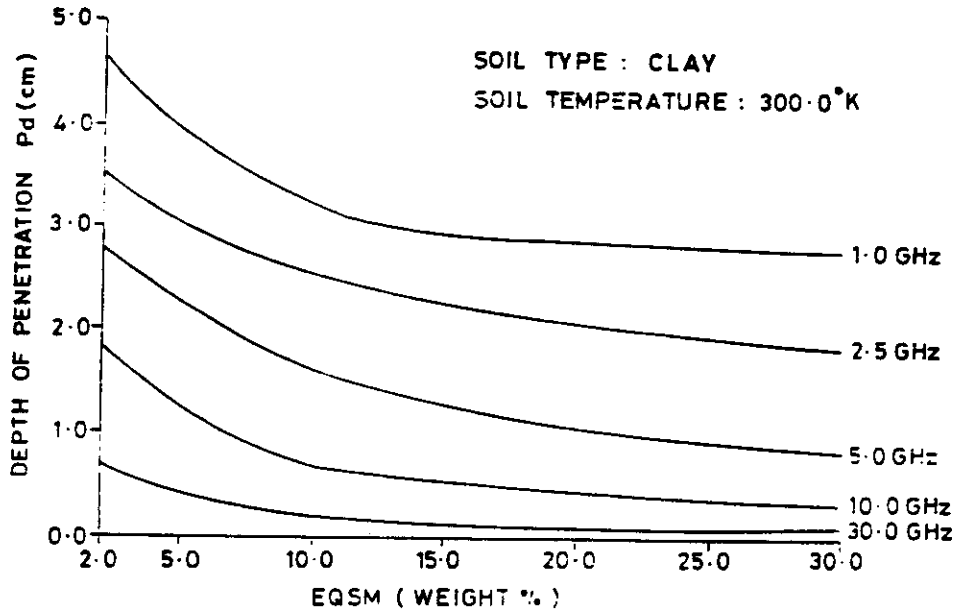

Fig. 7.1 Equivalent soil moisture (EQSM) Vs depth of penetration (Pd) for representative profiles of clay soils of Pune at different frequencies

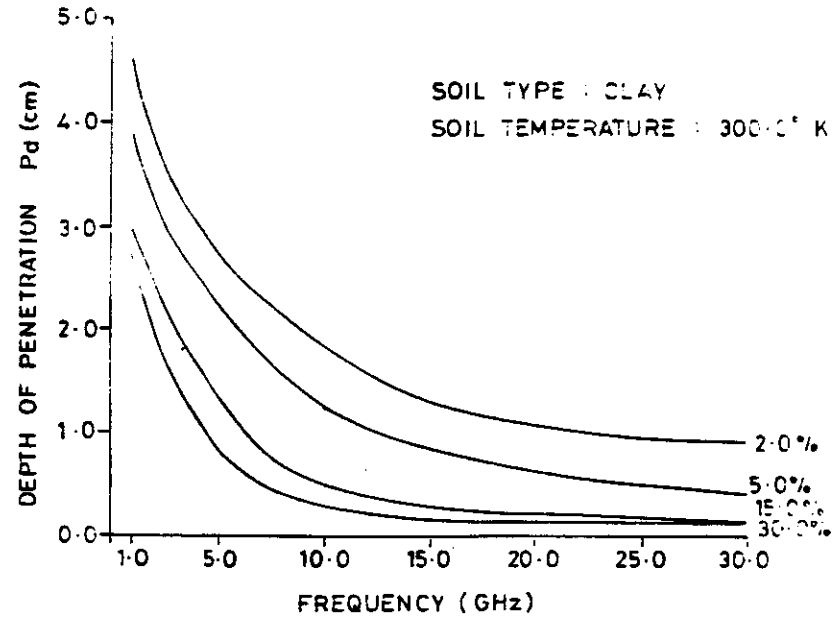

Fig. 7.2 Frequency Vs depth of penetration (Pd) for representative profiles of clay soils of Pune at different soil moisture conditions (weight %)

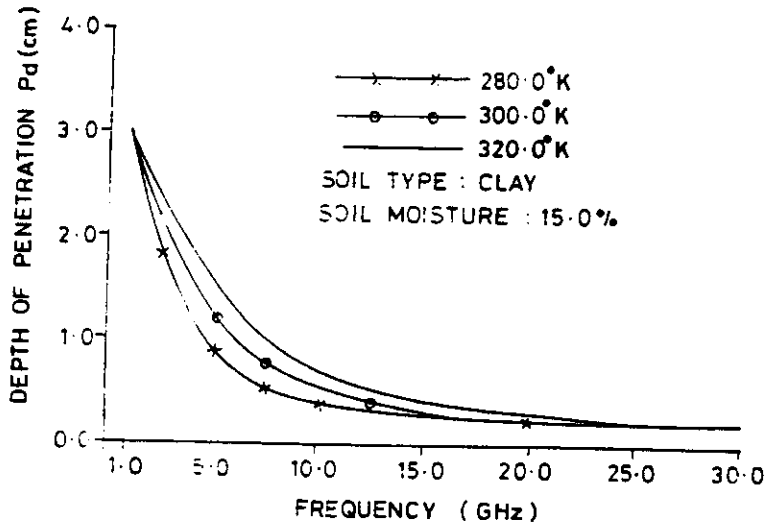

Fig. 7.3 Frequency Vs depth of penetration for different soil physical temperatures

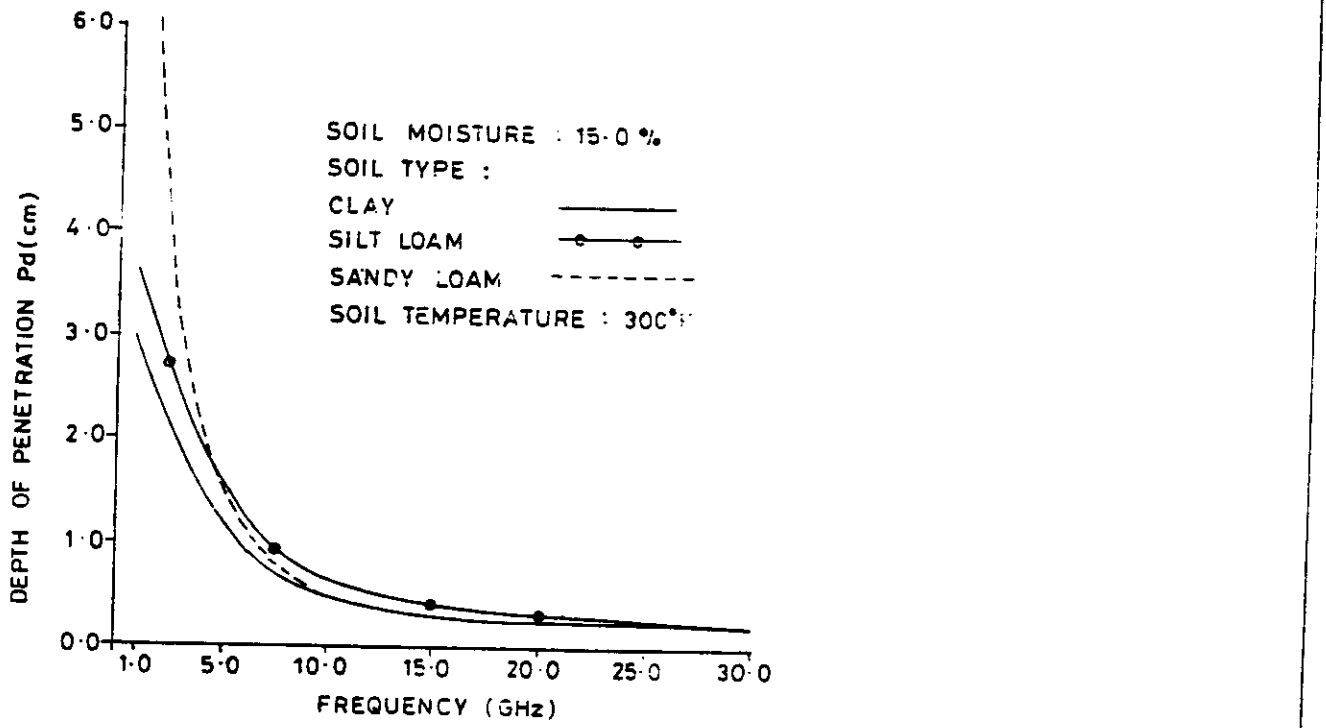

Fig 7.4 Frequency Vs depth of penetration for different soil textures

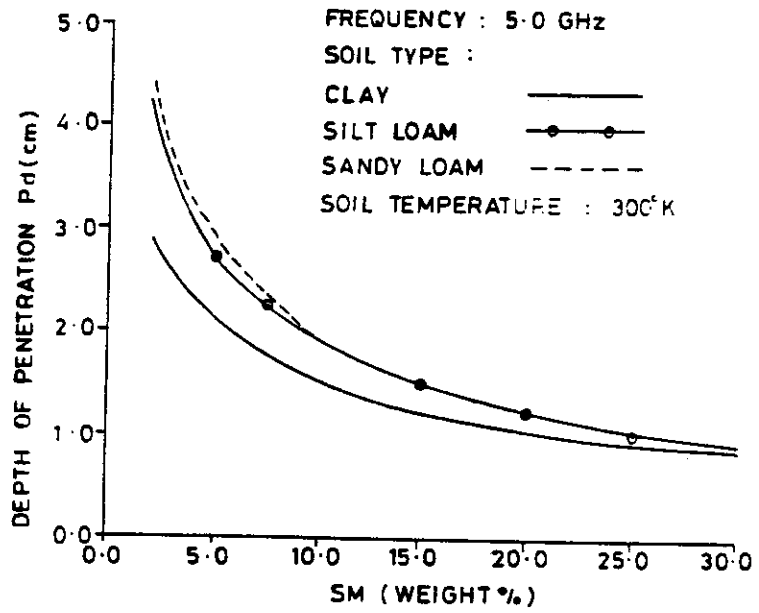

Fig. 3.5 Soil moisture (SM) Vs depth of penetration for different soil fextures

39

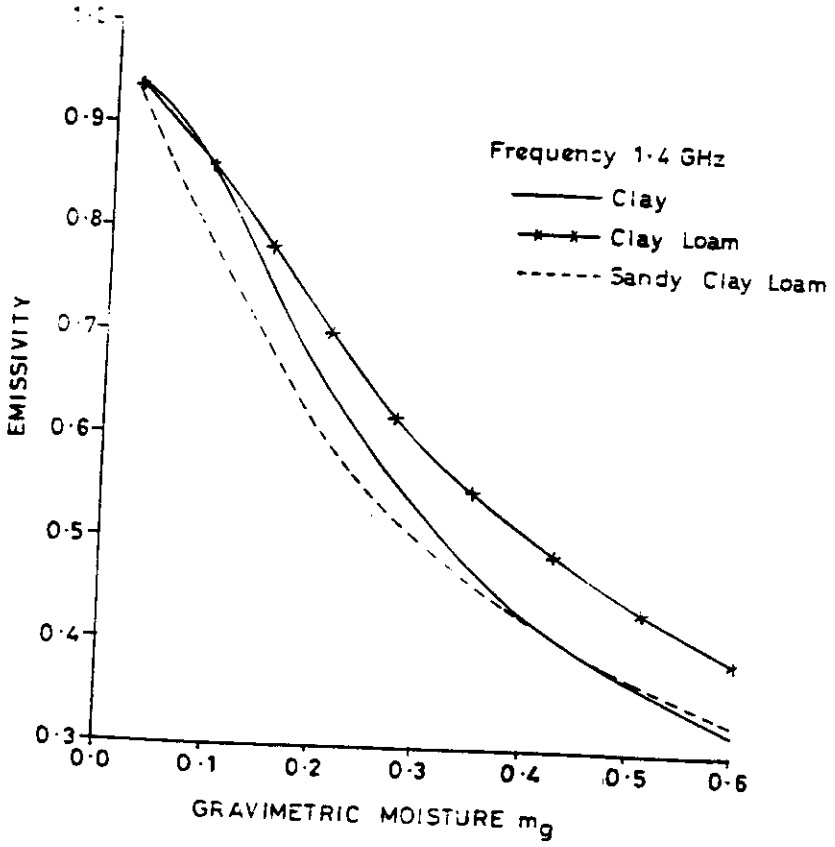

Figure 8.1 Calculated emissivity at 1.4 GHz and 0° incident angle as a function of gravimetric soil moisture(m_g).

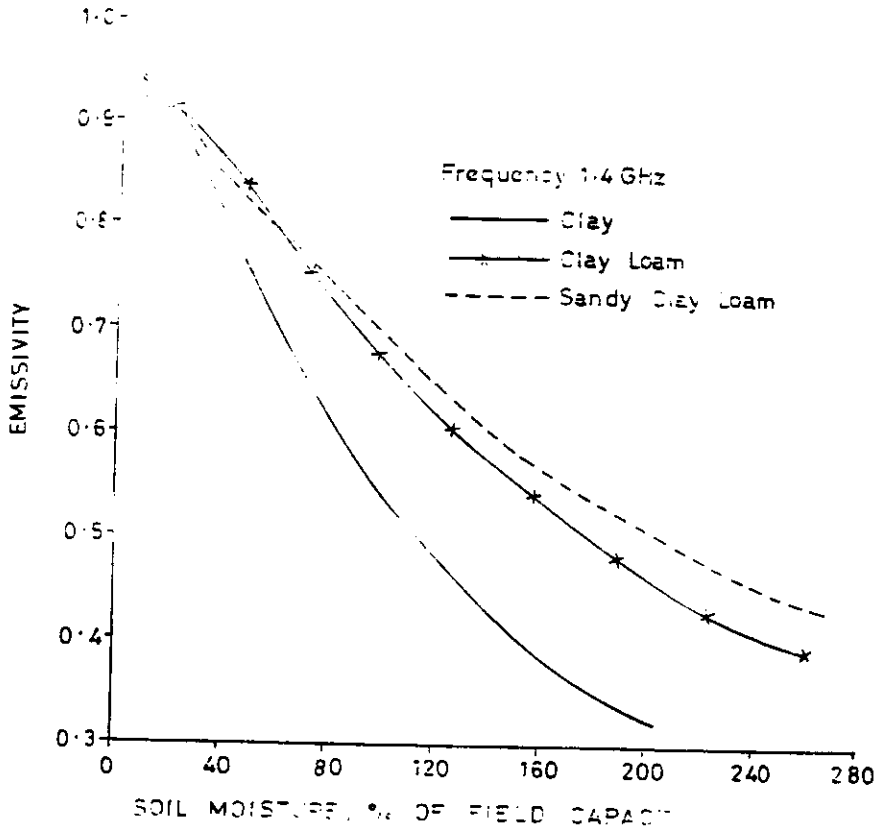

Figure 8.2 Calculated emissivity at 1.4 GHz and 0^{o} incident angle as a function of soil moisture in percentage of field capacity.

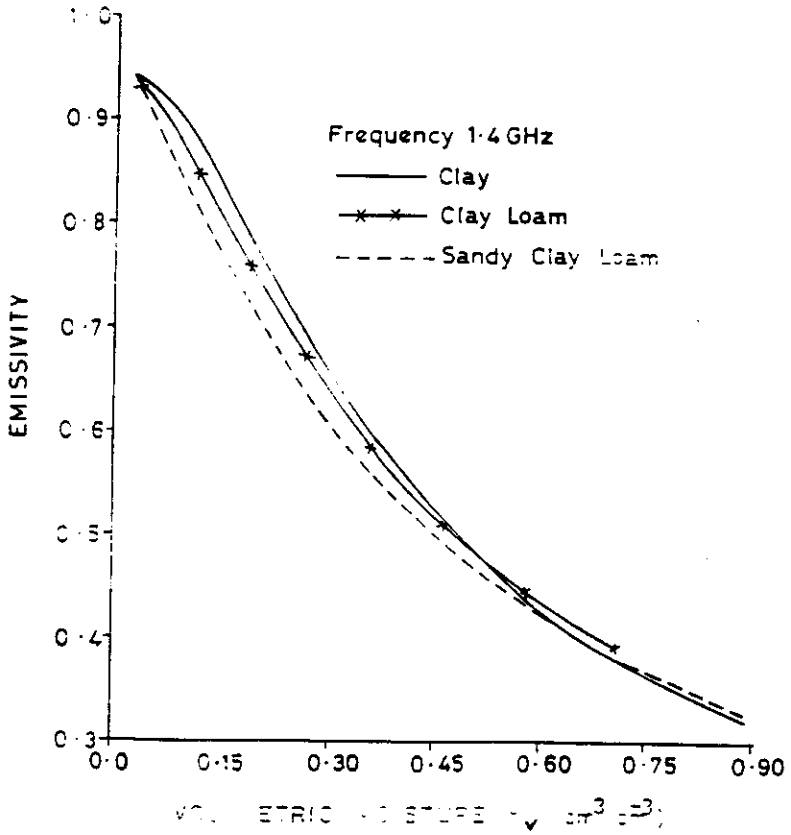

Figure 8.3 Calculated emissivity at 1.4 GHz and 0^{o} incident angle as a function of volumetric soil moisture(m_v).

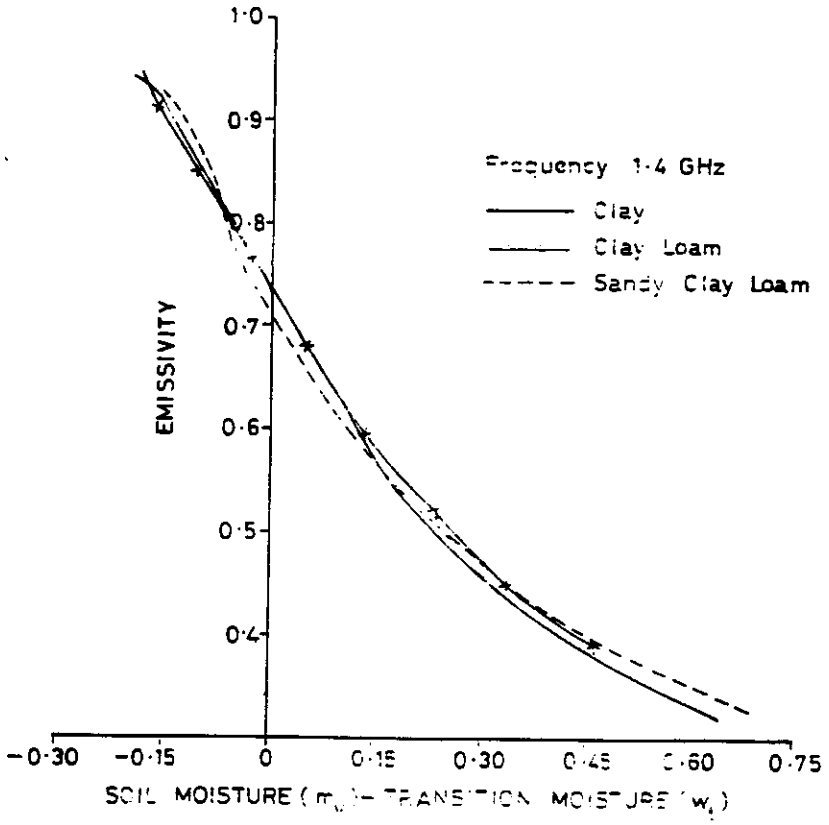

Figure 8.4 Calculated emissivity at 1.4 GHz and 0 incident angle as a function of soil moisture in terms of $(m_v - w_t)$.

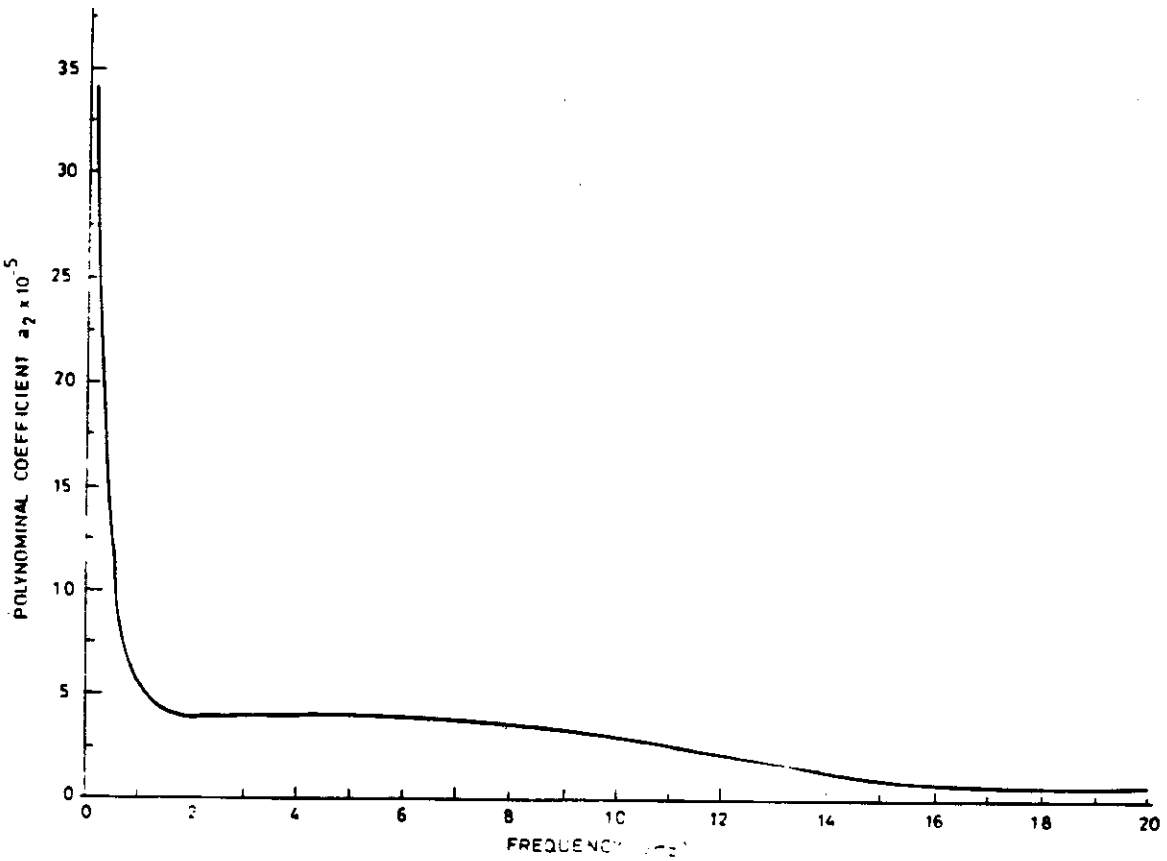

Fig. 9.1 a_2 vs Frequency for constant soil moisture profile

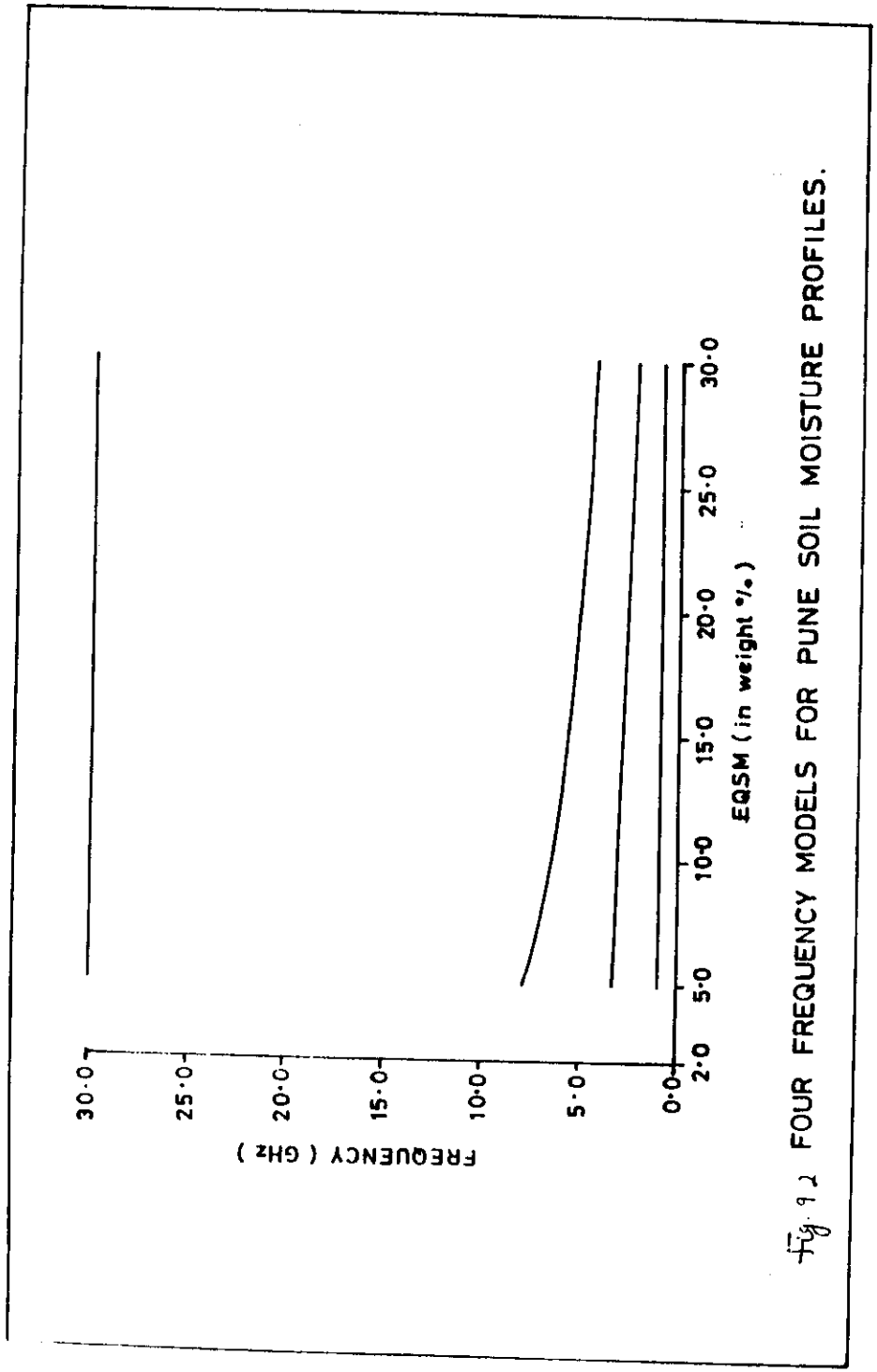

Fig. 9.2 FOUR FREQUENCY MODELS FOR PUNE SOIL MOISTURE PROFILES.

Analysis of Bhaskara - II Satellite Microwave Radiometer Data for Land Based Studies

K.S. Rao, B.K. Mohan, P.V. Narasimha Rao

Centre of Studies in Resources Engineering
Indian Institute of Technology, Powai, Bombay, INDIA

and

R.L. Karale, K.K. Narula

All India Soil and Landuse Survey (AIS & LUS)
I.A.R.I. New Delhi, INDIA

Realizing the importance of microwave remote sensing, India has launched Bhaskara - I and II satellites with microwave radiometers operating at 19.35, 22.235 and 31.4 GHz. The brightness temperature (TB) data was acquired during the period Dec 1981 - July 1983 by the radiometers onboard Bhaskara II. Even though these frequencies are ideally suited for atmospheric studies, attempts are made to utilize these data for land based studies also, in view of extensive coverage over Indian subcontinent. The results are presented in this paper.

INTRODUCTION

It is well known that microwave remote sensing has several advantages over other remote sensing techniques. These are broadly, all-weather capability, day and night operability and penetration into the soil. These qualities of microwave remote sensors are ideally suited for continuous assessment and monitoring of earth resources operationally.

Realising this, India has launched, in a big way, a programme

on microwave remote sensing. As a first step in this direction, Bhaskara - I and II satellites were launched with microwave payloads operating at frequencies 19.35, 22.235 GHz (Bhaskara - I) and 19.35, 22.235, 31.4 GHz (Bhaskara - II) respectively. Bhaskara - II was launched on November 20, 1981 and collected TB data over the Indian subcontinent for a period of 18 months in 325 passes. The specifications of the Bhaskara - II satellite microwave radiometer (SAMIR) payload are given in table 1 (Utilization Cell, 1982).

There are two modes of data collection of SAMIR namely, normal (nonscanning) mode and alternate (scanning) mode. In the normal mode the data is collected at four look angles -5.6^{o}, -2.8^{o}, 2.8^{o} and 5.6^{o} around nadir along the direction of the satellite pass. The TB data is acquired for each spin of the satellite since Bhaskara is a spinning satellite. The data is recorded against each spin nummber starting from 1 for each pass. The size of the radiometer foot print is 125 KM circular diameter. The TB resolution is 1 K.

The frequencies chosen for SAMIR are ideally suited for the retrieval of atmospheric parameters like liquid water content and water vapour (Pandey et al. 1980). However, from the field (Pampaloni, 1983), aircraft (Schmugge, 1974) and satellite (Rao et al. 1986c) experiments, it has been demonstrated that these frequencies can also be used for land based studies. Keeping this in mind several attempts are made to analyse the SAMIR data for the assessment of soil moisture on a large area basis. The work carried out is mainly the specific case studies, statistical

analysis, extraction of broad temporal signatures and generation of colour TB map. In this paper the results on the analysis of SAMIR data have been summarized.

THEORY

The models for the calculation of TB are broadly categorized into two groups namely, coherent (Tsang et al., 1975; Wilheit 1978) and noncoherent (Burke et al. 1979). Through a detailed investigation (Rao et al. 1987a) it has been noticed that the coherent models are more accurate compared to noncoherent ones. From these models it can be seen that there is a need to know the dielectric constant (C) and also the vertical profiles of soil moisture and temperature for the calculation of TB. A study was made (Rao et al. 1987b) to identify the theoretical model for the estimation of dielectric constant. It was concluded from these studies that the Dobson model (Dobson et al., 1985) is more general and covers a wider range of frequencies.

A test site in the agricultural farm land, Pune (India) was selected for the study of soil moisture and temperature profiles. Through a careful analysis of soil moisture and temperature collected over a year, the representative soil moisture and temperature profiles have been obtained (Rao et al. 1986b) as shown in Fig.s 1 and 2.

Using the above models on the representative profiles the TB is calculated as a function of frequency and soil moisture. The results are illustrated in Fig.s 3 and 4. It can be seen from

43

Fig. 5 that as the frequency increases, the TB increases. However, the increase is marginal in the frequency range 19 - 30 GHz. It can be seen from Fig. 4 that TB decreases as the soil moisture increases at all frequencies. The average sensitivity of TB to soil moisture is 3 K per percent soil moisture (Rao et al. 1987c).

The penetration depth of microwaves is calculated as a function of frequency and soil moisture as illustrated in Fig. (Rao et al. 1987d). It can be seen from Fig. 5 that in the frequency range considered here, the penetration depth is very small and particularly responds only to surface soil moisture

DATA QUALITY ASSESSMENT

For quick observation of the data, the TB is plotted as a function of the radiometer spin number as shown in Fig. 6. An observation of all the passes data acquired indicated that the overall quality of the data is good for various applications (R et al. 1987e). However, a careful observation of individual passes data reveal the following points:

(a) Whenever the satellite pass crosses from land to sea or sea to land, sharp overshoots and undershoots in TB values are observed for 19.35 GHz and 31.4 GHz. This can be attributed to the electrical characteristics of the radiometer.

(b) At the begining and end of the satellite passes, the TB data exhibited unduly rapid fluctuations in TB values. These can be attributed to the data acquisition for areas

outside the visibility zone of the receiving station.

(c) The data acquired by SAMIR during the time 20.00 - 04.00 hrs of the day is fairly good and the data acquired during the rest of the day time is completely noisy for 31.4 GHZ and 22.235 GHz and partly noisy for 19.35 GHz.

(d) There is an inaccuracy of about 100 km in the location of satellite foot prints, particularly for ascending passes.

(e) The magnitude of TB values increases with frequency over land which is in agreement with the theoretical observations as illustrated in Fig 3. Over sea it is seen that 22.235 GHz data departs from this trend, which is due to the presence of water vapour which has a resonance line at this frequency.

SPECIFIC CASE STUDIES

From the study of the data of all the passes individually, it has been noticed that inspite of the coarse resolution of the TB data, it is possible to interpret the changes in TB in terms of broad ground features such as soil moisture variations, vegetation cover differences, agroclimatic conditions, and sea and desert areas. There are several passes wherein the radiometers responded very closely to the changes in the ground phenomenon (Rao et al. 1987f). Following are a few examples to illustrate the same. The ground traces are given in Fig. 7 and the TB plots in Fig. 8.

A. Passes referred to Land Data

(1) **PASS 1188:** This pass passes through the Northern Indian state of Jammu and Kashmir (J&K) acquired at 0034 hrs on 7 Feb. 1982 (Fig. 8a). A dip in the TB data is seen at ground location centred at 35° 16' latitude and 77° 23' Longitude The radiometer wise TB values are indicated below:

	Average TB	TB at the dip position	Decrease in TB
R1 (31.4 GHz)	252	213	39
R2 (19.35 GHz)	236	206	30
R3 (22.235 GHz)	251	222	29

An observation of the complete data show that the TB values are fairly low in the areas of Arabian sea, rise sharply near the coastal areas and attain maximum values in Thar desert (Pakistan) through Rann of Kuchchh. This trend is valid for all the three frequencies of the data. However R2 shows lowest values followed by R1 and R3 over Arabian sea area whereas over the deserts the response by R1 and R3 is almost similar. The relatively high values in the desert areas are attributable to the arenaceous nature of soils, lack of soil moisture and scant thorny vegetation. The TB values show a declining trend in the areas over Punjab plains where coarse loamy soils (Ochrepts and Ustalfs) that are mostly underirrigated agriculture during Feb., predominate. Further dip in the TB values over the areas of J & K is, presumably, due to high organic matter content of brown hill forest soils (Udolls) and the luxuriant forest vegetation that they support. The minimum values of TB in all the three different

frequencies are observed over the areas of J & K hills covered with glaciers and snow and register steady increase over cold desert areas in China.

(2) **PASS 835:** This pass passes over the Indus river in northern India to the left of Jammu and Kashmir (Fig. 8b). The data was acquired around 1700 hours on 14 Jan. 1982. A dip in TB has been observed at 36° 11' deg. latitude and 72° longitude. The radiometerwise TB data are as follows:

	Average TB	TB at the dip	Decrease in TB
R1 (31.4 GHz)	260	244	16
R2 (19.35 GHz)	249	240	9
R3 (22.235 GHz)	254	242	12

It can be seen from figure 4b that the TB values (R1) are highest at 40° 26' NL - 65° 01' EL in USSR and decrease slowly attaining a low value at 36° 11' NL, 71° 56' EL in Himachal Pradesh. The low TB values over Himachal Pradesh are partly attributable to heavy foliage in the coniferous forests during this part of the season (14 Jan 1982) and partly to the natures of soils which are predominantly Udalfs with minor inclusions of Ageupts. Further rise in the TB value over U.P. is related to the lack of vegetation and dry nature of light coloured alluvial soils (Ochrepts and Psamments) low in organic matter. A little high TB value at 23° 44' - 86° 19' over Ranchi plateau is not related to soils or vegetation but may perhaps be explainable on the basis of occurrence of exposed base rocks.

(3) **PASS 2887:** This pass passes through Jammu & Kashmir acquired around 0530 hours on 30 May 1982 (Fig. 8c). A dip in TB

data is observed around 36° 24' latitude and 78° 11' longitude. The data of R1 and R3 are completely noisy. The mean value of R2 is 250 K and the TB at the dip position is 215 K, thus giving a change of 35 K. Due to Himalayan snow, the region where the dip is observed is with high soil moisture content which is responsible for the decrease in TB.

The TB values register decrease over Punjab reflecting less emission in Ochrepts and Udalfs compared to light coloured sandy soils of Thar desert and further drop down over snow bound mountains of J & K reaching to minimum in China.

(4). PASS 3130: The pass is acquired on 15 June, 1982 around 7 Hrs (Fig. 8d). The high values of TB with both the R1 and R2 frequencies over the south eastern Bihar area are attributable to lack of vegetaion, industrial activities (mining etc.,) and dominance of skeletal nature of soils with low water holding capacity. A dip in the TB values over the Kosi plains is related to the hydromorphic nature of the soils (Aquepts and Aquents). Minimum TB values are observed over U.P. Himalayas (Sivaliks) where dense cover of sal vegetaion is prevalent. Rise in TB values over areas near Bijnor are again due to loak of vegetaion and dry nature of soils (Orthents, Ochrepts). Sandy and coarse textural soils (Psamments and Orthents) of Punjab plains show maximum TB values.

(5) PASS 3065: The data of this pass was acquired on 10 June 1982 around 2300 Hrs (Fig.8e). The TB values are fairly low over the western coast region, owing presumably to the preponderance

of dense forest vegetaion of tropical ever green nature. A peak high value of TB is observed over Telangana region which is in confirmity with the scanty vegetation of deciduous nature and skeletal soils with low soil moisture content (Haplustalfs and Rhodustalfs) over this pediplain. Sharp decline in the TB values over snow bound mountains of Nepal Himalayas, however, does not need an explanation.

(6) PASS 3145: The pass is acquired on 16 June 1982 at 0630 Hrs (Fig. 8f). This pass shows similar trends in TB values and represents more or less the same soilscapes as that of 3130.

(7) PASS 1158: The pass is acquired on 5 Feb. 1982 at about 0100 Hrs (Fig. 8g). The TB values of this pass are comparable to that of pass 2887 described earlier, having similar soilscapes. The low values over Arabian sea and coast of gulf of Kuchchh rise over the Rann of Kuchchh and register further gradual rise over Barmer area of Rajasthan where sandy soils (psamments, orthids) and thin scruby thorny vegetation predominate. Further decrease over Punjab plains corresponds closely with the nature of soils exhibiting sequential decrease from Orthids to Fluvents and Ochrepts through Orthents. As expected further decrease is observed over snow clad mountains of U.P. Himalayan and Tibet.

(8) PASS 299: The data of this pass was acquired on 10 Dec. 1981 around 0722 Hrs. (Fig. 8h). The R2 value is low at 29° 16' NL, 78° 10' EL (near Dehradun) owing to the soils with high organic matter content (Udolls, Udalfs) and high density of

GE

vegetation with profuse foliage cover that is expected in the month of December. The values rise sharply upto 28 51' - 78 37' near Bijnor and remain uniform upto 25 31' - 82 05' near Allahabad having Ochrepts and Fluvents. These are mostly cultivated areas lying fallow during this period of the year. further rise upto 23 23' - 84 09' at Daltonganj and 20 48' - 86 35' near Dhankenal relate to lack of vegetation, dry nature of soils (Ustalfs, Orthents) with exposed bare rocks at places. The TB values sharply decline near Bay of Bengal where deltaic conditions prevail. After reaching a minimum value over Bay of Bengal it shows a slight rise over the Andamans having Fluvents and Orthents under very dense forest cover.

B. Passes around Sri Lanka

(9) **PASS 323:** This pass is over the middle of Sri Lanka acquired on 11 Dec 1981 at 2030 hours.

	Average TB	TB at the peak	Increase in TB
R1 (31.4 GHz)	168	212	44
R2 (19.35 GHz)	150	194	44
R3 (22.235 GHz)	188	208	20

The large difference in TB over sea between 19.35 and 22.235 GHz is due to the presence of high water vapour content. As the pass extneds to Sri Lanka land, the difference in TB between these two frequencies has decreased considerably.

(10) **PASS 1142:** This pass is over Sri Lanka adjacent to the earlier pass 323. The data has been collected on 3 Feb. 198[illegible] at about 2330 hours. The average TB difference observed here is of

the order of 30 K.

(11) **PASS 2841:** This pass is also over Sri Lanka with an average TB difference of 20 K. A comparison of the three passes over Sri Lanka indicates that, depending on the land portion covered in the resolution cell, the extent of the increase of TB varied.

(12) **PASS 2856:** This pass is going through the middle of Sri Lanka and India acquired on 23 Feb. 1982 at 0145 Hrs. Therefore it encounters land-sea-land alternately, thus showing multiple peaks in TB data.

C. Pass over Andaman and Nicobar Islands

(13) **PASS 1246:** This pass is over Andaman, Nicobar islands in the Bay of Bengal. As the size of these islands is very small, there is a difference of only 10 K in TB. Thus it indicates that even though the ground resolution is extremely poor, the smaller objects will be noticed whenever there is a very high TB contrast.

A detailed ground truth survey has to be conducted to analyse the variations in TB with reference to the ground phenomena and arrive at quantitiatve conclusions.

HISTOGRAM ANALYSIS

It may be noted from the above analyses that the correlations reported are only qualitative in nature and not quantitative. This is mainly due to the coarse resolution of the

64

system. Therefore it is felt appropriate to draw some general conclusions also over the complete Indian landmass in view of its coarse resolution. For this purpose, the data acquired in Feb. 1983 comprising 23 passes have been used. The ground traces of these passes are shown in Fig. 9. It can be seen from the above figure that there is a good coverage over the Indian subcontinent. The data corresponding to individual radiometers are pooled separately and TB histograms are drawn for each of them, as shown in Fig.10. It may be noted that the TB data corresponding to 2.8 have only considered for each spin in view of large overlap between footprints of different lookangles.

The TB data acquired over Himalayan snow/ice regions is separated on the basis of a geographical threshold. The histograms shown in the figure comprise three major peaks corresponding to sea, land and snow/ice data. The atmospheric corrections have been carried out for 19.35 GHz data based on the two frequency model developed by Rao et al. (1983), and shown in the same figure. The following observations can be made from the histograms (Rao et al. 1984):

a) As the histograms shown symmetric gaussian-like distributions, the standard deviation σ of each of the peaks is estimated and it is found to be about 6 K. The temperature resolution of the radiometer is about 1 K. The large value of σ may be attributed to varying conditions of sea and atmosphere as the total data used in these analyses is spread over 12 days.

b) The influence of atmospheric water vapour on TB is considerable over sea compared to over land. This can be noticed from the shift of the sea peak position in the corrected data histograms by about 8 K as compared to the negligible shift of the land peak.

c) The spread in the snow/ice data is of the order of 45 K. This may be due to partial coverage of land and snow regions and different stages of wetness of snow. The spread in the land peak is around 50 K. It may be noted that the data used for the histogram is collected over different times of the day. Therefore the spread in the land peak TB may be attributed partially to the changes in physical temperature and to the changes in the surface soil moisture conditions.

The TB signatures extracted from these histograms for sea, snow/ice regions and moist soils are summarized in Table 2.

BROAD TB SIGNATURES

As indicated earlier, the SAMIR system has collected TB data in about 325 passes during the period Dec. 1981 - June 1983. Statistical analysis of the data indicated that most of the data have been acquired during specific time intervals of the day and during certain months of the year. Table 3 shows the number of passes acquired in each interval.

Histograms are generated for each data set and around 100 temporal TB signatures at 19.35, 22.235 and 31.4 GHz pertaining to broad regions of land, sea and snow/ice have been extracted

(Rao et al. 1986a). Statistical techniques have been adopted to arrive at these signatures by careful study of TB data acquired over the Indian subcontinent. The results are given in Tables 4a-c. The following can be seen from the above tables.

In general it has been observed from tables 4a-c that the TB signatures obtained during 1500 - 2000 hours have higher TB values compared to the other timings of the day. This may be partially due to the higher physical temperatures and partially due to lower surface moisture conditions. The TB signatures during Dec. 1981 - Feb. 1982 and Dec. 1982 - Feb. 1983 are more or less same. Similarly, the TB signatures of April - June 1982 and April 1983 - June 1983 also agree with each other. Moreover the TB signatures of winter season are lower compared to those of summer season. A comparison of the three frequency signatures shows that they are in increasing order of TB.

The comparison of 19.35, 22.235 and 31.4 GHz signatures of snow/ice (Table 4c) shows that 19.35 GHz data has lower TB signatures compared to that of the other frequencies. However, the signatures of 22.235 GHz and 31.4 GHz data show more or less same signatures. The signatures of 31.4 GHz data are slightly (about 1 K) on the higher side of 22.235 GHz data.

In general it has been observed from Table 4b that the TB of sea is highest for 22.235 GHz and lowest for 19.35 GHz. The TB signatures of 31.4 GHz data are in between those of the other two frequencies data.

COLOR TB MAP OF INDIAN SUBCONTINENT - INFERENCE ON SOIL MOISTURE VARIATIONS

So far the analyses of the TB data have been carried out in terms of single individual passes for correlating to the ground phenomena. It is felt that it would be useful to have a two-dimensional image data for mapping purposes and for better interpretability. By suitably interpolating for data over ground locations not covered, a TB map of the Indian subcontinent is generated using digitl image processing techniques as described below.

From the timewise distributions of the passes as given in Table 3, the data acquired during April - June 1982 around 0 hours has a good geographical coverage over the Indian subcontinent. A quick appraisal of the data indicated that the TB data for 31.4 GHz and 22.235 GHz were noisy for many of the passes whereas the data for 19.35 GHz were of good quality (Table 4). Therefore, only these data were chosen for generating a colour TB map of the Indian subcontinent (Rao et al., 1986c). It may also be noted that among the three frequencies, 19.35 GHz data has better correlation with surface soil moisture. While generating the TB map, care is taken to eliminate the noisy data.

The boundary of India and Sri Lanka is digitized manually and stored in a raster form in a 400x400 matrix which comes to a spatial resolution of 6' x 6' in terms of latitude - longitude. The TB data of all the passes at 19.35 GHz are filled in the grids according the geographic positions. The geographical distribution of the blank pixels is highly random and so simple

49

linear interpolation technique is adopted to fill the blank pixels.

The histogram of the data is analyzed to note the ranges of TB for land and sea peaks. The TB range has been stretched nonlinearly between 0 and 255. Greater attention is given to the land peak while stretching the data in such a way that (i) most of the dynamic range is allotted to the land peak and (ii) the stretching function is derived from the land peak histogram. The latitude - longitude grid with boundary of India and Sri Lanka is superimposed over the TB data matrix. The colour TB map is produced by generating two more data sets as given in Table 6 and superimposed on the first set with different colours assigned to different sets (using Optronics Colormation photoread/write system).

A comparison of the colour TB map with the moisture retention characteristics of soils reveals that a broad general trend does emerge. The cyan colour on the TB map (Fig. 11) exhibited over the Jammu and Kashmir (J&K) state and Terai belt of Uttar Pradesh corresponds to the soils rich in organic matter high moisture retention. The regions of Kashmir have exhibited dark blue colours representing maximum moisture. Likewise the coastal regions of the country corresponding to soils characterized by high water retention have appeared as having cyan colours. The dark red colours supposed to be representing the driest conditions have been exhibited over parts of Rajasthan south central and southern parts of the country. The dark red

colour on the eastern part of the country correspond to the soil with low moisture retention at the surface.

In contradiction to the agreements in the soil moisture retention and colour TB map, at certain places, the black soil regions have appeared in dull red and dark grey colours representing low to moderate moisture conditions. It is worth mentioning in this context that the colours exhibited by the TB map represent average values for moisture conditions over very broad regions whereas the soil moisture conditions within this region may vary widely depending on the local physiographic conditions, irrigation and several other factors.

CONCLUSIONS

This paper presents a consolidated work on the use of Bhaskara-II SAMIR data for land based studies. The results presented here demonstrate the capability of 19.35, 22.235 and 31.4 GHz for extracting information on land features, soil moisture etc. inspite of coarse resolution.

ACKNOWLEDGEMENTS

The authors thank the Head, CSRE for his continued encouragement throughout the course of this work. The authors are grateful to Space Applications Centre, Ahmedabad for providing the Bhaskara-II SAMIR data and also for allowing the use of their photo-read/write system. The authors thankfully acknowledge the help extended by various colleagues of CSRE through several fruitful discussions. Finally, the authors the Department of Science and Technology for providing financial support for this research.

REFERENCES

Burke, W.J., Schmugge, T.J., and Parks, J.F., (1978). Compari of 2.8 and 21cm microwave radiometer observations of inte erence effects, J. Geophy. Res., 83, 2077-2083.

Dobson, M.C., Ulaby, F.T., Hallikainen, M.T., and El Rayes, M.A., (1985). Microwave dielectric behaviour of wet soils - Part II: dielectric mixing models, IEEE Trans. Geosci. and Rem Sensing, GE-23, 35-46.

Eagleman, J., and Lin, W., (1976). Remote Sensing by a 21cm Passive Radiometer, J. Geophy. Res., 81, 3660-3666.

McFarland , M.J., (1976). The Correlation of Skylab 2 Band Brightness Temperature with Antecedent Precipitation, proc. Conf. Hydrometeorology, 60, American Meteor. Soc., Boston.

Newton, R.W., (1977). Microwave Remote Sensing and its Applications to Soil Moisture Detection, Tech. Report, RSC-81, Texas A&M Univ., College Station.

Pampaloni, P., Paloscia, S., Zipoli, G., (1983). Microwave emission of soil and vegetation at X and Ka bands. International Geoscience and Remote Sensing Symposium held at Sanfrancisco, California, IEEE Catalogue no. 83CH1837-4.

Pandey, P.C., Sharma, A.K., and Gohil, B.S., (1980). Capability of Bhaskara SAMIR to distinguish atmospheric water vapour and liquid water contents, Pro. Ind. Acad. Sci. 89(2).

Rao, K.S., Murthy, Y.V.S., Gopalan, A.K.S., Ramakrishnan, R., and Majumdar, T.J., (1983). Model for the atmospheric corrections to microwave brightness temperature data, Rem. Sen. of Env., 13, 209-236.

Rao, K.S., Venkatachalam, P.,Sowmya, A., Majumdar, T.J., (1985). Capability of Bhaskara - II Microwave Radiometer Brightness Temperature Data to Discriminate Soil Moisture Condition Indian Landmass, Adv. Space Res., 4: pp 91-96.

Rao, K.S., Mohan, B.K., Venkatachalam, P., Karale, R.L., and Saini, K.M., (1986a). Temporal Brightness Temperature signatures of Land, Sea and Snow/Ice at 19.35, 22.235, and 31.4 GHz, J. Indian Soc. Remote Sensing, 14, pp 9-22.

Rao, K.S., Y. Subrahmanyeswara Rao, Girish Chendra, B. K. Mohan and P. Venkatachalam, (1986b). Representative profiles of soil moisture and temperature of black soil in the context of Microwave Remote Sensing, Proceedings of the fifth annual conference on hydrology, Bhopal.

Rao, K.S., Sowmya, A., Mohan, B.K., Venkatachalam, P., and Ahmed, N., Karale, R.L., and Narula, K.K., (1986c). Computer-Aided Brightness Temperature Map of Indian Subcontinent - Influence on Soil Moisture Variations, Remote Sensing of Environment, 20.

Rao, K. S., Rao, Y. S., Suresh Raju, C., (1987a). A study on theoretical models for the calculation of Brightness Temperature - comparison with the expreimental results, communicated to Remote Sensing of Environment.

Rao, K.S., Girish Chandra, and Suresh Raju, C.,(1987b). Comparative study on different dielectric models - computation representative profiles of black soils, to be published in Journal of Indian Society of Remote Sensing, Vol. 15 (2).

Rao, K. S., Girish Chendra, Narasimha Rao, P. V., (1987c). study on relation between Brightness Temperature and moisture; selection of frequency range for Microwave Remote Sensing, to be published in International Journal of Remote Sensing.

Rao, K. S., Girish Chandra, Narasimha Rao, P. V., (1987d), Study on penetration depth and its dependence on frequency, moisture, texture and temperature, communicated to Indian Journal of Society of Remote Sensing.

Rao, K.S., Mohan, B.K., Narasimha Rao, P.V., and Karale, R.L. (1987e), Some Useful Observations in the Analysis of Brightness Temperature Data Acquired by Bhaskara - II SAMIR System, to be published in Int. J. of Remote Sensing.

Rao, K. S., Narasimha Rao, P. V., Mohan, B.K., Karale, R. L. and Narula, K. K., (1987f), Capability of Bhaskara Satellite Microwave Radiometer for land studies: correlation with ground truth, communicated to International Journal of Remote Sensing.

Schmugge , T.J., (1974), Remote Sensing of surface Soil Moisture J. Geophy. Res., 79, pp 317-323.

Tsang, L., Njoku, E., and Kong, J.A., 1975, Microwave Thermal Emission from a Stratified Medium with Nonuniform Temperature Distribution , J. Applied Physics, 46, 5127-5133.

Utilisation cell, (1982), Bhaskara II SAMIR data User's guide, SAC - RSA - UC - IN - 02, Space Applications Center, ISRO, Ahmedabad, India.

Wilheit, T.T., 1978, Radiative Transfer in a Plane Stratified Dielectric , IEEE Trans. Geosci. Electronics, GE-16, pp 138-143.

S1

Table 2: Radiometer Signatures (TB in deg. K)

		R1 (31.4 GHz)	R2 (19.35GHz)	Atmospheric Corrected R2(19.35 GHz)	R3 (22.235 GHz)
1).	Complete Data Sea Peak	165 ± 7	142 ± 7	134 ± 8	183 ± 6
					196 ± 3
	Land Peak	265 ± 6	246 ± 6	245 ± 6	260 ± 4
2).	Excluding snow/ice Sea Peak	165 ± 7	142 ± 8	134 ± 8	183 ± 6
	Land Peak	265 ± 7	246 ± 6	245 ± 7	260 ± 4
3).	Snow/ice regions	228	213 227 237	215	229
4).	Moist soil range	210-276	211-256	217-261	225-270
5).	Snow/ice range	217-249	201-245	198-245	215-260

52

Table 1. Salient features of Bhaskara - II SAMIR system

1. Frequency of operation (GHz)	: 19.35, 22.235, 31.4
2. Look angles around nadir (for TB measurement)	: $\pm 2.8^{o}$, $\pm 5.6^{o}$
3. TB resolution of radiometers	: 1 K
4. Modes of operation	: Non-scanning (normal) Scanning (alternate)
5. Radiometer foot print size	: 125 Km circular diameter (1^{o} lat. X 1^{o} lon. approx)

Table 4a. Peak position and Spread in TB data over Land (deg. K)

		00.00–04.00hrs.	04.00–08.00hrs.	15.00–20.00hrs.	20.00–24.00hrs
M1	f1	241,246,250,(218–255)	244,(227–254)	257,(245–266)	252,(225–257)
	f2	249,258(234–271)	-	263,(251–272)	260,(236–270)
	f3	256,261,(224–272)	-	270,(255–282)	265,(215–272)
M2	f1	252,(222–260)	254,(197–267)	265,(234–274)	256,(226–265)
	f2	264,(Data has a spread upto 274 deg k)	-,(197–281)	267,275,(248–278)	270,(250–280)
	f3	269,(242–276)	-	—	271,(243–282)
M3	f1	246,(225–251)	-,(228–254)	—	248,(220–256)
	f2	261,(246–266)	251,(236–266)	—	262,(252–271)
	f3	262,(239–268)	--	—	265,(233–274)
M4	f1	252,(210–258)	256,(232–265)	269,(238–276)	257,(233–262)
	f2	267,(239–274)	269,(254–280)	—	272,(251–278)
	f3	266,(225–277)	--	--	275,(263–280)

For every entry:

First value(s): Peak positions; - denotes no peak
Values inside paranthesis: Range of TB

Table 3. Availability of data Passes

Duration	00.00hrs to 400hrs	400hrs to 800hrs	1500hrs to 2000hrs	2000hrs to 2400hrs
Dec. 1981 to Feb 1982	15	18	22	25
April 1982 to Jun 1982	12	30	11	20
Dec 1982 to Feb 1983	17	12	-	17
Apr. 1983 to Jun 1983	9	15	14	10

Note : The numbers indicate the number of passes during that specific interval

Table 4c. Peak position and Spread in TB data over Himalayan Snow/Ice Regions (deg. K)

		00.00-04.00hrs.	04.00-08.00hrs.	15.00-20.00hrs.	20.00-[illegible]0hrs
M1	f1	217,227,233,240 (200-243)	-,(215-241)	227,247,(224-254)	220,(2[illegible]250)
	f2	Multiple peaks,(219-256)	-	234,251,(-)	228,([illegible]259)
	f3	227,244,256,(213-259)	-	-,(221-269)	-,(218-264)
M2	f1	219,(205-253)	-,(215-257)	-,(249-271)	-,(22[illegible])
	f2	232,(222-267)	198,204,(211-272)	-	249,(239-270)
	f3	231,(217-269)	-	--	-,(234-271)
M3	f1	213,231,(205-238)	-,(219-237)	--	-,(215-235)
	f2	229-243,(223-254)	243,(236-251)	--	-,(226-253)
	f3	-,(219-256)	--	--	-,(222-253)
M4	f1	243,(223-254)	236,244,(232-248)	254,(249-265)	-,(228-260)
	f2	260,(238-267)	-,(238-264)	--	-,(247-273)
	f3	261,(255-268)	--	--	250,(245-277)

For every entry:

First value(s): Peak positions; - denotes no peak
Values inside paranthesis: Range of TB

Table 4b. Peak position and Spread in TB data over Sea (deg. K)

		00.00-04.00hrs.	04.00-08.00hrs.	15.00-20.00hrs.	20.00-24.00hrs
M1	f1	142,155,(127-475)	142,157,164(137-190)	155,(139-171)	145,(134-185)
	f2	182,(170-210)	Multiple peaks(169-220)	177,184,193(169-215)	182,198(163-)
	f3	164,(157-183)	161,176 (-)	176,(162-188)	167,(157-195)
M2	f1	136,154,(125-180)	-,(136-186)	148,162,(141-194)	156,(137-187)
	f2	-, (168-)	179,(173-190)	211,(195-)	210,(217-)
	f3	160,172,(153-193)	-	--	174,(160-194)
M3	f1	138,(127-182)	144,(136-173)	--	146,(132-193)
	f2	178,(168-)	186,196,(172-)	--	186,202,(175-)
	f3	163,(156-196)	--	--	171,(159-192)
M4	f1	159,(147-184)	-,(144-181)	163,(150-189)	160,(137-184)
	f2	218,(204-)	-,(186-)	--	-,(206)
	f3	180,200,(169-217)	--	--	181,(172-194)

For every entry:

First value(s): Peak positions; - denotes no peak
Values inside paranthesis: Range of TB

Table.6 Gray Level Assignments to Red, Blue and Green Components

ACTUAL RANGE	ASSIGNED RANGE		
	RED	BLUE	GREEN
120-180	4-33	254-224	91-200
181-230	34-253	224-5	74
231-290	254	4	74
291-300	0	0	0
301			

Table 5. Data Quality of Passes

Sr. No.	Orbit No.	Date	Time	RADIOMETER (G/B) R 1	R 2	R 3
1.	2191	14.4.82	7:02	B	G(all)	B
2.	2206	15.4.82	6:49	B	G(all)	G(all)
3.	2221	16.4.82	6:36	B	G(all)	G(all)
4.	2236	17.4.82	6:24	B	G(all)	G(all)
5.	2251	18.4.82	6:10	B	G(all)	G(all)
6.	2266	19.4.82	5:56	B	G(19,100)	G(19,100)
7.	2737	20.5.82	7:41	B	G(all)	B
8.	2752	21.5.82	7:31	B	G(all)	B
9.	2767	22.5.82	7:15	B	G(12,100)	B
10.	2782	23.5.82	7:01	B	G(12,100)	B
11.	2812	25.5.82	6:34	B	G(all)	B
12.	2827	26.5.82	6:22	B	G(all)	B
13.	2841	27.5.82	4:28	B	G(all)	B
14.	2842	27.5.82	6:07	B	G(all)	B
15.	2856	28.5.82	4:15	B	G(all)	B
16	2871	29.5.82	4.01	B	G(all)	G(all)
17.	2872	29.5.82	5.41	B	G(all)	B
18.	2887	30.5.87	5.28	B	G(all)	B
19	2902	31.5.82	5:11	B	G(all)	B
20.	3130	15.6.82	6:54	B	G(7,100)	G(7,100)
21.	3145	16.6.87	6:39	B	G(all)	G(all9
22.	3160	17.6.82	6:27	B	G(all)	G(all)
23.	3175	18.6.82	6.13	B	G(all)	G(all)

G(all) : Entire pass is good

G(m,n) : Data good from spon m to spin n.

B : Bad

LIST OF CAPTIONS OF FIGURES

FIGURE 1. REPRESENTATIVE SOIL MOISTURE PROFILES OF BLACK SOILS OF PUNE, INDIA

FIGURE 2. REPRESENTATIVE SOIL TEMPERATURE PROFILES OF BLACK SOILS OF PUNE, INDIA

FIGURE 3. BRIGHTNESS TEMPERATURE V/S FREQUENCY FOR CONSTANT SOIL MOISTURE PROFILES

FIGURE 4. BRIGHTNESS V/S CONSTANT SOIL MOISTURE (BY WEIGHT PERCENTAGE) AT DIFFERENT FREQUENCIES (FOR T 300K)

FIGURE 5. FREQUENCY V/S DEPTH OF PENETRATION FOR DIFFERENT SOIL TEXTURES

FIGURE 6. BRIGHTNESS AS A FUNCTION OF SPIN NUMBER

FIGURE 7. GROUND TRACES OF BHASKARA II SATELLITE FOR WHICH VARIATIONS IN TB VALUES ARE OBSERVED

FIGURE 8a. BRIGHTNESS TEMPERATURE VARIATIONS OVER JAMMU & KASHMIR (ORBIT 1188)

FIGURE 8b. BRIGHTNESS TEMPERATURE VARIATIONS OBSERVED FOR THE PASS (ORBIT 805) OVER INDUS RIVER AND LEH SIDE OF JAMMU AND KASHMIR

FIGURE 8c. BRIGHTNESS TEMPERATURE VARIATIONS OVER JAMMU AND KASHMIR (ORBIT 2887)

FIGURE 8d. OBSERVED BRIGHTNESS TEMPERATURE VARIATION FOR THE ORBIT 3130 OVER BIHAR AND WEST BENGAL

FIGURE 8e. PLOT SHOWING THE VARIATION OF BRIGHTNESS TEMPERATURE OVER KARNATAKA, ANDHRA PRADESH, MADHYA PRADESH AND BIHAR (ORBIT 3065)

FIGURE 8f. BRIGHTNESS TEMPERATURE VARIATIONS OVER ORISSA, MADHYA PRADESH, UTTAR PRADESH, HARYANA AND PUNJAB (ORBIT 4135)

FIGURE 8g. PLOT SHOWING THE BRIGHTNESS TEMPERATURE VARIATION OVER HIMACHAL PRADESH AND EAST OF KASHMIR HIMALAYAN SNOW/ICE REGIONS (ORBIT 1150)

FIGURE 8h. BRIGHTNESS TEMPERATURE V/S SPIN NUMBER FOR THE ORBIT 299 OVER NORTH ANDAMAN ISLANDS

FIGURE 9. GROUND TRACES OF BHASKARA II SAMIR DATA ACQUIRED DURING 9 FEB 83 TO 21 FEB 83

FIGURE 10. HISTOGRAMS FOR THE THREE RADIOMETERS IN BOTH APC FOR 19.35 GHz CORRECTED DATA

FIGURE 11. [illegible] OF MEAN [illegible] FOR [illegible]

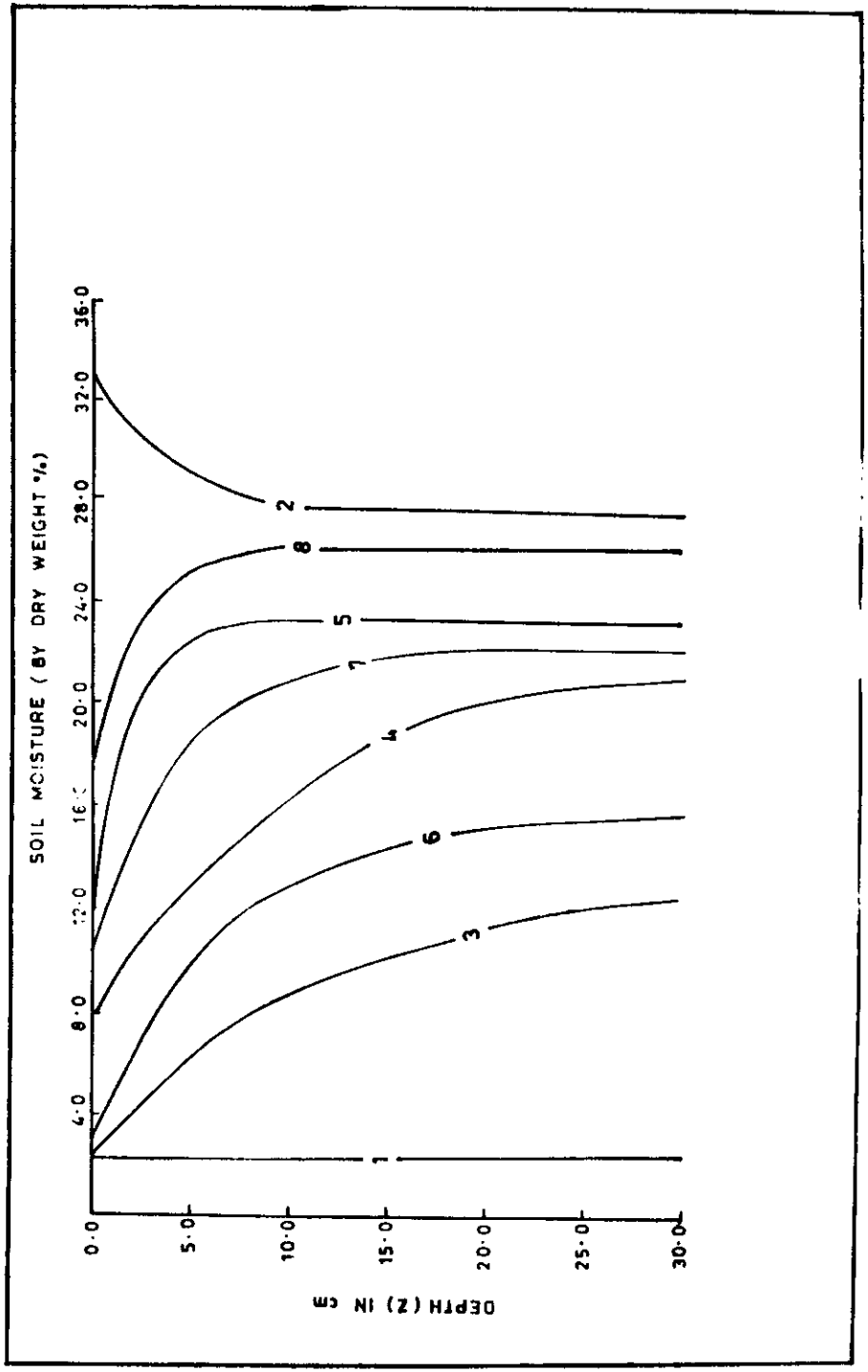

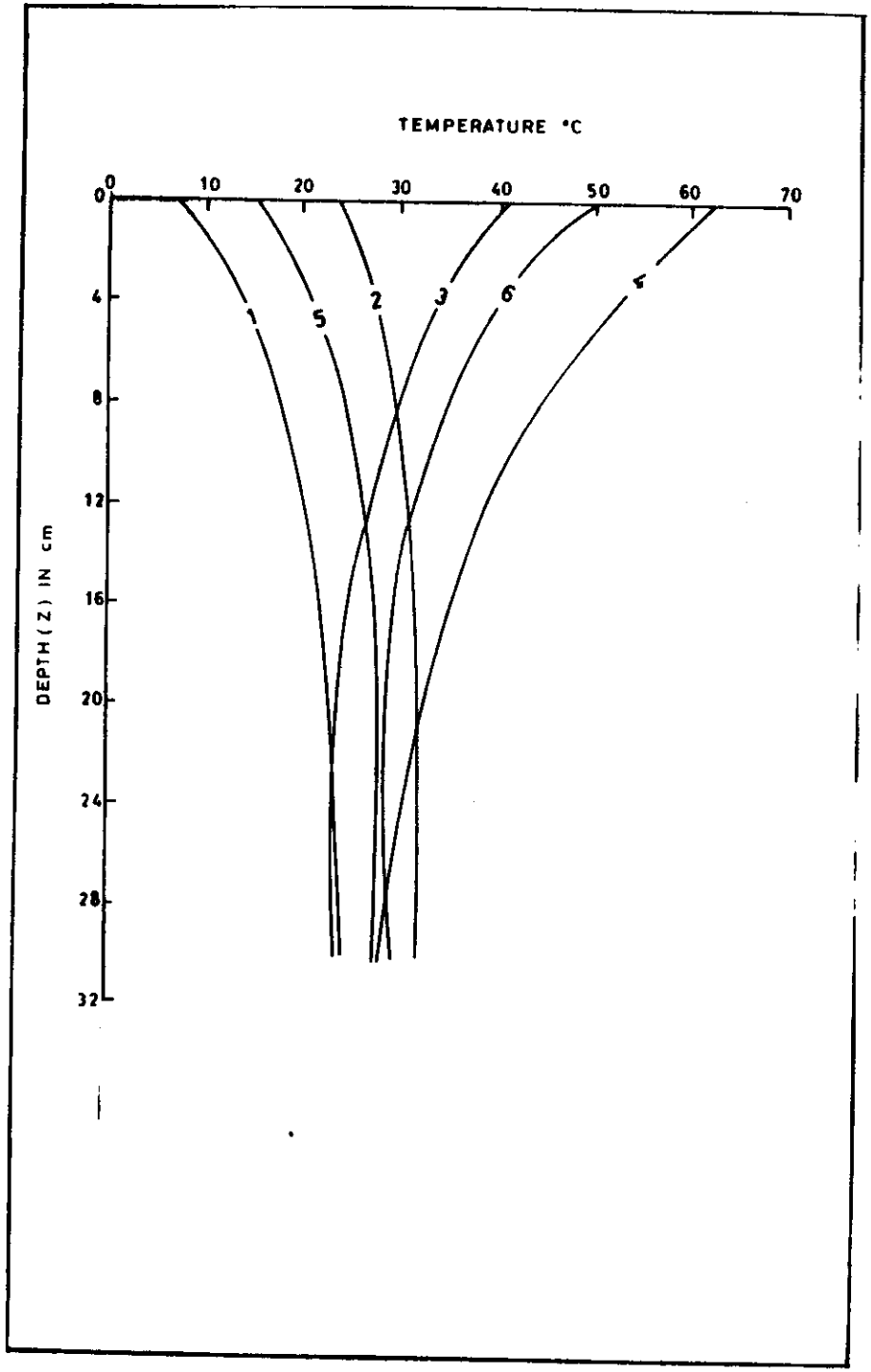
TEMPERATURE °C
0
10
20
30
40
50
60
70
0
4
8
12
16
20
24
28
32
DEPTH (Z) IN cm
1
5
2
3
6
4

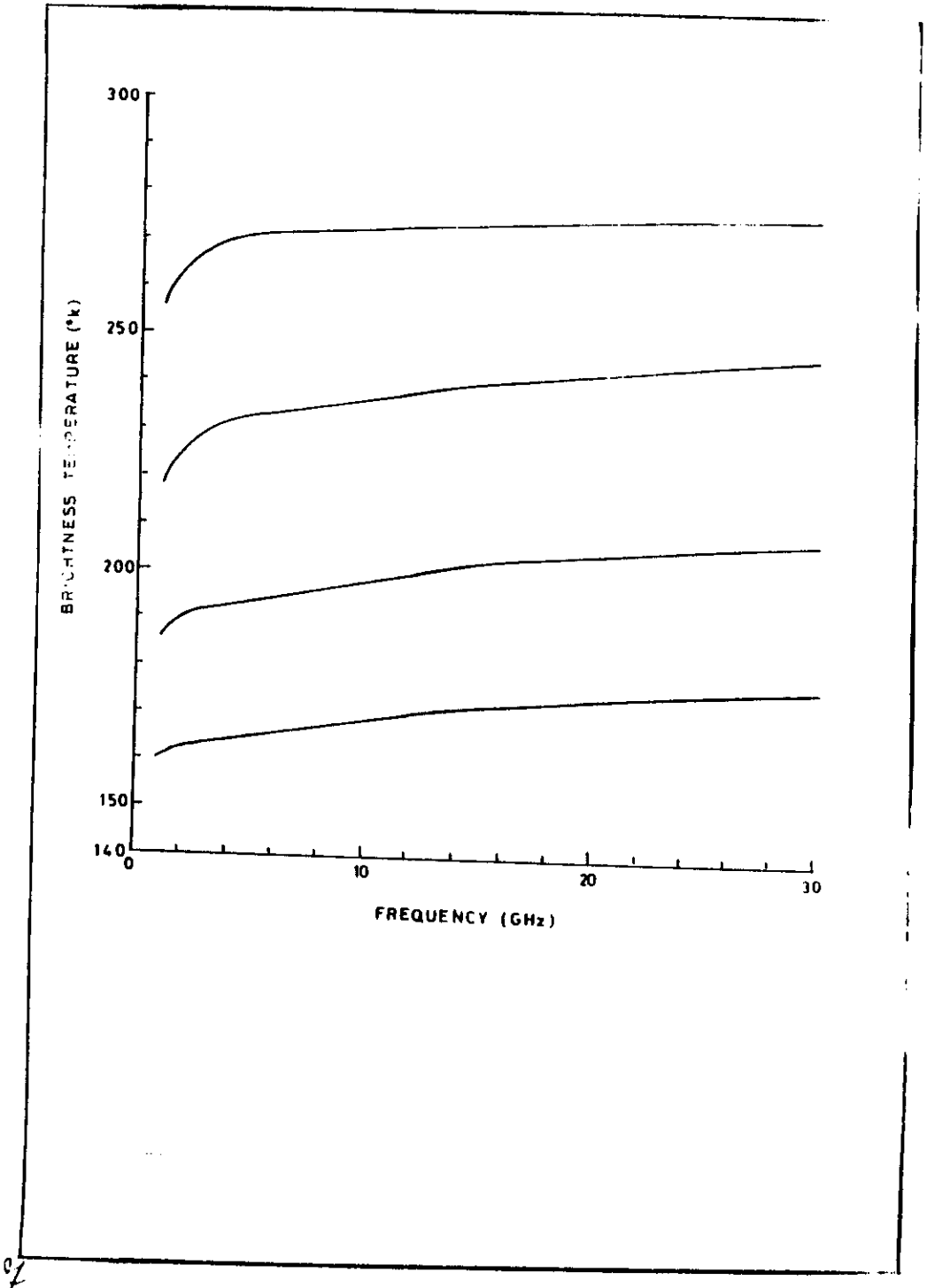
300
250
200
150
140
0
10
20
30
FREQUENCY (GHz)

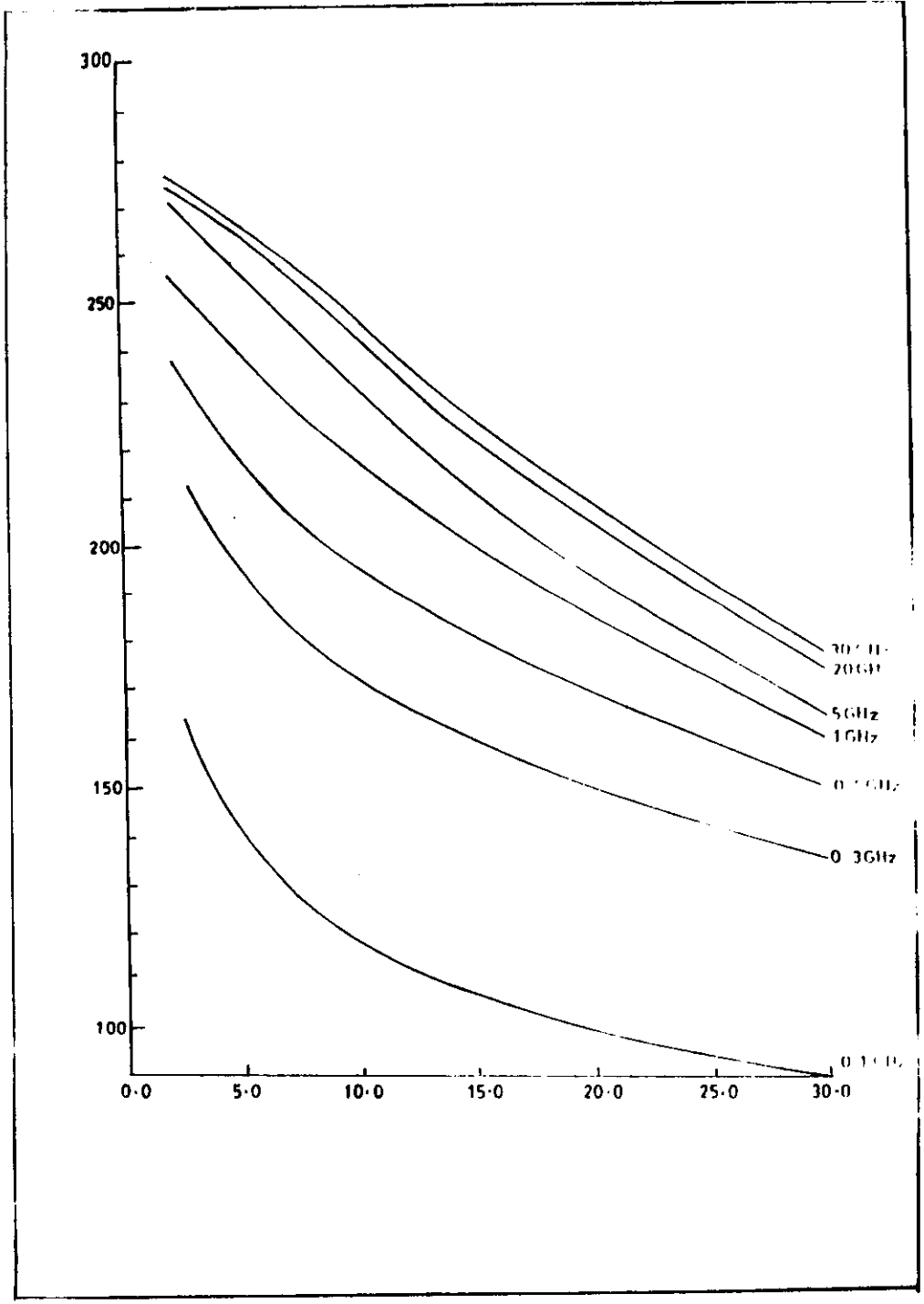
300
250
200
150
100
0·0
5·0
10·0
15·0
20·0
25·0
30·0
5GHz
1GHz
0 3GHz

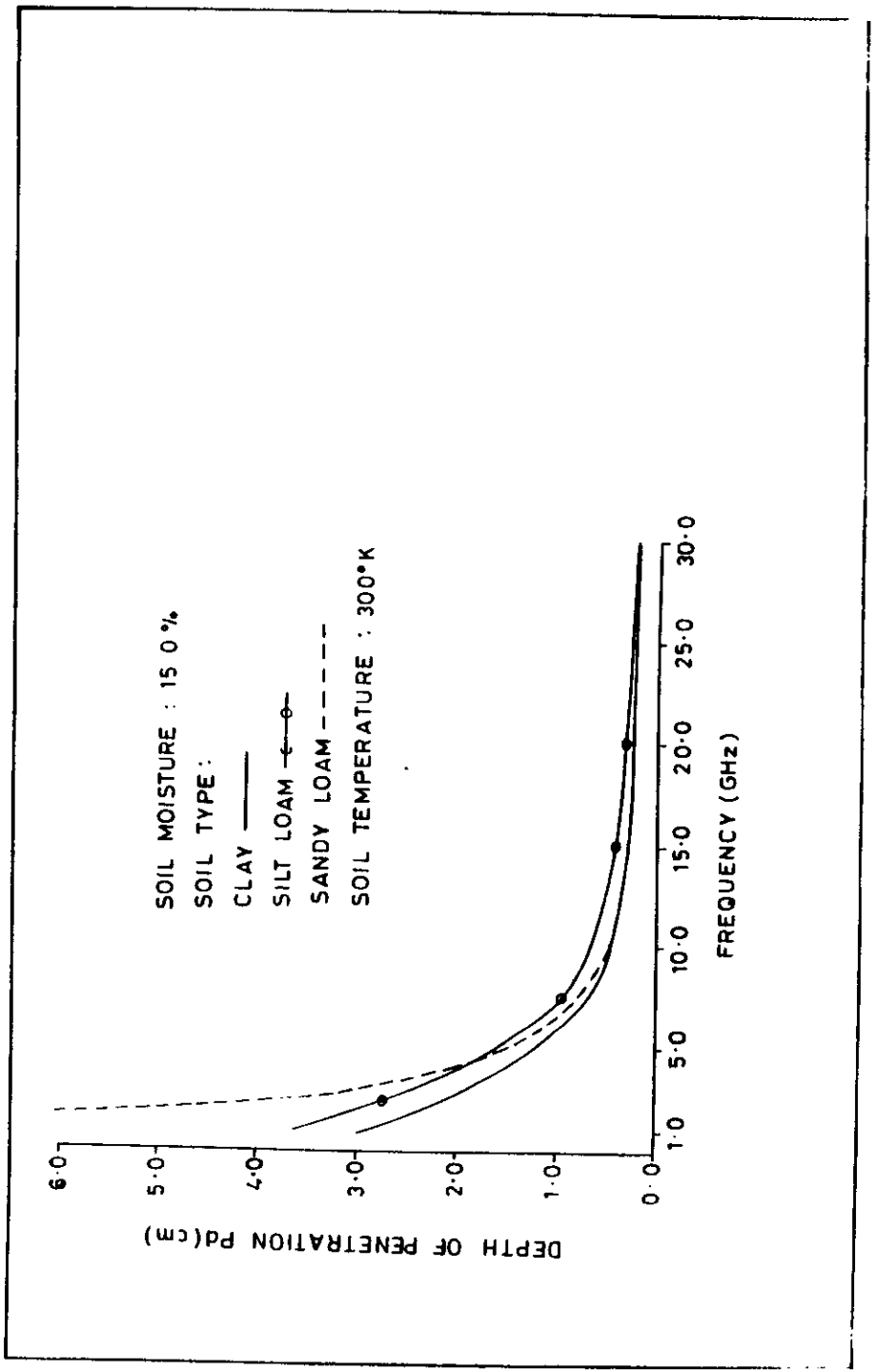
SOIL MOISTURE : 15 0 %
SOIL TYPE :
CLAY
SILT LOAM
SANDY LOAM
SOIL TEMPERATURE : 300°K
DEPTH OF PENETRATION Pd(cm)
FREQUENCY (GHz)
0·0
1·0
2·0
3·0
4·0
5·0
6·0
1·0
5·0
10·0
15·0
20·0
25·0
30·0

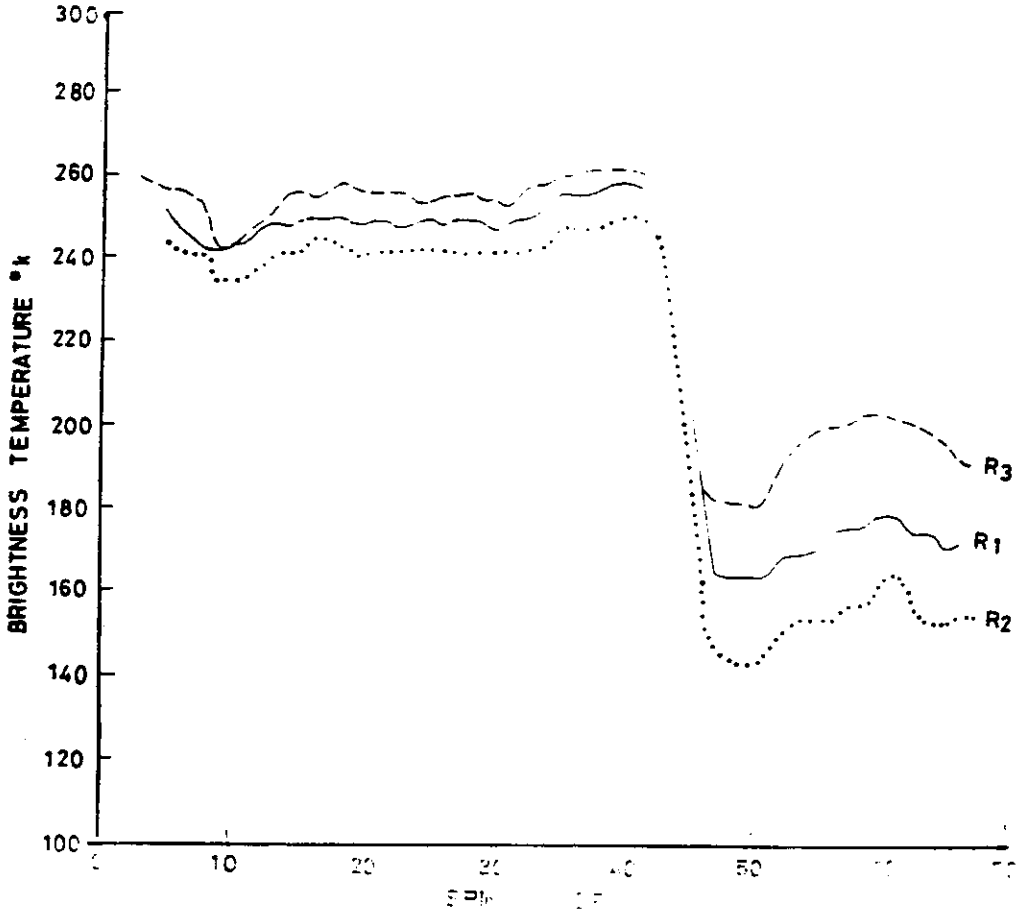
BRIGHTNESS TEMPERATURE °k
300
280
260
240
220
200
180
160
140
120
100
10
R3
R1
R2

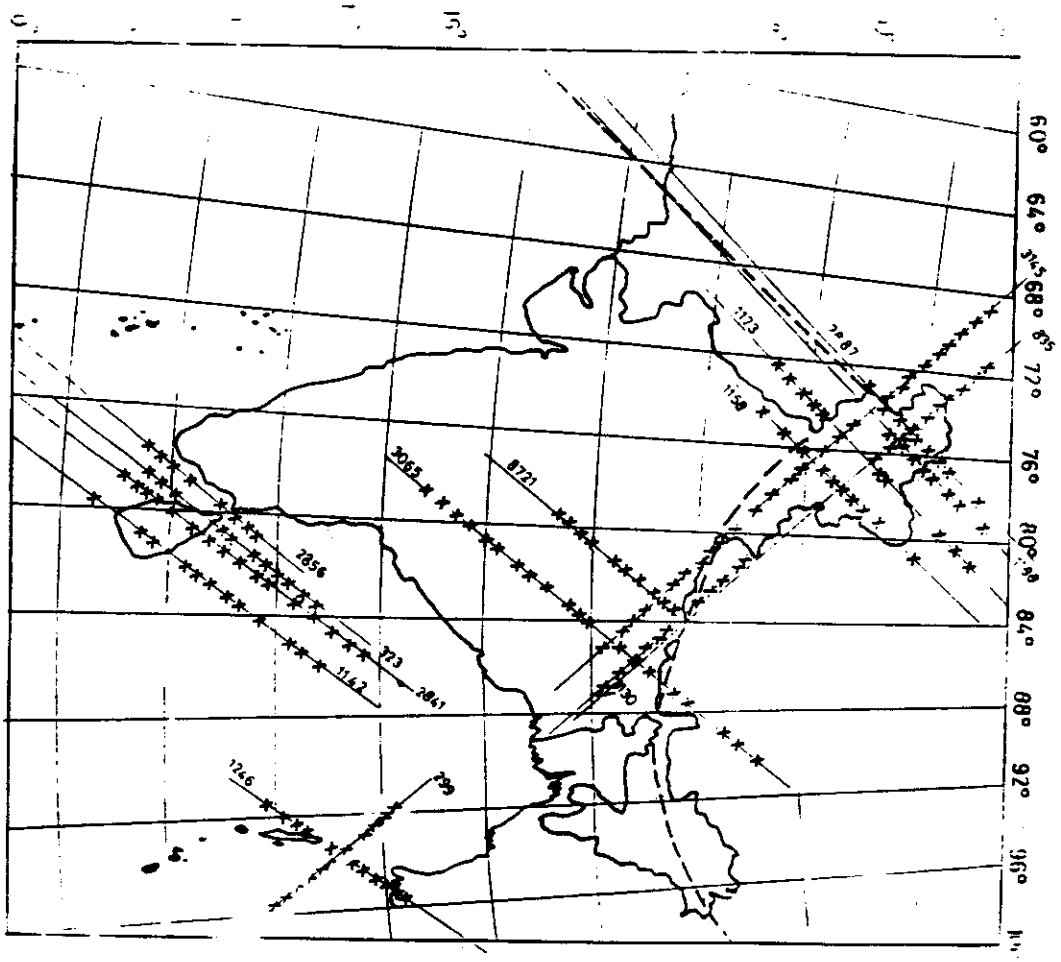
60°
64°
68°
72°
76°
80°
84°
88°
92°
96°
2085
8721
2856
373
2841
1246
239

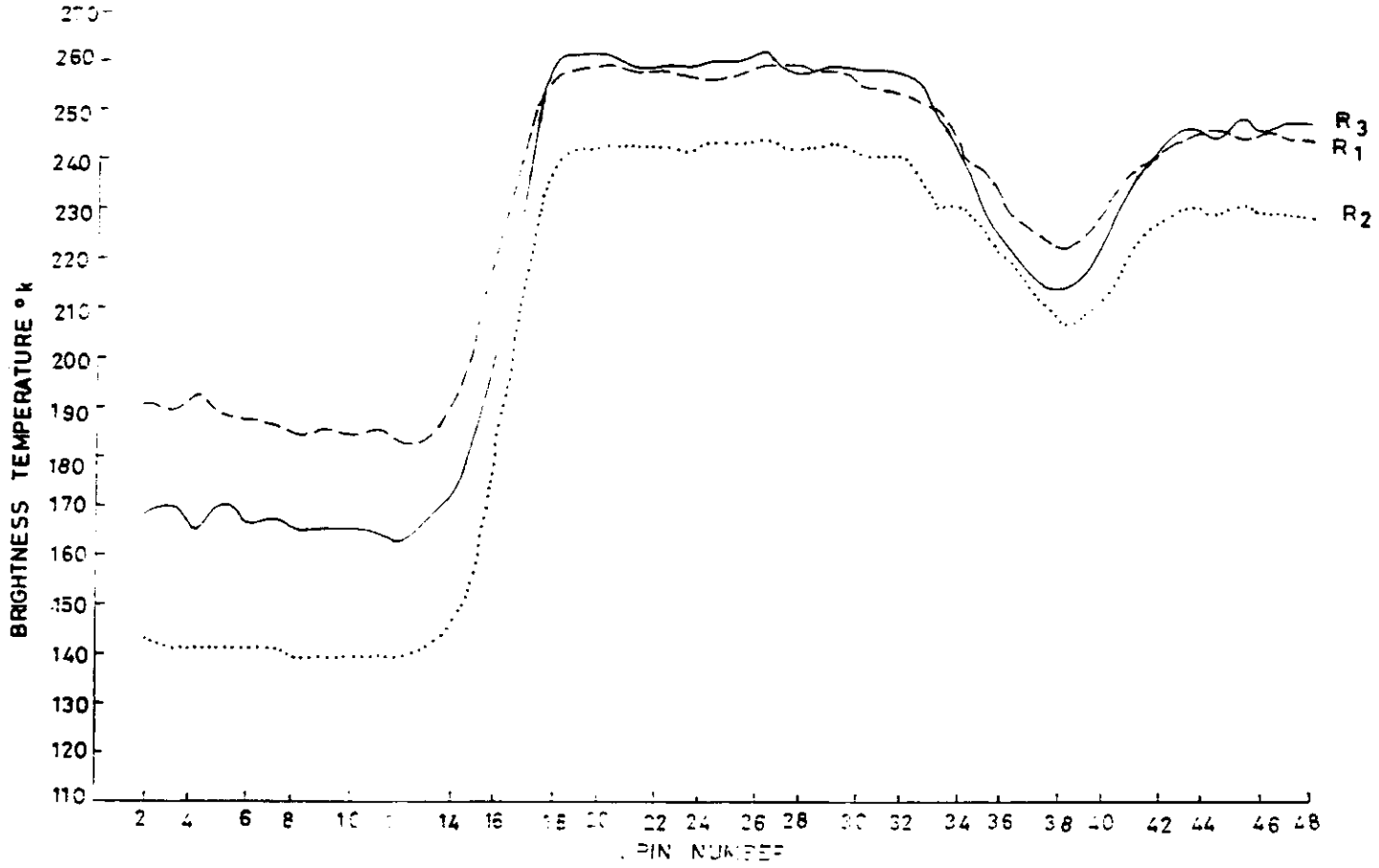
BRIGHTNESS TEMPERATURE °k
260
250
240
230
220
210
200
190
180
170
160
150
140
130
120
110
2 4 6 8 10 14 16 22 24 26 28 32 34 36 38 40 42 44 46 48
PIN NUMBER
R3
R1
R2

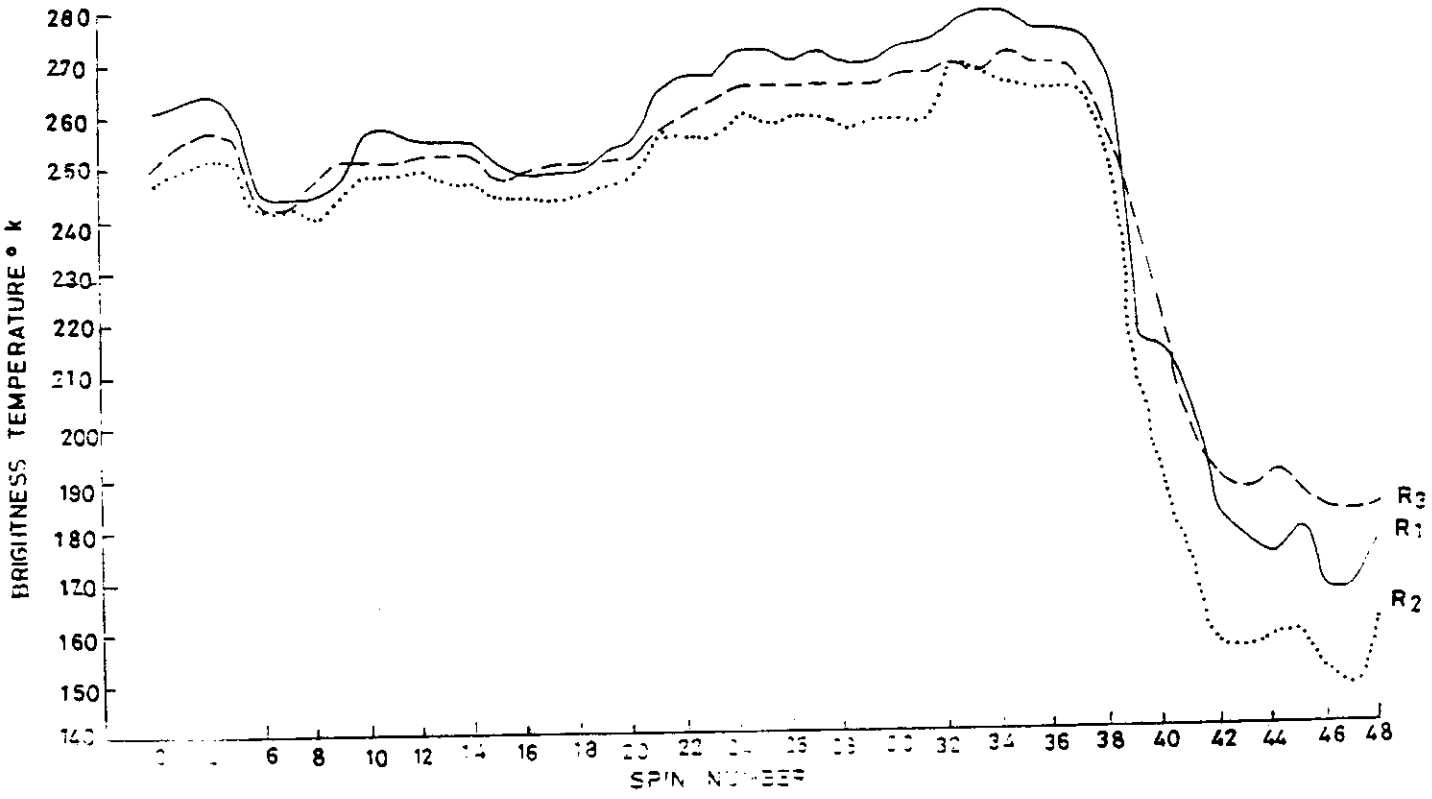
BRIGHTNESS TEMPERATURE °k
280
270
260
250
240
230
220
210
200
190
180
170
160
150
140
6 8 10 12 16 18 32 34 36 38 40 42 44 46 48
SPIN NUMBER
R3
R1
R2

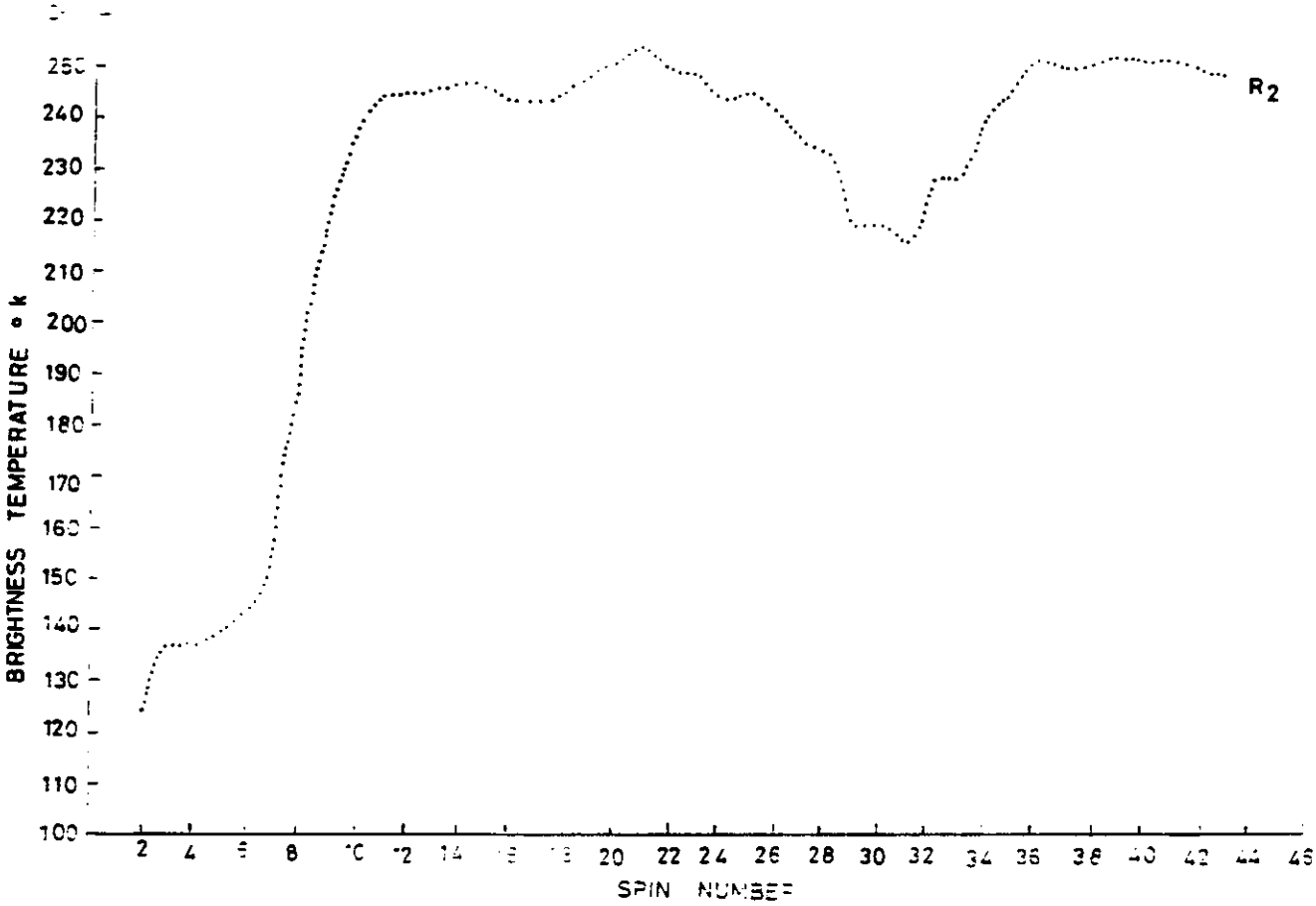
BRIGHTNESS TEMPERATURE ° k
250
240
230
220
210
200
190
180
170
160
150
140
130
120
110
100
2 4 6 8 10 12 14 16 18 20 22 24 26 28 30 32 34 36 38 40 42 44 46
SPIN NUMBER
R2

Z 9

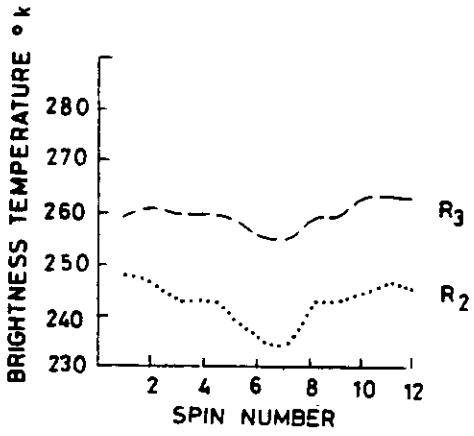
BRIGHTNESS TEMPERATURE ° k
280
270
260
250
240
230
2 4 6 8 10 12
SPIN NUMBER
R3
R2

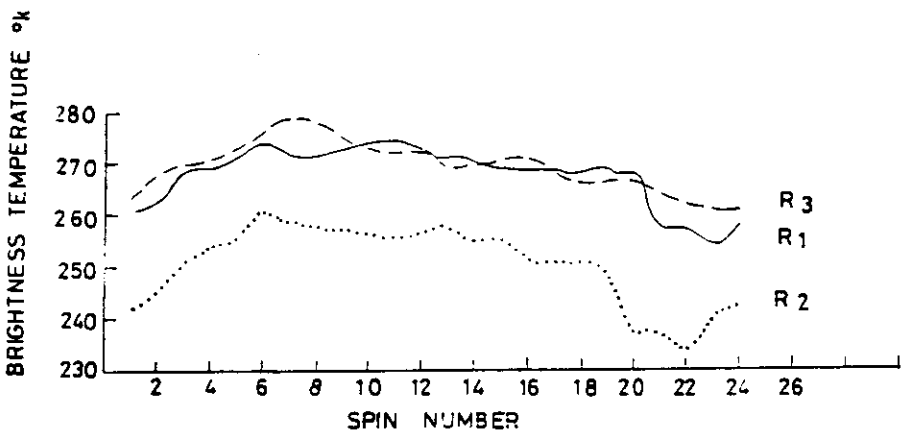
BRIGHTNESS TEMPERATURE °k
280
270
260
250
240
230
2 4 6 8 10 12 14 16 18 20 22 24 26
SPIN NUMBER
R 3
R 1
R 2

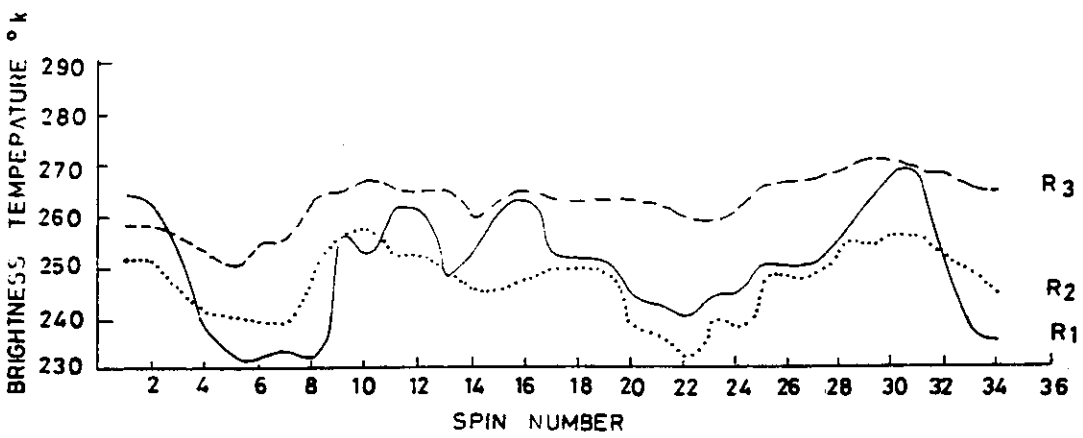
BRIGHTNESS TEMPERATURE °k
290
280
270
260
250
240
230
2 4 6 8 10 12 14 16 18 20 22 24 26 28 30 32 34 36
SPIN NUMBER
R3
R2
R1

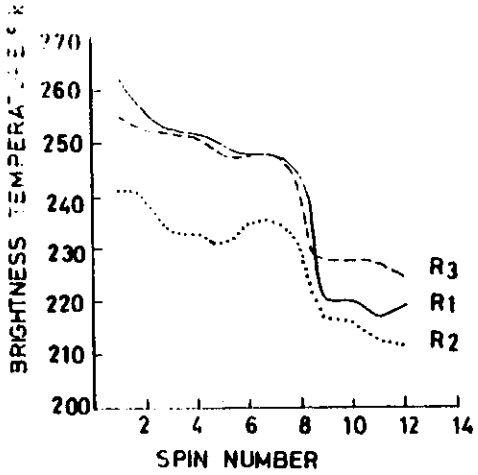
270
260
250
240
230
220
210
200
2
4
6
8
10
12
14
SPIN NUMBER
R3
R1
R2

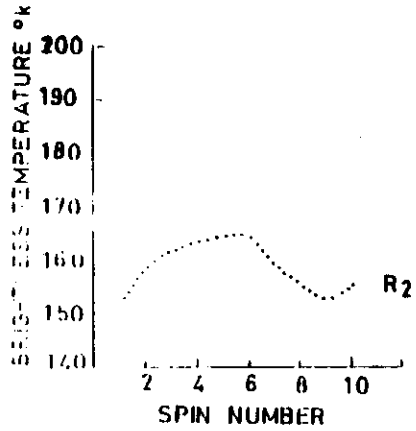
200
190
180
170
160
150
140
2
4
6
8
10
SPIN NUMBER
R2

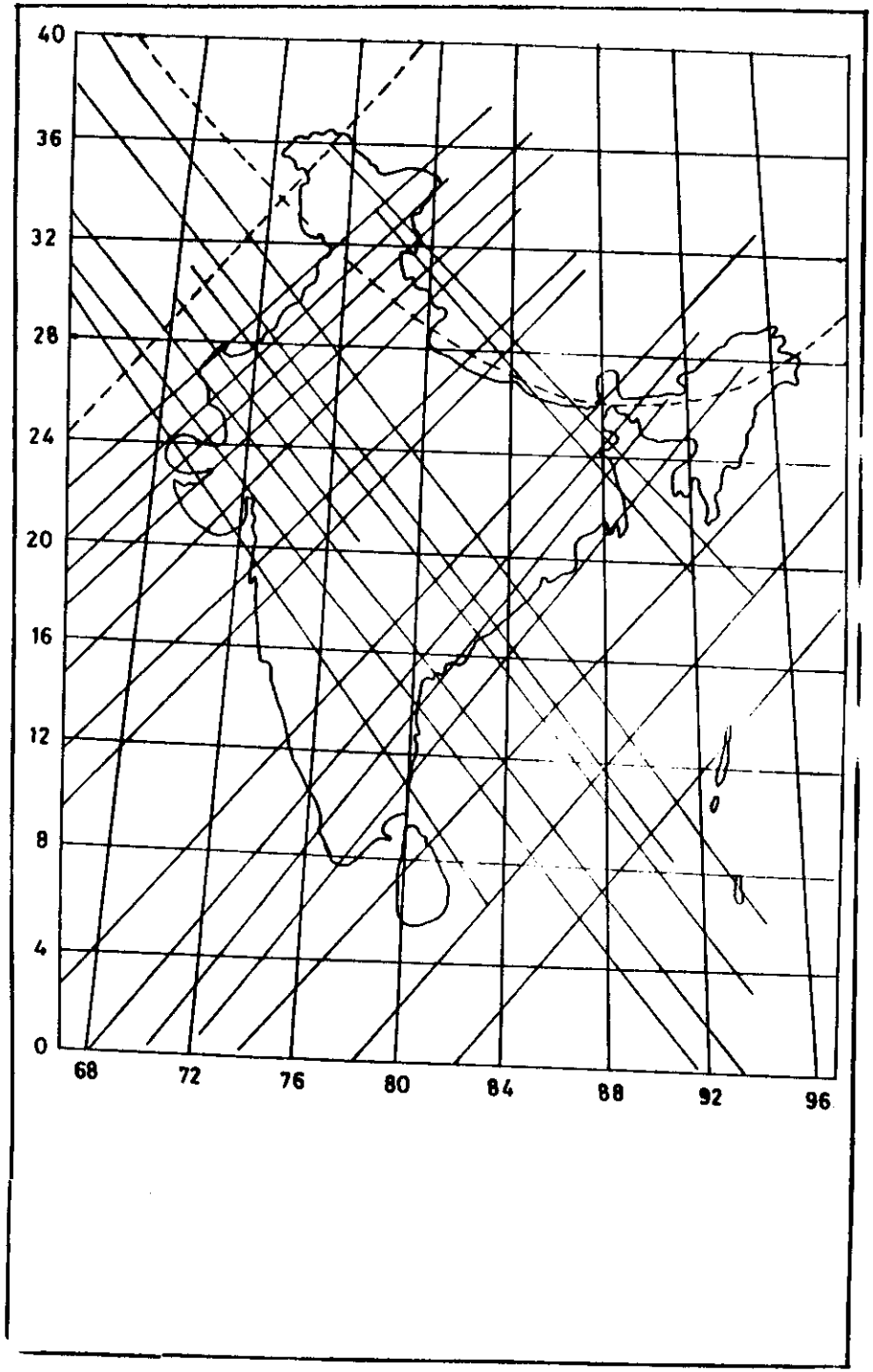

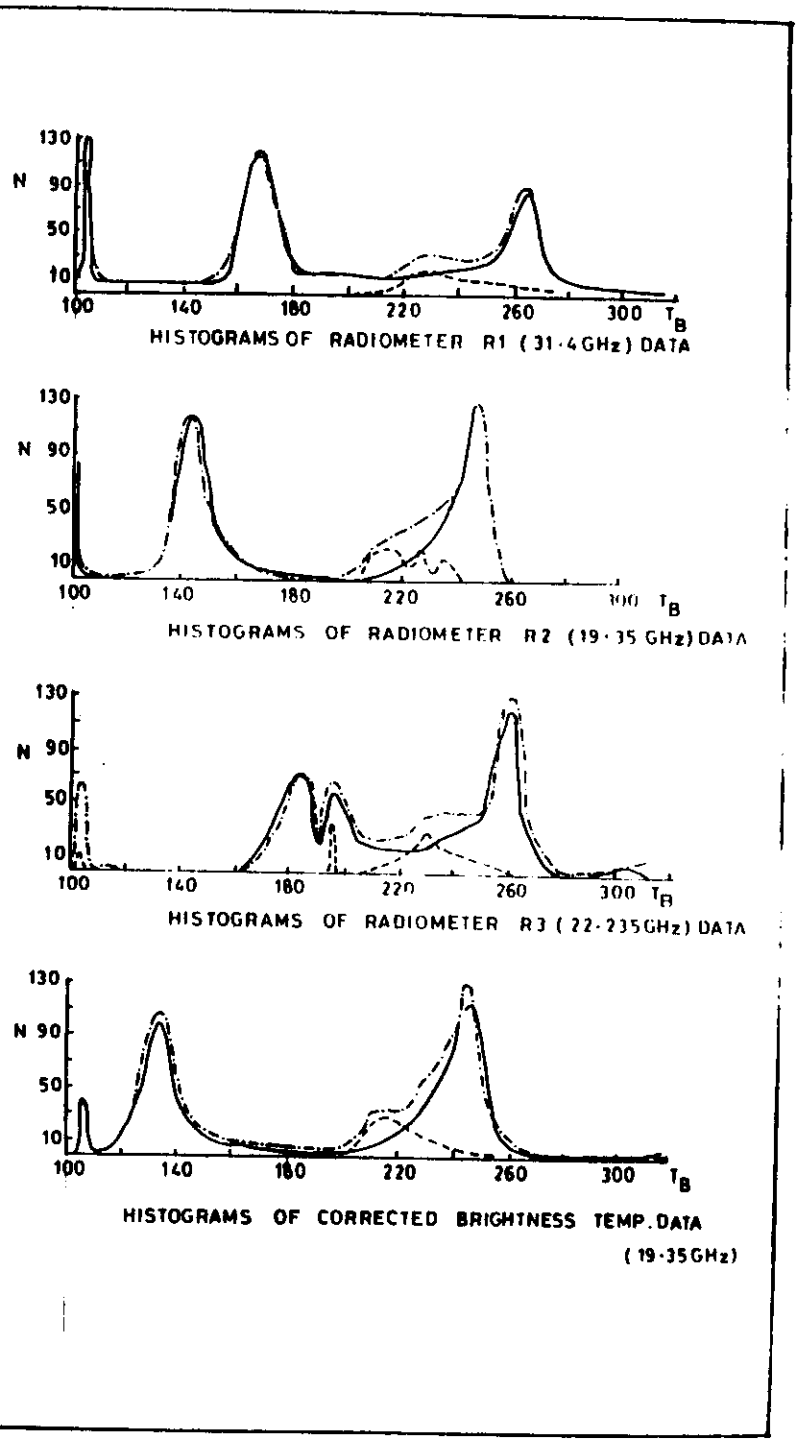

HISTOGRAMS OF RADIOMETER R1 (31·4 GHz) DATA

HISTOGRAMS OF RADIOMETER R2 (19·35 GHz) DATA

HISTOGRAMS OF RADIOMETER R3 (22·235 GHz) DATA

HISTOGRAMS OF CORRECTED BRIGHTNESS TEMP. DATA
(19·35 GHz)

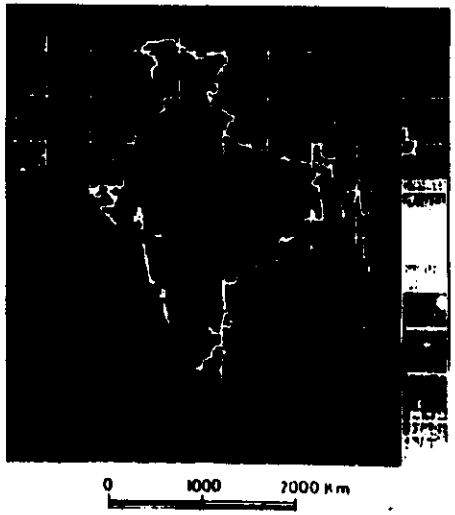

FIGURE 8. Color T_b map of Indian Subcontinent (original in color)